General Disclaimer

One or more of the Following Statements may affect this Document

- This document has been reproduced from the best copy furnished by the organizational source. It is being released in the interest of making available as much information as possible.

- This document may contain data, which exceeds the sheet parameters. It was furnished in this condition by the organizational source and is the best copy available.

- This document may contain tone-on-tone or color graphs, charts and/or pictures, which have been reproduced in black and white.

- This document is paginated as submitted by the original source.

- Portions of this document are not fully legible due to the historical nature of some of the material. However, it is the best reproduction available from the original submission.

Produced by the NASA Center for Aerospace Information (CASI)

DOE/NASA/0326-1
NASA CR-174820
Allison EDR 11869

An Investigation of Enhanced Capability Thermal Barrier Coating Systems for Diesel Engine Components

By: Robert L. Holtman
Jerry L. Layne
Berton Schechter

Allison Gas Turbine Division
General Motors Corporation
Indianapolis, Indiana 46206-0420

(NASA-CR-174820) AN INVESTIGATION OF ENHANCED CAPABILITY THERMAL BARRIER COATING SYSTEMS FOR DIESEL ENGINE COMPONENTS Final Report (General Motors Corp.) 140 p HC A07/MF A01 CSCL 11B G3/27 N85-16154 Unclas 14203

prepared for
National Aeronautics and Space Administration
NASA-Lewis Research Center
Cleveland, Ohio 44135
Contract No. DEN3-326

---

for
U.S. DEPARTMENT OF ENERGY
Conservation and Renewable Energy
Office of Vehicle and Engine R & D
Washington, D.C 20585
Under Interagency Agreement DE-A101-80CS50194

DOE/NASA/0326-1
NASA CR-174820
Allison EDR 11869

An Investigation of Enhanced Capability Thermal Barrier Coating Systems for Diesel Engine Components

By: Robert L. Holtman
Jerry L. Layne
Berton Schechter

Allison Gas Turbine Division
General Motors Corporation
Indianapolis, Indiana 46206-0420

August 1984

prepared for
National Aeronautics and Space Administration
NASA-Lewis Research Center
Cleveland, Ohio 44135
Contract No. DEN3-326

---

for
U.S. DEPARTMENT OF ENERGY
Conservation and Renewable Energy
Office of Vehicle and Engine R & D
Washington, D.C. 20585
Under Interagency Agreement DE-A101-80CS50194

FOREWORD

The low heat rejection (LHR) diesel engine technology utilized in this program was developed under a joint Allison Gas Turbine/Detroit Diesel Allison LHR diesel engine program sponsored by Detroit Diesel Allison. This technology included the following:

- o development of the experimental single cylinder LHR engine
- o development of the LHR diesel engine simulation model
- o development of heat transfer coefficients and boundary data utilized in the heat transfer analyses
- o definition of engine operation state points

TABLE OF CONTENTS

Section	Title	Page
I	Summary	1
II	Introduction	3
III	Task I--Analysis and Design	8
	3.1 Preliminary Design of Coating System Envelope	8
	3.2 Coating System Description	10
	3.3 Heat Transfer Analysis	14
	3.4 SI Pad Configuration	36
IV	Task II--Bench Test Evaluation	38
	4.1 Coating System Morphology	38
	4.2 Test Coupon Preparation	42
	4.3 Thermal Conductivity Evaluation	42
	4.4 Erosion Resistance	57
	4.5 Corrosion/Oxidation Resistance	57
	4.6 Thermal Shock/Fatigue Resistance	62
	4.7 Coating Selection for Engine Testing	84
V	Task III--Engine Component Testing	87
	5.1 Approach	87
	5.2 Engine Component Design	87
	5.3 Fabrication of Coated Engine Components	91
	5.4 Engine Testing	98
VI	Conclusions and Recommendations	127
	6.1 Description of Investigation	127
	6.2 Program Goals	127
	6.3 Results and Conclusions	127
	6.4 Recommendations	128
	Appendix A--List of Terms, Abbreviations, and Symbols	129
	References	130

PAGE [illegible] BLANK NOT FILMED

LIST OF ILLUSTRATIONS

Figure	Title	Page
1	Engine components with applied thermal barrier coatings	5
2	Program plan diagram	6
3	Zirconia powder particle morphology	12
4	Thermal barrier coating cross section	14
5	Three-dimensional low heat rejection finite element model of the fire deck assembly	16
6	Two-dimensional axisymmetrical finite element model of the piston	16
7	Two-dimensional axisymmetrical finite element models of the valves	17
8	The effect of the thickness of the strain isolator on the thermal effectiveness of the thermal barrier coating on the piston	20
9	The effect of the thickness of the strain isolator on the surface temperature of the thermal barrier coating on the piston	20
10	The effect of the thickness of the thermal barrier coating on the thermal effectiveness of the piston	22
11	The effect of the thickness of the thermal barrier coating on the surface temperature of the piston	22
12	Contour plot of temperatures in a coated piston	25
13	Contour plot of temperatures in an uncoated piston	26
14	Metal temperature of the piston versus engine power	28
15	Contour plot of temperatures in a coated low heat rejection fire deck	32
16	Contour plot of temperatures in an uncoated low heat rejection fire deck	33
17	Temperatures of uncoated (top) and plasma-sprayed zirconia coated (bottom) intake valves	34
18	Temperatures of uncoated (top) and plasma-sprayed zirconia coated (bottom) exhaust valves	35
19	Vendor coating A on strain isolator pad in system 2	39
20	Brazed and coated strain isolator pad	40
21	Vendor coating B in system 3	41
22	80/20 SYSZ/Eccosphere coating in systems 4 and 5	44
23	Plasma-sprayed hollow yttria-stabilized zirconia coating developed by Allison	45
24	Thermal conductivity measurement fixture	46
25	Thermocouple locations in the thermal conductivity measurement rig	47
26	Waspaloy thermal conductivity	50
27	Measured thermal conductivity of Ni-Resist D5B, EMS 1, and EMS 235	51
28	Thermal conductivity of Waspaloy with and without a bond coat	52
29	Conductivity versus temperature for ceramics	53
30	Thermal conductivity of a strain isolator pad	54
31	Conductance versus temperature for ceramic systems without strain isolator pads	55
32	Conductance versus temperature for ceramic systems with strain isolator pads	55

LIST OF ILLUSTRATIONS (CONT)

Figure	Title	Page
33	Thermal conductivities of zirconia coatings, monolithic zirconia, strain isolator pad, and metallic engine materials	56
34	Erosion test fixture	58
35	Erosion test results	59
36	Systems 1-7 2 hr after the erosion test	60
37	Corrosion/oxidation test fixture	61
38	Corrosion/oxidation test samples	63
39	Corrosion test results as seen through a scanning electron microscope	64
40	Overall view of the thermal shock test fixture	65
41	Burner station of the thermal shock test rig	66
42	Typical thermal shock test cycle	69
43	Thermal shock testing to system 1--vendor coating A without a strain isolator pad; substrate of EMS 235; 20 cycles to failure	70
44	Thermal shock testing to system 1--vendor coating A without a strain isolator pad; substrate of D5B; 6723 cycles to failure	71
45	Thermal shock testing to system 1--vendor coating A without a strain isolator pad; substrate of Waspaloy 192 cycles to failure	72
46	Thermal shock testing to system 2--vendor coating A with a strain isolator pad; substrate of Waspaloy; completed 25,260 cycles without failing	73
47	Results of thermal shock testing to system 2--vendor coating A with a strain isolator pad on a Waspaloy; substrate after the completion of 25,260 cycles without failing	74
48	Thermal shock testing to system 3--vendor coating B without a strain isolator; substrate of D5B; 17 cycles to failure	75
49	Thermal shock testing to system 3--vendor coating B without a strain isolator pad; substrate of EMS 235; 0.5 cycles to failure	76
50	Thermal shock testing to system 4--80/20 SYSZ/Eccosphere coating without a strain isolator pad; substrate of Waspaloy; completed 25,260 cycles without failing	78
51	Results of thermal shock testing to system 4--80/20 SYSZ/Eccosphere coating without a strain isolator pad on a Waspaloy substrate after the completion of 25,260 cycles without failing	79
52	Thermal shock testing to system 5--80/20 SYSZ/Eccosphere coating with a strain isolator pad; substrate of Waspaloy; 24,350 cycles to failure	80
53	Thermal shock testing to system 6--PS/HYSZ coating without a strain isolator pad; substrate of Waspaloy; completed 25,260 cycles without failing	81

LIST OF ILLUSTRATIONS (CONT)

Figure	Title	Page
54	Results of thermal shock testing to system 6--PS/HYSZ coating without a strain isolator pad on a Waspaloy substrate after completion of 26,250 cycles without failing	82
55	Results of thermal shock testing to system 7--PS/HYSZ coating with a strain isolator pad on a Waspaloy substrate after the completion of 25,260 cycles without failing	83
56	The placement of an assembled fire deck in an engine	89
57	Fire deck insulating rings	90
58	Final design configuration of coated valves	94
59	Strain isolator pad installed on a Waspaloy fire deck	95
60	Equipment that applies a plasma-sprayed coating to piston, fire decks, and valves	96
61	As-sprayed coated valves	97
62	Uncoated/coated piston dome contour	99
63	Spray-coated piston (top) and fire deck (bottom)	100
64	Finish-machined coated components	101
65	Single-cylinder diesel test engine	102
66	Cross sections of coated engine components	106
67	A piston with a thermal barrier coating before testing	107
68	A coated piston after 4 hr of testing	108
69	A coated piston after 14 hr of testing	109
70	A coated piston after 24 hr of testing	110
71	A fire deck with a thermal barrier coating before testing	111
72	A coated fire deck after 4 hr of testing	112
73	A coated fire deck and coated valves after 4 hr of testing	113
74	A coated fire deck and coated valves after 14 hr of testing	114
75	A coated fire deck and coated valves after 24 hr of testing	116
76	A coated fire deck after 24 hr of testing	117
77	Valves with thermal barrier coatings before testing	118
78	Coated valves after 4 hr of testing	119
79	Coated valves after 24 hr of testing	119
80	Exhaust gas temperature versus air/fuel ratio at 1900 rpm	121
81	Exhaust gas temperature versus air/fuel ratio at 1300 rpm	122
82	Thermocouple instrumentation on a coated fire deck	123
83	Metal temperatures of the fire deck along symmetrical centerline	124
84	Reduction in metal temperatures of the fire deck versus air/fuel ratio	126

LIST OF TABLES

Table	Title	Page
I	Test conditions for TBCs on the single-cylinder research engine with NASA DEN3-326 coated components	7
II	Thermal barrier system composition matrix	11
III	Summary of the preliminary heat transfer analysis of the piston for specific coating system thicknesses	19
IV	Summary of the preliminary heat transfer analysis of the fire deck for specific coating system thicknesses	21
V	Summary of the preliminary heat transfer analysis of the intake and exhaust valves for specific coating system thicknesses	21
VI	Summary of the final piston heat transfer results	24
VII	Reduction in the metal temperatures of the piston due to the TBC	24
VIII	Summary of the final fire deck heat transfer analysis results	29
IX	Reduction in the metal temperatures of the fire deck due to TBC	29
X	Summary of the final intake and exhaust valve heat transfer analysis results	30
XI	Reduction in the metal temperatures of the valves due to TBCs	31
XII	Summary of the final heat transfer analysis on the piston, fire deck, and valves	31
XIII	Physical characteristics of the SI pad for diesel applications	37
XIV	Single-cylinder diesel engine component materials	43
XV	Thermal conductivity test plan	49
XVI	Thermal shock test results	68
XVII	Summary of deflections and stresses in intake and exhaust valves	92
XVIII	Typical spray parameters for PS/HYSZ coating	93
XIX	Coating system constituent thickness	98
XX	Comparison of engine loading	103
XXI	Single-cylinder LHR diesel engine test conditions	104

I. SUMMARY

The primary objective of this program was to investigate materials systems and processes for the development of effective and durable thermal barrier coatings for heavy-duty diesel engines. This effort systematically evaluated specimens of several thermal barrier coating (TBC) systems and tested a selected system in a single-cylinder low heat rejection (LHR) diesel engine.

Specimens of seven coating systems were systematically evaluated for thermal conductivity, erosion resistance, corrosion/oxidation resistance, thermal shock fatigue resistance, and microstructure. These systems included coatings with the following four basic compositions:

- o Allison plasma-sprayed/hollow particle yttria-stabilized zirconia (PS/HYSZ)
- o Allison 80/20 solid particle yttria-stabilized zirconia/Eccosphere (80/20 SYSZ/Eccosphere)
- o vendor coating A zirconia-based coating
- o vendor coating B zirconia-based coating

The first three basic coatings were also combined with a strain isolator (SI) pad, increasing the number of coating systems tested to seven.

The selected TBCs were expected to provide better coating thickness capability than the current state-of-the-art coatings, which are typically 0.38 mm to 0.64 mm (0.015 in. to 0.025 in.) thick. Each TBC also incorporated structural modifications to provide more effective crack stoppers and, thus, to provide greater durability at increased thicknesses.

Experimental results showed that the thermal conductivity of the zirconia-based TBCs ranged from 0.872 to 0.976 W/m °C at 371°C (0.042 to 0.047 Btu/hr-in.-°F at 700°F), one-third to one-half of the thermal conductivity of monolithic zirconia. These TBCs, therefore, achieved insulation effectiveness comparable to monolithic zirconia in a significantly reduced space envelope.

The PS/HYSZ coating was judged superior in the specimen screening tests and was applied to the piston crown, fire deck, and valves of an uncooled single-cylinder diesel engine. The nominal thickness of the coating was 1.52 mm (0.060 in.). A 1.02 mm (0.040 in.) thick SI pad was also used in the coating system on the fire deck.

A planned 24 hour test of the coated piston, valves, and fire deck was conducted an uncooled single-cylinder LHR diesel engine at power levels from 0.83 MPa to 1.17 MPa (120 lb/in.^{2} to 170 lb/in.^{2}) brake mean effective pressure (BMEP). Testing included a 4-hr proof test of each coated component individually, followed by two 10-hr tests of the coated components combined. The coatings on all of the components survived the engine testing with a minimum of distress.

The measured engine exhaust gas temperature increased 28°C (50°F) with all of the coated components installed while measured fire deck metal temperatures (measured at a point 2.54 mm [0.100 in.] from the combustion surface) decreased 86°C (155°F) on the intake side and 42°C (75°F) on the exhaust side.

The average temperature drop across the TBC was calculated by finite element heat transfer analysis to be 107°C (192°F) on the piston, 53°C (95°F) on the fire deck, 80°C (144°F) on the intake valves, and 33°C (60°F) on the exhaust valves.

II. INTRODUCTION

BACKGROUND

Energy use by heavy-duty diesel trucks is substantial and growing. In 1980, diesel powered heavy trucks used 1.8 x 10^{18}EJ (1.7 x 10^{15} Btu) of fuel energy. This 1980 usage represented 17% of the total of all highway fuel energy usage; up from 14% in 1975. By the year 2000, heavy truck fuel use is expected to approach 25% of the total highway fuel consumption.

In recognition of a growing impact on national fuel use, the DOE is placing increased emphasis on conservation technologies applicable to heavy duty diesel trucks. Because the passenger car conservation strategy of downsizing cannot realistically be applied to heavy trucks, the attention has been directed toward a revolutionary concept in diesel engine technology; the low heat rejection (LHR) diesel.

The LHR designs are distinguished by the complete absence of water cooling; a system that traditionally included flow passages in the engine block as well as a fan and radiator mounted in front of the engine. Elimination of the water cooling significantly alters the engine heat balance; with resulting overall efficiency improvement. Correlcative advantages in the areas of engine packaging and multifuel capability are also expected to contribute to highway fuel conservation.

A major technology challenge associated with the LHR engine is that of insulation and metal protection for the in-cyclinder components that formerly were water cooled. It is generally agreed that "ceramics" have the potential for meeting the requirements projected for the LHR components. Presently there are two approaches to ceramic technology for diesels; (1) monolithics, and (2) coatings.

The monolithic approach involves simply the use of an appropriate ceramic as the material of construction for selected parts. This approach is being pursued in various industry and government funded efforts involving a variety of specific ceramic materials and in-cylinder components.

The coatings approach involves the plazma spray application of ceramic material as a protective coating over the component metalic substrate. The lower average thermal conductivity of the "as-sprayed" materials makes the coating attractive as a thermal barrier. There remains, however, a significant technology challenge regarding the durability of the relatively thick coatings required for specific LHR diesel applications.

The current state-of-the-art for diesel in-cylinder ceramic coatings extends to thicknesses of 0.64 mm (0.025 in.). This report relates results from an experimental investigation of durability for coatings of 1.53 mm (0.060 in.) thickness; and coating systems, including special strain isolator pad, of 2.54 mm (0.100 in.) thickness.

OBJECTIVE OF PROGRAM

The overall objective of this program was to advance state-of-the-art coating technology through the systematic development of an enhanced TBC system for

application in a diesel engine environment. More specifically, the objectives were as follows:

- o to systematically investigate coating application parameters to develop an advanced thick coating system with enhanced insulating capability
- o to evaluate the thermal and mechanical durability characteristics, such as thermal conductivity, erosion, corrosion/oxidation, and thermal shock fatigue resistance, of selected advanced zirconia-based coatings
- o to evaluate the performance of a selected TBC system applied to the piston, fire deck, and valves in a LHR diesel engine environment (uncooled single cylinder diesel engine)
- o to conduct a heat transfer analysis of the coating systems to determine the operating conditions of the engine components
- o to evaluate the performance of a strain isolator (SI) pad as part of a TBC system

The engine components on which the TBCs were evaluated are pictured with TBCs in Figure 1.

PROGRAM PLAN

The technical effort of this program was accomplished in three tasks as shown in Figure 2. Task I determined the general composition of the coating systems to be evaluated and provided the heat transfer analysis of the coating systems as applied to modified engine components. In Task II, characteristics of seven coating systems were determined in screening tests to provide data for the selection of one coating for evaluation in engine testing. Task II also developed the coating system morphology. In Task III, the selected coating was applied to modified engine parts and tested in an uncooled single-cylinder diesel engine.

DESCRIPTION OF TASKS

In Task I, the compositions of four developmental coatings were defined. Two of the coatings were vendor coatings. Three of the coating systems were also combined with an SI pad, resulting in a total of seven systems for evaluation in Task II. A preliminary heat transfer analysis was conducted to determine the effect of coating and SI thickness trade-offs and the effect of coating system thickness on engine component temperatures.

The development of a unique Allison PS/HYSZ coating (one of the four developmental coatings) was also undertaken in Task II. This effort involved investigating coating application parameters to obtain the desired coating morphology.

Test coupons of the coating systems (with and without SI pads) were prepared and tested in bench test fixtures to determine thermal conductivity, erosion resistance, corrosion/oxidation resistance, and thermal shock fatigue resistance. These results determined the coating performance rank and were the basis on which one coating system was selected for evaluation in engine testing.

In Task III, modified designs for the piston, fire deck, and valves were prepared; the parts fabricated; the selected coating (from Task II) applied; and tests performed in an uncooled single cylinder LHR diesel engine. The ceramic coatings on all of the components were nominally 1.52 mm (0.060 in.) thick (tapered to 0.51 mm [0.020 in.] on the intake valves and 0.76 mm [0.030 in.]

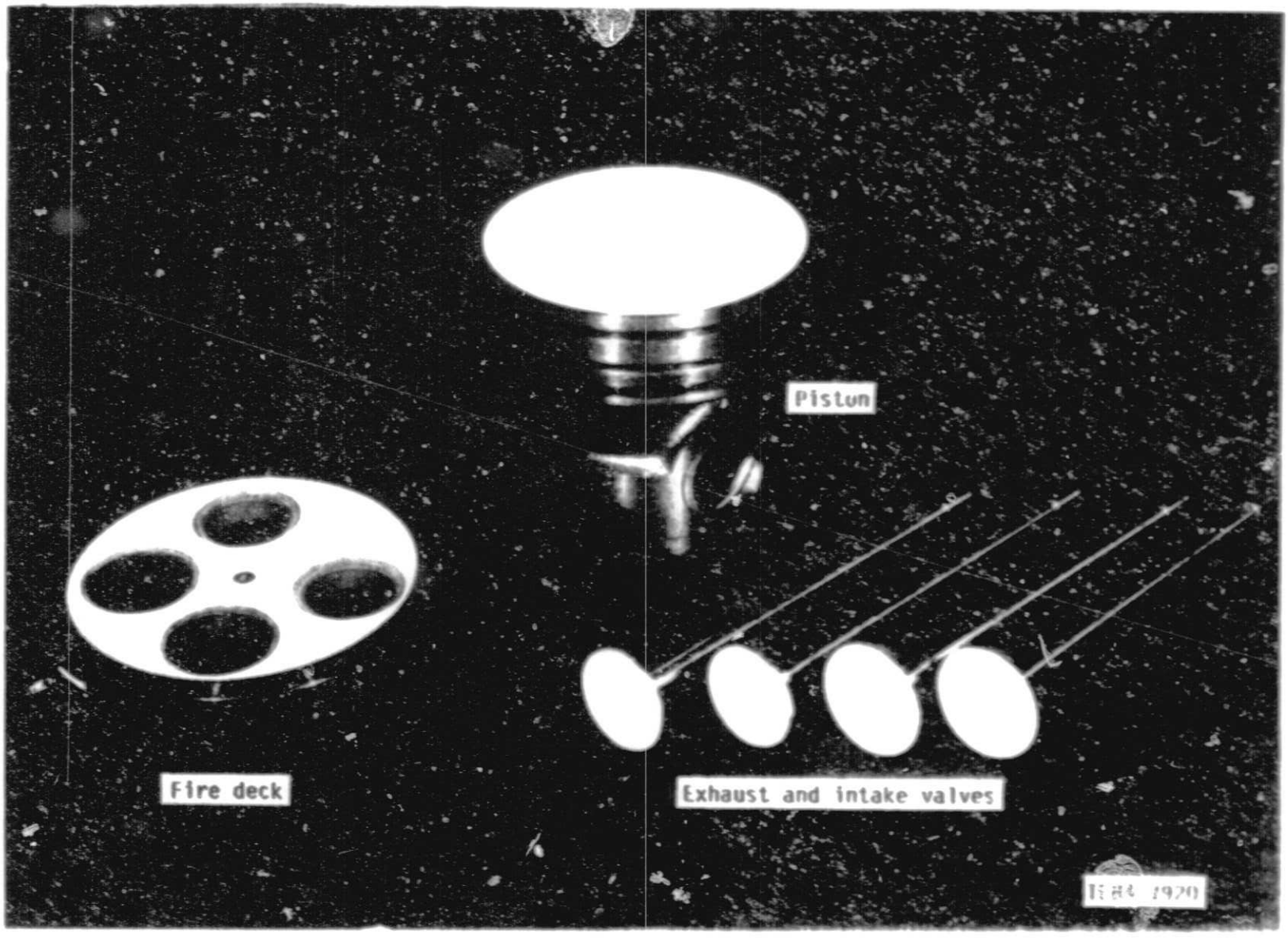

Figure 1. Engine components with applied thermal barrier coatings.

ORIGINAL PAGE IS
OF POOR QUALITY

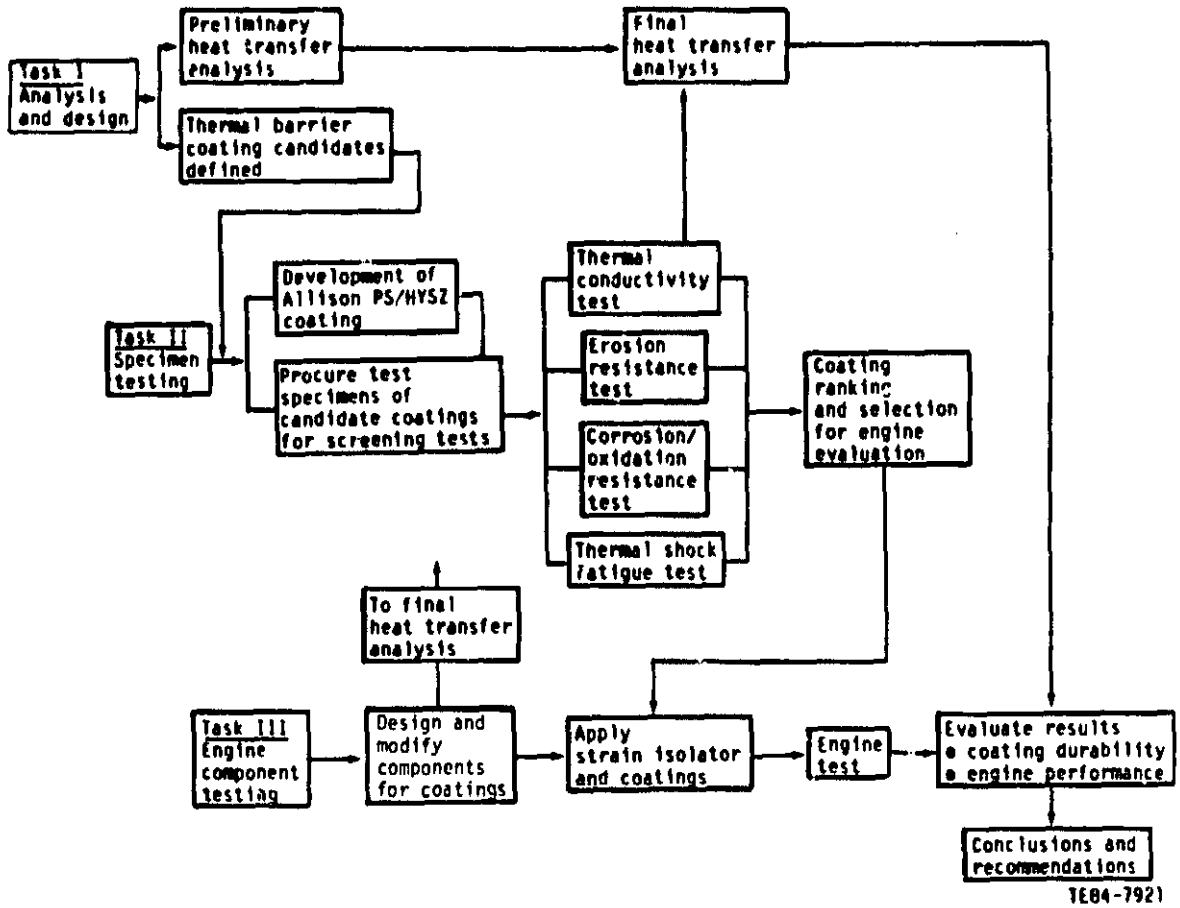

Figure 2. Program plan diagram.

on the exhaust valves). The coating system on the fire deck included an SI pad 1.02 mm (0.040 in.) thick giving a 2.54 mm (0.100 in.) total system thickness. The components were tested individually for 4 hr each and collectively until 24 hr total test time was accumulated on each component. Testing was conducted at power levels of 0.827 MPa to 1.172 MPa (120 lb/in.^{2} to 170 lb/in.^{2}) BMEP. Engine exhaust gas temperature and specific fire deck metal temperatures were compared for coated and uncoated components.

TEST ENGINE

A heavy-duty research single-cylinder engine was selected to test TBCs applied to the piston, fire deck, and valves. The engine selection was based on the following:

- The engine provides a relevant LHR operating environment in which to evaluate TBCs.
- The engine has demonstrated the ability to operate without water cooling continuously at power levels above that specified in this program (1.17 MPa [170 lb/in.^{2}] BMEP) so there is little risk of program delays due to engine-related problems.)

- o TBCs could be applied to the piston, fire deck, and valves with minimum redesign and minimum development of the metal hardware.
- o Engine was actively being used in an LHR engine program and available to this program.

The test engine was a 1.8 L (110 $in.^3$) displacement single cylinder version of a multicylinder heavy-duty diesel truck engine. The engine was of rugged construction and readily adaptable to different cylinder liner, piston, and head configurations. Its bore and stroke (130 mm and 139 mm [5.12 in. and 5.47 in.], respectively), operating speed (1000 rpm to 2300 rpm), and direct injection high pressure unit injector fuel system were typical of modern heavy-duty diesel truck engines. Typical components tested in the engine included the piston, piston rings, cylinder liners, cylinder head, valves, valve operating mechanism, and fuel injector.

The engine was connected to a motoring absorbing dynamometer. The engine had temperature-controlled fuel and lubricating systems, controlled temperature and pressure intake, and controlled pressure exhaust systems that permitted simulation of turbocharged or turbocompounded operation.

Standard instrumentation for speed, torque, fuel flow, exhaust temperature, etc was installed to determine the engine operating parameters and performance. In addition, the test stand was equipped to acquire data from specially instrumented components.

ENGINE TEST CONDITIONS

The thermal barrier coated components were tested from 0.83 MPa to 1.17 MPa (120 $lb/in.^2$ to 170 $lb/in.^2$) BMEP at 1300 and 1900 rpm. Table I shows the thermal and mechanical loading of the coated components tested in this program.

Table I.
Test conditions for TBCs on the single-cylinder research engine with NASA DEN3-326 coated components.

	Power	
	23.3 kW (31 hp)	34.5 kW (46 hp)
Speed--rpm	1300	1900
BMEP--MPa ($lb/in.^2$)	1.17 (169)	1.17 (170)
Air-fuel ratio	27.6	26.9
Average cycle gas temperature--°C (°F)	839 (1545*)	851 (1563*)

*Estimated

III. TASK I--ANALYSIS AND DESIGN

Task I was comprised of the following three primary activities:

- o design of coating envelope for engine components
- o selection of TBC systems to be evaluated in screening tests
- o heat transfer analysis of coated engine components

The TBC envelope on the piston, fire deck, and valves was defined in two steps. First, a preliminary study was conducted to determine the maximum coating system thickness (material removal) that could be accommodated on the existing engine components. Second, design modifications to the piston, fire deck, and valves were finalized after preliminary results from the TBC screening tests (Task II) were available and the SI pad geometry was defined.

Four basic TBC material compositions were identified for evaluation in the screening tests. Each system incorporated features intended to enhance durability with increased coating thickness. Three of the systems were also combined with an SI element to determine the performance of a coating system incorporating this unique feature. Ceramic coating and SI thickness trade-off and overall thermal effectiveness versus coating system thickness were investigated in the preliminary analysis in the early stages of the program. These results impacted the design of the SI pad.

Heat transfer analysis of the coating systems applied to the modified engine components was carried out in two steps--preliminary analysis and detailed final analysis. The total system thickness identified in the preliminary design of the coating envelope was used in the preliminary heat transfer analysis. The detailed final heat transfer analysis was completed after detailed designs of the modified engine components were completed, thermal conductivity of the coating system to be tested in the engine was determined (in Task II), and final specification of the SI pad design was determined.

The final heat transfer analysis calculated the operating temperatures of the coated engine components and the reduction in heat loss to surfaces in the cylinder.

3.1 PRELIMINARY DESIGN OF COATING SYSTEM ENVELOPE

The preliminary design of the coating system envelope was conducted to determine the maximum thickness of a coating system that could be applied to modified engine hardware. The modified piston, fire deck, and valves were designed to be interchangeable with uncoated components so the coated components could be tested individually as well as collectively. The design heat transfer and structural analyses conducted on the existing uncoated fire deck and piston of the LHR test engine were deemed appropriate for this program and were reviewed to determine how much material could be removed from the fire deck and piston to provide an envelope for a TBC.

Fire Deck

The uncoated metal LHR fire deck assembly used in this engine was fabricated of a high-strength alloy material, Waspaloy. Analysis of the fire deck design showed that up to 2.54 mm (0.100 in.) could be removed from the combustion

surface while maintaining adequate stress margin and minimal deflection (flexing). It was assumed that the coating system did not contribute to fire deck stiffness.

Piston

The preliminary study of the piston design showed that a coating up to 1.52 mm (0.060 in.) thick could be applied to the piston crown with minor modifications to the piston structure. Unlike the fire deck, the piston crown was designed originally to allow a minimum metal thickness in the combustion bowl region to maintain a low reciprocating mass. Therefore, a structural margin that would allow the substitution of a TBC in the amount planned in this program in place of the piston structure did not exist. The ability of the piston crown to provide a rigid substrate for the coating application was a major consideration in this analysis. The design review of the piston-connecting rod assembly for the test engine showed the connecting rod could be shortened by 1.52 mm (0.060 in). The shortened rod would lower the piston by 1.52 mm (0.060 in.) in the cylinder, leaving a space envelope for a TBC with an insignificant removal of material rom the piston combustion bowl surface. To accommodate a TBC thickness greater than 1.52 mm (0.060 in.) (such as the 2.54 mm (0.1 in.) thick coating that could be accommodated by the fire deck) a major redesign of the piston assembly would be required. This redesign would have entailed reducing the combustion bowl diameter (with a corresponding increase in bowl depth) and repositioning unmachined cast surfaces to maintain an adequate piston crown wall thickness. This approach was not pursued for two reasons. First, experience has shown that a reduced combustion bowl diameter would have a detrimental effect on engine performance. Second, a major piston design effort was beyond the scope of this program.

Valves

The structural analysis of the intake and exhaust valves showed deflection of the valve head under high-cylinder gas pressure loading to be the major consideration in determining how much material could be removed for the application of a TBC. To ensure the durability of the coating, the valve heads must remain rigid during engine operation. An analysis of the intake and exhaust valves showed that a coating of varied thicknesses would be required to maintain adequate valve head stiffness. Valve head deflection under cylinder gas pressure loads would be excessive if more than 0.51 mm (0.020 in.) of material were removed near the outside diameter (o.d.) of the intake valve and 0.76 mm (0.030 in.) from the exhaust valve. The practical maximum coating thickness in the center portion of the valves was about 1.52 mm (0.060 in.).

In summary, the results of this preliminary study showed the following:

- a coating up to 2.54 mm (0.100 in.) thick could be accommodated on the fire deck
- a coating up to 1.52 mm (0.060 in.) thick could be applied to the piston with minor redesign
- a coating of variabled thicknesses was required on the valves to retain adequate valve stiffness

3.2 COATING SYSTEM DESCRIPTION

The enhanced diesel TBC developed in this program built on coating technology developed at NASA and used in the thin coatings now in use. This technology included the following:

- o NiCrAlY bond coat--an oxidation resistant bond coat material with a high chrome content
- o plasma-sprayed (PS) coating--8% by weight yttria prestabilized zirconia powder
- o application of coating at low velocity and low power to create a porosity of 12%, which improves coating durability

The features required to ensure durability of the thicker coating include the following:

- o increased ability to withstand internal strains caused by increased thermal gradients
- o closed pore porosity to impede penetration of combustion contaminants

A unique method considered for isolating the ceramic coating from the metallic substrate was to place an SI between the coating and the substrate. The function of the SI was to accommodate thermal expansion mismatch between the coating and metal substrate, a common cause of coating separation.

Ceramic Coatings

Four developmental TBC compositions were evaluated in this program. Each of these four coatings incorporated specific characteristics intended to improve their durability with increased thickness. The coating candidate compositions were:

- o vendor coating A--YSZ
- o vendor coating B--calcia-stabilized zirconia
- o PS 80/20 SYSZ/Eccosphere coating
- o PS/HYSZ coating

The first, third, and fourth coating compositions were also evaluated in bench tests in combination with an SI element. Vendor coating B was not available on an SI. Thus, seven coating systems were evaluated and are listed in Table II.

Vendor Coating A and Vendor Coating B

Vendor coating A and vendor coating B are proprietary coatings that consist of vendor-modified zirconia powders to increase thermal shock resistance. Vendor coating A (system No. 1 and 2 in Table II) was a YSZ coating with a MgO secondary phase and was supplied with and without an SI element. Vendor coating B (system No. 3 in Table II) was a calcia-stabilized zirconia with a MgO secondary phase. Vendor coating B did not include an SI element.

The bond coats used in the two vendor coating systems were approximately 0.102 mm (0.004 in.) thick compared to 1.52 mm (0.006 in.) in the 80/20 SYSZ/ Eccosphere and PS/HYSZ coating systems described thereafter.

Table II.
Thermal barrier system composition matrix.

Thermal barrier system composition	SI treatment: None	SI treatment: 1.02 mm (0.040 in.,) thick
0.102 mm (0.004 in.) NiCrAlY bond coat, 1.42 mm (0.056 in.) vendor coating A	System 1	System 2
0.102mm (0.004 in.) NiCrAlY bond coat, 1.42 mm (0.056 in.) vendor coating B	System 3	Not recommended for use with SI pad
0.127-0.175 mm (0.005-0.007 in.) NiCrAlY bond coat, 0.254 mm (0.010 in.) SYSZ sublayer, 1.13 mm (0.044 in.) 80/20 SYSZ/Eccosphere coating	System 4	System 5
0.127-0.175 mm (0.005-0.007 in.) NiCrAlY bond coat, 0.254 mm (0.010 in.) SYSZ sublayer, 1.13 mm (0.044 in.) PS/HYSZ coating	System 6	System 7

Note: Coating system components listed in order of application

80/20 SYSZ/Eccosphere Coating

The 80/20 SYSZ/Eccosphere coating system (system No. 4 and 5 in Table II) used the NASA-developed NiCrAlY bond coat and an 88% dense solid yttria-stabilized zirconia (SYSZ) coating as a base coat for a PS combination of 80% (by volume) SYSZ and 20% hollow Eccosphere (alumino-silicate). The bond coat and sublayer SYSZ coating had a combined thickness of about 0.41 mm (0.016 in.). The 80/20 SYSZ/Eccosphere top layer filled out the remainder of the total coating system envelope. The 80/20 SYSZ/Eccosphere material provided the closed pore porosity characteristic desired of a diesel engine coating to prevent infiltration of combustion products. It did not, however, offer the reduced thermal conductivity characteristic of the hollow zirconia powder incorporated in the PS/HYSZ coating described hereafter, because the Eccosphere material has greater thermal conductivity than zirconia. The 80/20 SYSZ/Eccosphere coating system was evaluated both alone and in combination with an SI pad.

PS/HYSZ Coating

The PS/HYSZ coating system (system No. 6 and 7 in Table II) was a developmental coating combining a high chrome content NiCrAlY bond coat and SYSZ coating with a new HYSZ coating material. As in the 80/20 SYSZ/Eccosphere coating, the NiCrAlY bond coat and the 88% dense SYSZ coating served as a base coat on which the HYSZ coating was applied. Figure 3 is a scanning electron microscope (SEM)

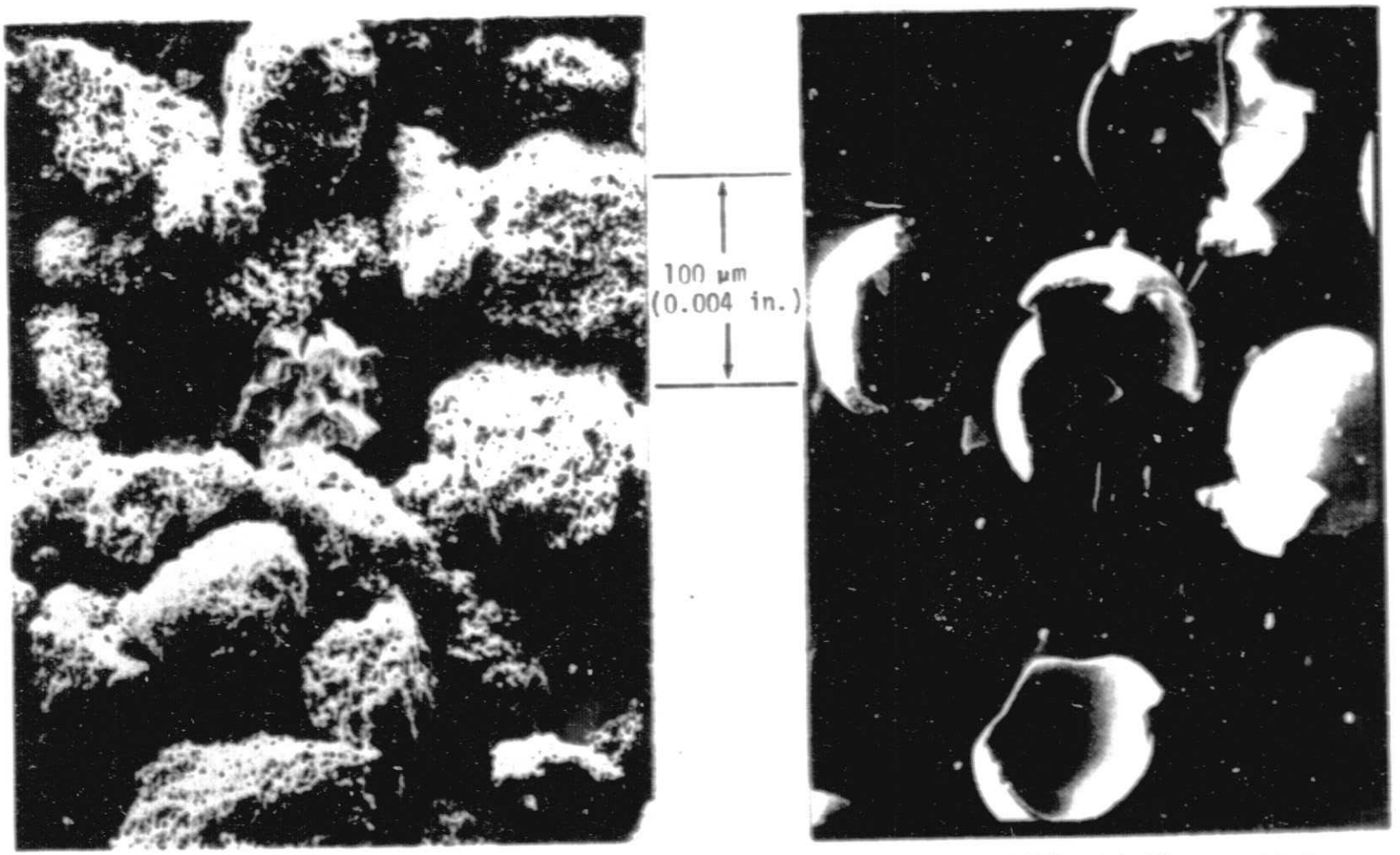

a. Prestabilized solid particle zirconia powder (8% by weight Y_2O_3)

b. prestabilized hollow particle zirconia powder (8% by weight Y_2O_3)

ORIGINAL PAGE IS
OF POOR QUALITY

Figure 3. Zirconia powder particle morphology.

photograph that shows HYSZ and SYSZ powder. The hollow particles pictured are intentionally fractured to illustrate the extremely thin walls of the particle. The goal of plasma-spraying the hollow particle powder is to preserve the morphology of the hollow particles through proper selection of PS parameters.

Figure 4 shows a schematic cross section of a PS/HYSZ coating system. The sintered-fiber metal SI element is included in the schematic for illustration purposes. The SI pad provides additional isolation between the thick ceramic coating and the metal substrate. The pad is composed of oxidation resistant Hoskins 875 metal fibers in a sintered configuration, which is 50% dense. The bond coat, nominally 0.15 mm (0.006 in.) thick with high chromium content NiCrAlY, provides a firm attachment base for the ceramic layers to follow. The bond coat, shown deposited on the SI pad, is applied to the substrate if the SI pad is not used. A normal density YSZ layer is applied to the bond coat. This layer is approximately 0.25 mm (0.010 in.) thick and nominally 88% dense. This 12% porosity allows the coating to accommodate some mismatch with the metallic substrate due to thermal expansion and provides a compatible surface for the attachment of the final TBC. The top layer of the coating system is the 8% percent by weight HYSZ coating.

The HYSZ powder has a dual effect on the characteristics of the coating system. First, it produces a closed pore coating structure compared with the open pore coating structure obtained with SYSZ powder. This closed pore structure results in a reduction in length or in the elimination of migratory paths into the coating through which combustion products can penetrate. At the same time, the strain relief characteristic of the open pore structure obtained with SYSZ powder is retained in the closed pore HYSZ powder coating. The second effect is a reduction in the thermal conductivity of the hollow particle layer compared with a solid particle layer due to the increased porosity of the HYSZ coating.

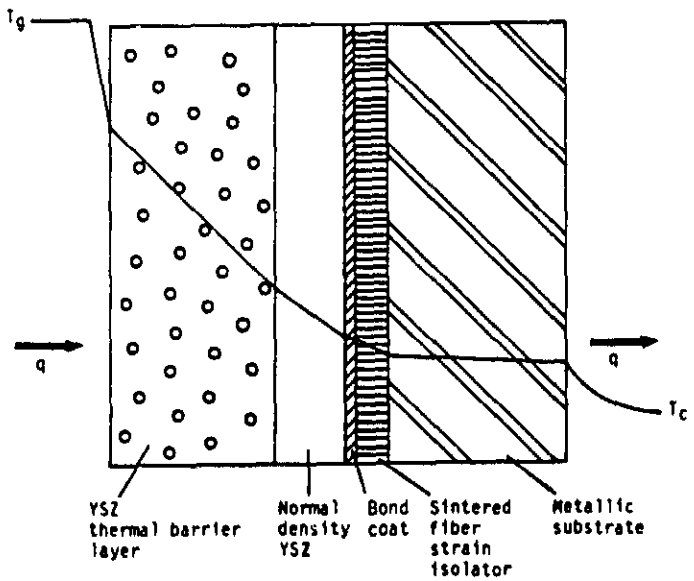

Figure 4. Thermal barrier coating cross section.

The PS/HYSZ coating system was evaluated both with and without an SI element.

3.3 HEAT TRANSFER ANALYSIS

Heat transfer analysis of the TBCs applied to the piston, fire deck, and valves was conducted in two phases: a preliminary heat transfer analysis and a final heat transfer analysis.

The preliminary heat transfer analysis was conducted on the piston, fire deck, and valves to determine the following:

- o the effect of the thickness of the SI as opposed to the thickness of the zirconia coating on the coating system's thermal effectiveness and on its combustion surface temperature
- o the effect of the thickness of the zirconia coating on thermal effectiveness and on combustion surface temperature

The estimated values of the thermal conductivity for the SI pad and zirconia coating were used in the preliminary heat transfer analysis as was a generalized definition of the coating system envelope on the engine components.

The final heat transfer analysis was conducted on the as-coated piston, fire deck, and valves to determine the following:

- o thermal effectiveness of the TBC
- o operating temperature of the coating surface
- o reduction in component metal temperature
- o temperature drop through coating systems

The final heat transfer analysis was accomplished after data unavailable for the preliminary heat transfer analysis were determined in other program activities. These data included the following:

- o thermal conductivity of the coating system selected for engine testing
- o final definition of the SI pad configuration
- o final definition of the coating system envelope on the piston, fire deck, and valves
- o definition of the engine test condition

3.3.1 General Approach to Heat Transfer Analyses

Heat transfer analysis of engine components was performed with two analytical tools: an engine cycle simulation model and a finite element method (FEM) heat transfer analysis program. The engine cycle simulation model calculated instantaneous and average engine operating parameters to predict engine performance for a total cycle. The calculated average gas temperature in the cylinder, heat transfer coefficients, and average component wall temperatures were used as boundary conditions in the FEM heat transfer analysis. The FEM heat transfer analysis calculated heat transfer data and operating temperatures on detailed two dimensional (2-D) and three-dimensional (3-D) engine component models of the piston, fire deck, and valves.

Engine Simulation Model

The engine cycle simulation model calculated engine airflow, combustion rate, and heat transfer between combustion gas and walls in the cylinder on a crank angle by crank angle basis to calculate engine performance for a total cycle. The heat transfer model within the cycle simulation model was a one-dimensional (1-D) network of connected nodes that represented the combustion chamber walls. This thermal circuit was used to calculate single point temperatures on the piston, fire deck, and valves and at three vertical locations on the cylinder liner. FEM heat transfer analysis of the piston, fire deck, and valves was conducted in an iterative manner with the cycle simulation model to converge calculated average component wall temperatures. In this manner the 1-D heat transfer model within the engine cycle simulation model was tuned to the hardware configuration being investigated. The cycle average gas temperature, average heat transfer coefficients, exhaust gas temperature, and wall temperatures in the cylinder, all of which were calculated in the engine cycle simulation model, were used as thermal boundary conditions in the detailed FEM heat transfer analysis of the engine components.

Heat Transfer FEM Analysis

The FEM heat transfer analysis program calculated component local temperatures based on the boundary condition data from the engine cycle simulation program. The FEM heat transfer analysis program used FEMs of the fire deck, piston, and valve shown in Figures 5, 6, and 7, respectively. The fire deck model shown in Figure 5 was a 3-D model of one-half of the fire deck assembly and supporting head structure. The fire deck, the steel fire deck retaining ring, the steel plate above the fire deck, and the inner and outer insulation supports above the fire deck ring assembly are included in this model. Experience in the LHR diesel engine program showed that the 3-D model of the fire deck gave more accurate results when compared with a 2-D model. Factors contributing to this state are the temperature gradient from intake to exhaust side, the non-axisymetric configuration of the fire deck, and the differing thermal boundary conditions in the intake and exhaust port openings.

The piston model, shown in Figure 6, was a 2-D, axisymmetric model that includes the Ni-Resist crown, the piston base or body, and the fire ring (upper compression ring). The intake and exhaust valve models shown in Figure 7 were also axisymmetric models. Two-dimensional axisymmetric models were used for the piston and valves because the components are axisymmetric and the thermal and structural load boundary conditions imposed in the analysis were also 2-D.

3.3.2 Preliminary Heat Transfer Analysis

Preliminary heat transfer analysis was conducted on the piston, fire deck, and valves by using the engine cycle simulation model and FEM heat transfer analysis program to determine the following:

- o the effect of SI/zirconia coating thickness trade-off on thermal effectiveness and combustion surface temperature
- o the effect of zirconia coating thickness on thermal effectiveness and combustion surface temperature

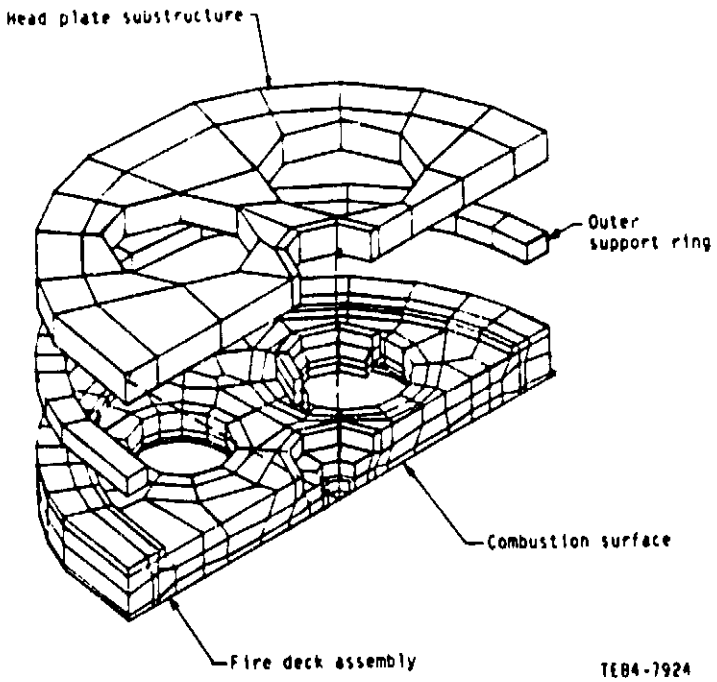

Figure 5. Three-dimensional low heat rejection finite element model of the fire deck assembly.

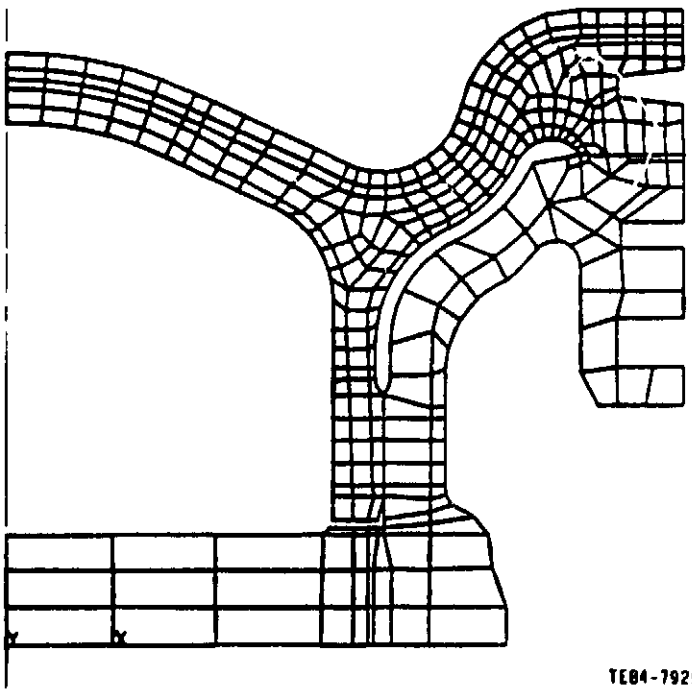

Figure 6. Two-dimensional axisymmetrical finite element model of the piston.

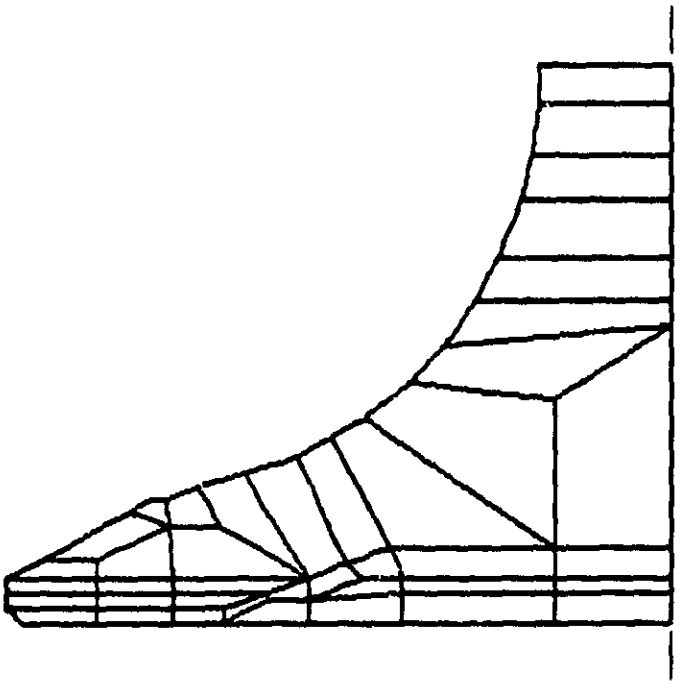

a. Intake valve

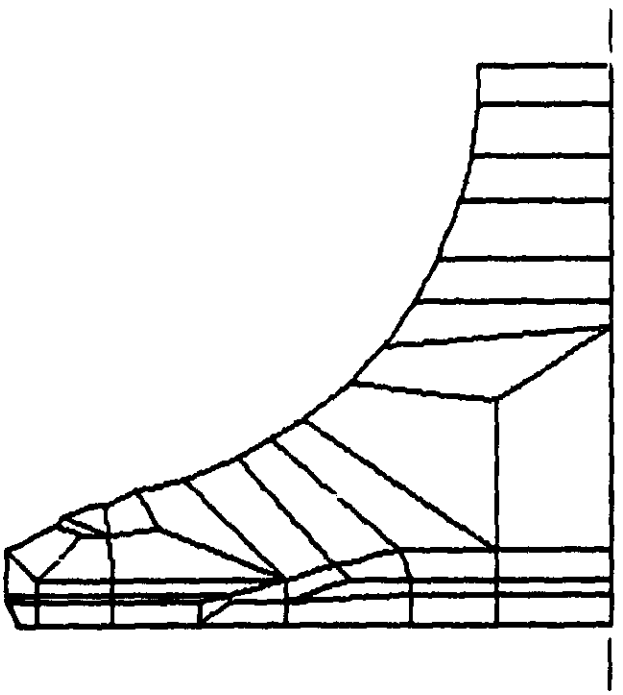

b. Exhaust valve

TE84-7926

Figure 7. Two dimensional axisymmetrical finite element models of the valves.

Three coating system geometries, all with up to 2.54 mm (0.100 in.) total thickness, were analyzed as follows:

- o 1.52 mm (0.060 in.) thick SI pad with up to 1.02 mm (0.040 in.) thick zirconia coating
- o 1.02 mm (0.040 in.) thick SI pad with up to 1.52 mm (0.060 in.) thick zirconia coating
- o up to 2.54 mm (0.100 in.) thick zirconia coating without an SI pad

The maximum total coating system thickness of 2.54 mm (0.100 in.) was based on the results of the preliminary coating system envelope study discussed in section 3.1. In that study, 2.54 mm (0.100 in.) was found to be the maximum possible coating thickness on the modified fire deck. In the preliminary heat transfer analysis, the 2.54 mm (0.100 in.) coating thickness was also evaluated on the piston for the following reasons.

First, the study to determine the effect of the SI/zirconia coating thickness trade-off on thermal effectiveness could be accomplished more effectively by conducting the analysis with the 2-D axisymmetrical FEM heat transfer analysis of the piston instead of the more complex 3-D analysis of the fire deck. This method was used because less effort was required to construct and modify the 2-D piston model and thermal boundary conditions for the various coating configurations and because less computer time was required to complete the 2-D FEM heat transfer calculations than the 3-D FEM calculations.

The study to determine the effect of varying zirconia coating thicknesses on thermal effectiveness was also conducted more efficiently with the 2-D FEM heat transfer analysis of the piston for the same reasons. Following the detailed analysis of the piston, calculations were made for specific coating thickness configurations on the fire deck and valves. The second reason for evaluating the 2.54 mm (0.100 in.) coating on the piston was that the results of the study would allow a direct comparison of identical coating systems on all of the engine components.

Thermal conductivity data for the zirconia coating and SI pad were estimated for the preliminary heat transfer analysis because data from thermal conductivity testing in Task II were not yet available and the design of the SI pad was not finalized. The thermal conductivity assumed for the zirconia coating was 1.37 W/m °C (0.066 Btu/hr-in-°F). This assumption was based on an estimated coating porosity and nominal monolithic zirconia properties. The thermal conductivity of the SI pad was estimated to be 11.4 to 12.5 W/m-°C (0.55 to 0.60 Btu/hr-in-°F). This estimate was based on vendor data for a 25% dense pad.

3.3.2.1 Results of the SI/Zirconia Coating Thickness Trade-Off

Two coating system configurations incorporating an SI pad were analyzed to determine the effect of SI pad thickness on overall thermal barrier system thermal effectiveness and on combustion surface temperature. Each coating system was analyzed for total thicknesses up to 2.54 mm (0.100 in.). Thermal effectiveness is defined as follows:

$$\frac{\text{Baseline component heat loss - Coated component heat loss}}{\text{Baseline component heat loss}} \times 100$$

Figures 8 and 9 show the thermal effectiveness and average combustion surface temperature for coating systems using 1.02 mm or 1.52 mm (0.040 in. or 0.060 in.) thick SI pads covered by PSZ coatings varying in thicknesses up to 2.54 mm (0.100 in.). The figures and Table III show that for a total coating-pad thickness of 2.54 mm, the case II system with the thinner 1.02 mm (0.040 in.) pad provides 32% greater thermal effectiveness and 16°C (28°F) higher piston average surface temperature than the case I system with the 1.52 mm (0.060 in.) pad. In other words, if the total thermal barrier system thickness is fixed a system with the thinnest SI pad will have the greatest thermal effectiveness. Conversely, in a system using a fixed zirconia coating thickness, the thermal effectiveness is greater with a thicker pad.

Table III.
Summary of the preliminary heat transfer analysis of the piston for specific coating system thicknesses.

Case	Heat loss--kW (Btu/min)	Thermal effectiveness--%	Average surface temperature--°C (°F)
Baseline (no coating)	1.66 (105.7)	--	485 (905)
I (1.02 mm [0.040 in.] zirconia coating/1.52 mm [0.060 in.] SI)	1.59 (90.6)	14.3	533 (991)
II (1.52 mm [0.060 in.] zirconia coating/1.02 mm [0.040 in.] SI)	1.51 (85.7)	18.9	548 (1019)
III (2.54 mm [0.100 in.] zirconia coating)	1.33 (75.7)	28.3	580 (1076)

3.3.2.2 Zirconia Coating Thickness Versus Thermal Effectiveness

The analysis of a case III system was conducted to evaluate the effect of the coating thickness on thermal effectiveness and the average combustion surface temperature. The case III system did not incorporate a SI pad. For case III, calculations were made for coating thicknesses up to 2.54 mm (0.100 in.). Figures 10 and 11 show the trend of increasing thermal effectiveness and of increasing average surface temperature of the piston with increasing coating thickness. Figure 10 shows that the thermal effectiveness of a 1.52 mm (0.060 in.) thick coating is 18% and increases to 28.3% at 2.54 mm (0.100 in.). Figure 11 shows that the average surface temperature of the piston increases from 485°C (905°F) without a coating to 546°C (1016°F) with a 1.52 mm (0.060 in.) thick coating and to 580°C (1076°F) with 2.54 mm (0.100 in.) thick coating. A summary of the heat transfer analysis on the piston for specific coating system thicknesses is shown in Table III.

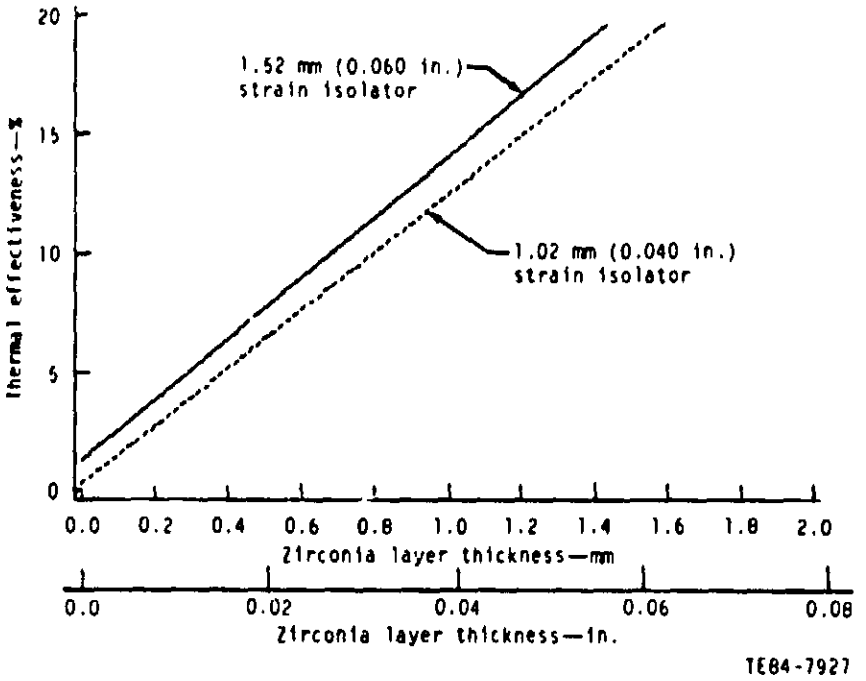

Figure 8. The effect of the thickness of the strain isolator on the thermal effectiveness of the thermal barrier coating on the piston.

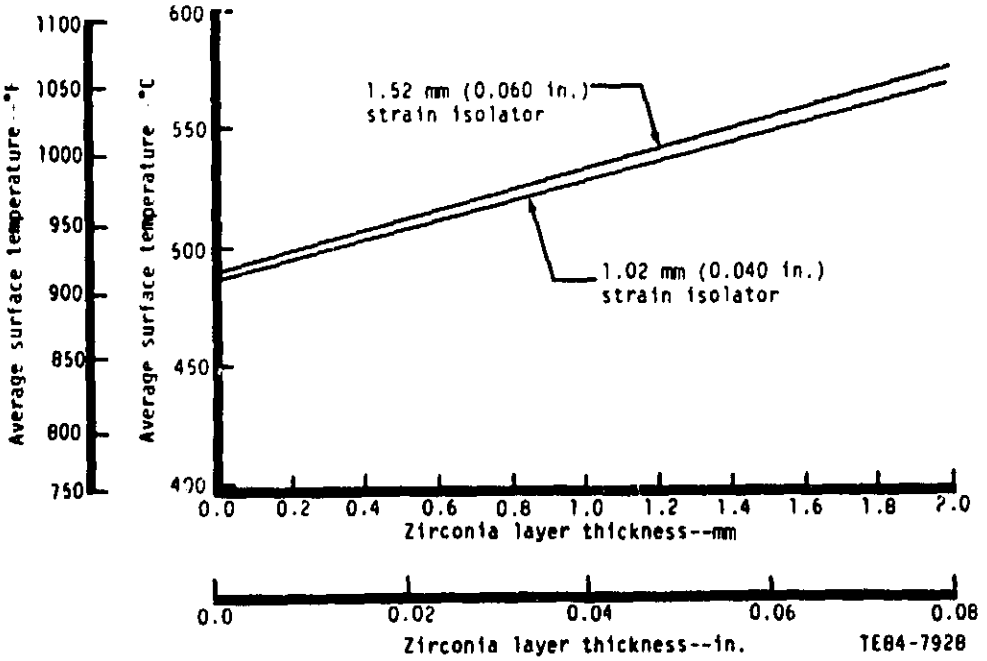

Figure 9. The effect of the thickness of the strain isolator on the surface temperature of the thermal barrier coating on the piston.

The fire deck and valves were analyzed also with the same coating configurations as described for the piston. The same general effects seen in the piston analysis were also observed in the results for the fire deck and valves. Table IV shows a summary of the preliminary heat transfer analysis results for specific coating configurations on the fire deck. Table V shows a summary of results for the intake and exhaust valves.

Table IV.
Summary of the preliminary heat transfer analysis of the fire deck for specific coating system thicknesses.

Case	Heat loss--kW (BTu/min)	Thermal effectiveness--%	Average surface temperature--°C (°F)
Baseline (no coating)	1.00 (56.88)	--	467.4 (873.3)
I (1.5 mm [0.060] YSZ/ 1.0 mm [0.040] SI)	0.902 (51.38)	9.8	516.1 (961.0)
II (2.5 mm [0.100] YSZ)	0.836 (47.16)	17.2	551.3 (1024.3)

Table V.
Summary of the preliminary heat transfer analysis of the intake and exhaust valves for specific coating system thicknesses.

	Heat loss--kW (Btu/min)		Thermal effectiveness--%		Average surface temperature--°C (°F)	
Case	Intake	Exhaust	Intake	Exhaust	Intake	Exhaust
Baseline (no coating)	0.233 (13.27)	0.142 (8.11)	---	---	381 (717)	502 (936)
I (1.0 mm [0.040 in.] YSZ/1.5 mm [0.060 in.] SI)	0.205 (11.64)	0.115 (6.53)	12.3	19.5	436 (316)	565 (1049)
II (1.5 mm [0.060 in.] YSZ/ 1.0 mm [0.040 in.] SI)	0.202 (11.51)	0.112 (6.39)	13.3	21.2	440 (824)	571* (1060)
III (2.5 mm [0.100 in.] YSZ)	0.193 (10.97)	0.106 (6.03)	17.3	25.6	458 (857)	586 (1086)

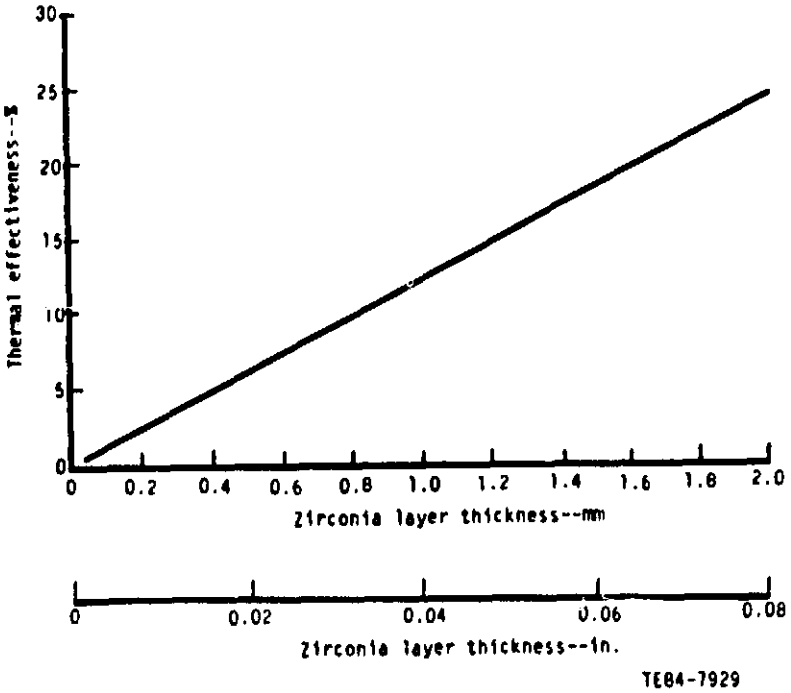

Figure 10. The effect of the thickness of the thermal barrier coating on the thermal effectivness of the piston.

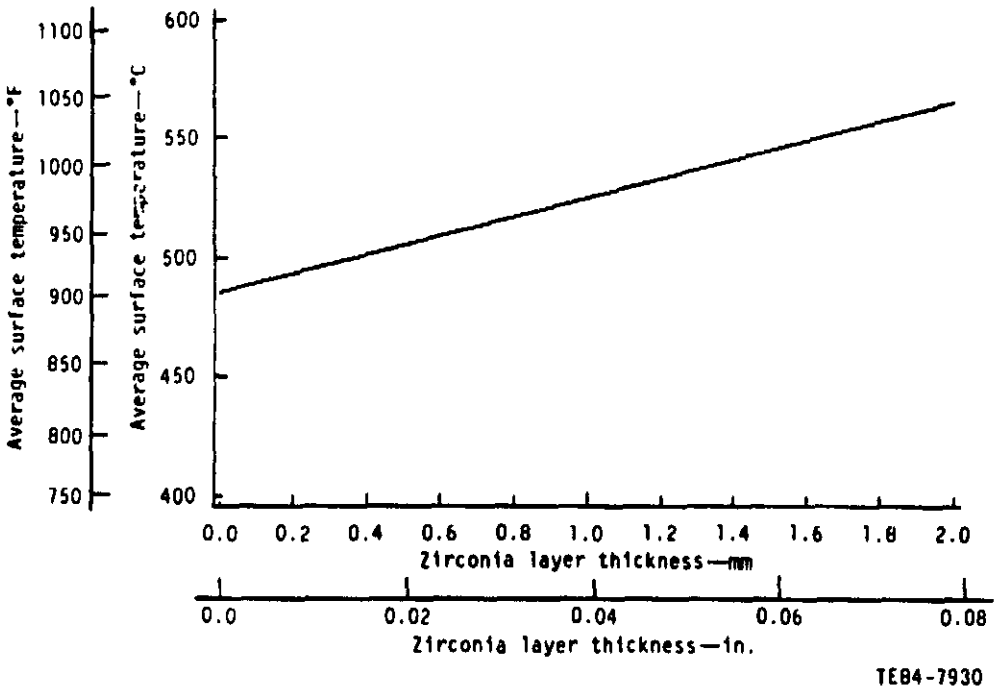

Figure 11. The effect of the thickness of the thermal barrier coating on the surface temperature of the piston.

The results of the preliminary heat transfer analysis show the following:

- o The case II thermal barrier system consisting of a 1.02 mm (0.040 in.) thick SI pad and 1.52 mm (0.060 in.) thick zirconia coating would be 32% more thermally effective than the case I coating system when applied to the piston.
- o The thermal effectiveness of the case II coating when applied to the fire deck would be 9.8% and the fire deck average surface would increase 49°C (88°F).
- o If, hypothetically, the zirconia coating thickness would be increased from 1.52 mm (0.060 in) to 2.54 mm (0.100 in.), it would result in an increase in the average surface temperature of the piston by 32°C (58°F), the fire deck would increase by 35°C (63 F), and the valves by about 17°C (30°F).
- o The SI pad is relatively ineffective in comparison with the zirconia coating in improving the thermal effectiveness characteristics of the coating system. Therefore, from a thermal effectiveness standpoint, a pad of minimal thickness is desirable.

3.3.3 Final Heat Transfer Analysis of Engine Components

3.3.3.1 Approach

Final heat transfer analyses of the tested coated piston, fire deck, and valve configurations were completed using the same approach as used in the preliminary heat transfer analysis. An engine cycle simulation model and FEM heat transfer analysis program were used in combination to complete the analysis of the piston, fire deck, and valves as tested in Task III.

The final analysis was accomplished after data unavailable for the preliminary heat transfer analysis were determined in other program activitites. These data included the following:

- o thermal conductivity of the coating system selected for engine testing
- o final definition of the SI pad configuration
- o final definition of the coating system envelope on the piston, fire deck, and valves
- o definition of the engine test condition for component design and analysis

Zirconia Coating Thermal Conductivity

A thermal conductivity value of 0.865 W/m °C (0.042 Btu/hr-in.-°F) was used for the zirconia coating in the final heat transfer analyses. This value was based on results of the thermal conductivity tests conducted in Task II.

Design Engine Test Condition

A single engine operating condition was selected for the final heat transfer and cycle simulation analysis. The engine operating condition was as follows:

- o speed--3600 rpm
- o power--34.3 kW (46 hp)
- o BMEP--1.17 MPa (170 lb/in.^{2})
- o air/fuel ratio--33.4
- o fuel flow rate--6.53 kg/h (14.4 lb/hr)
- o intake pressure--220 kPa absolute (32 psia)

- o exhaust pressure--220 kPa absolute (32 psia)
- o engine configuration--uncooled cylinder liner, uncooled head, LHR piston

3.3.3.2 Final Piston Heat Transfer Analysis

Temperatures were calculated for coated and uncoated pistons using the finite element analysis model shown in Figure 6. A layer of elements at the combustion chamber surface was used to model the coating and appropriate coating thermal conductivity values.

Heat transfer analysis results of a 1.52 mm (0.060 in.) thick coating applied to the LHR piston are summarized in Table VI. This coating is the nominal coating thickness tested on the piston in Task III. Isotherm plots for a coated and an uncoated baseline piston are shown in Figures 12 and 13, respectively. A 107°C (192°F) temperature drop was calculated across the low thermal conductivity coating, as shown by the closely grouped isotherm lines in the coating layer in Figure 12.

Table VI.
Summary of the final piston heat transfer results.

Configuration	Average surface temperature--°C (°F)	Heat loss--kW (Btu/min)	Thermal effectiveness--%
Uncoated (baseline)	474 (885)	1.58 (90.00)	---
1.52 mm (0.060 in.) PSZ coating (tested configuration)	536 (996)	1 27 (72.38)	20%

In addition to increased surface temperature, another result of using a TBC is reduced metal temperature below the coating for the same engine operating condition. Data in Table VII quantities this metal temperature reduction for the coated piston. The metal temperatures listed are at the combustion chamber surface of the uncoated piston and at the surface just below the coating layer of the coated pistons. The average metal surface temperature was reduced 45°C (81°F) with the 1.52 mm (0.060 in.) coating. Comparison of the isotherm lines shown in Figures 12 and 13 illustrates the reduction in metal temperature throughout the piston assembly when the 1.52 mm (0.060 in.) coating is applied.

Table VII.
Reduction in the metal temperatures of the piston due to the TBC.

Condition	Metal temperatures--°C (°F) Maximum	Average
Uncoated piston	544 (1012)	474 (885)
1.52 mm (0.060 in.) PSZ coating (tested configuration)	518 (965)	429 (804)

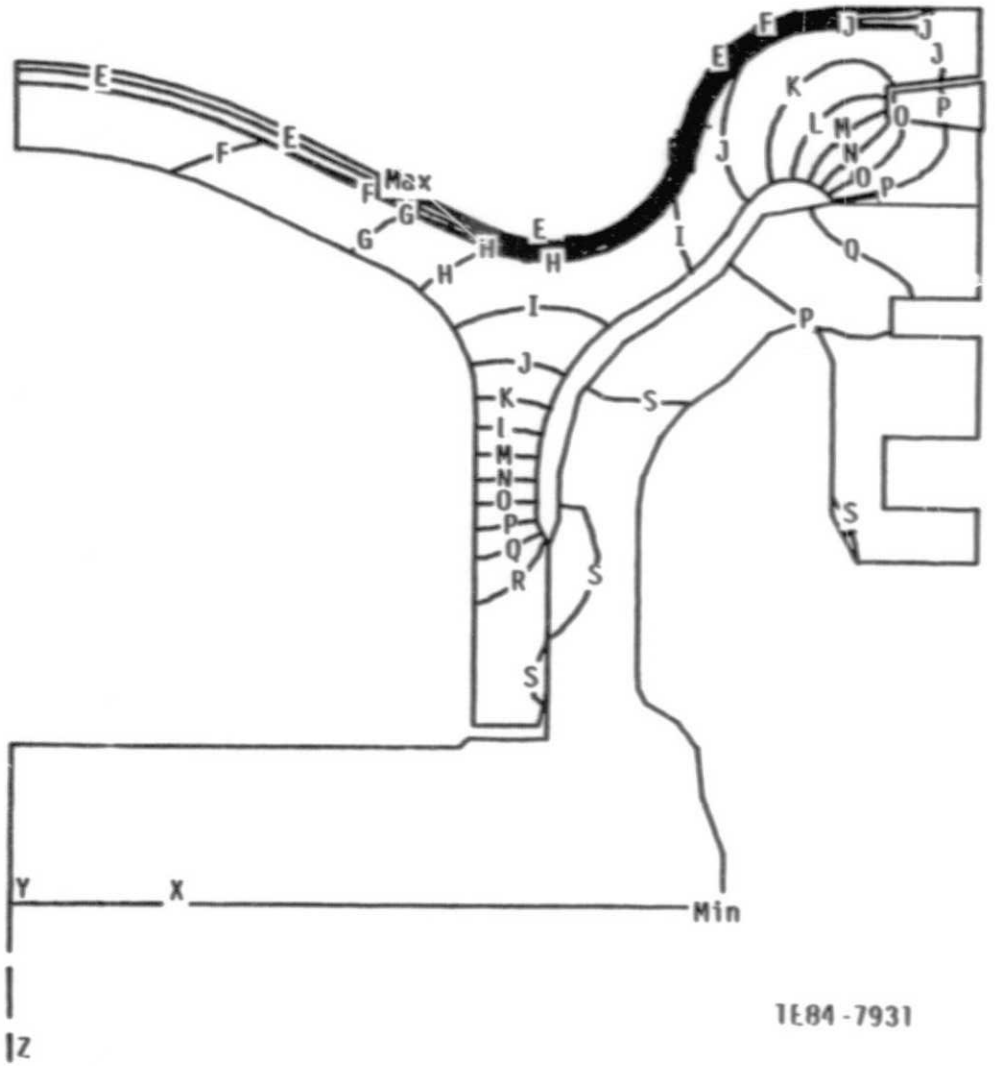

1E84-7931

Legend

	°C	°F
A	648.89	1200.0
B	621.11	1150.0
C	593.33	1100.0
D	565.56	1050.0
E	537.78	1000.0
F	510.00	950.0
G	482.22	900.0
H	454.44	850.0
I	426.67	800.0
J	398.89	750.0
K	371.11	700.0
L	343.33	650.0
M	315.56	600.0
N	287.78	550.0
O	260.00	500.0
P	232.22	450.0
Q	204.44	400.0
R	176.67	350.0
S	148.89	300.0
T	121.11	250.0
Max	565.39	1049.7
Min	127.35	261.2

Figure 12. Contour plot of temperatures in a coated piston.

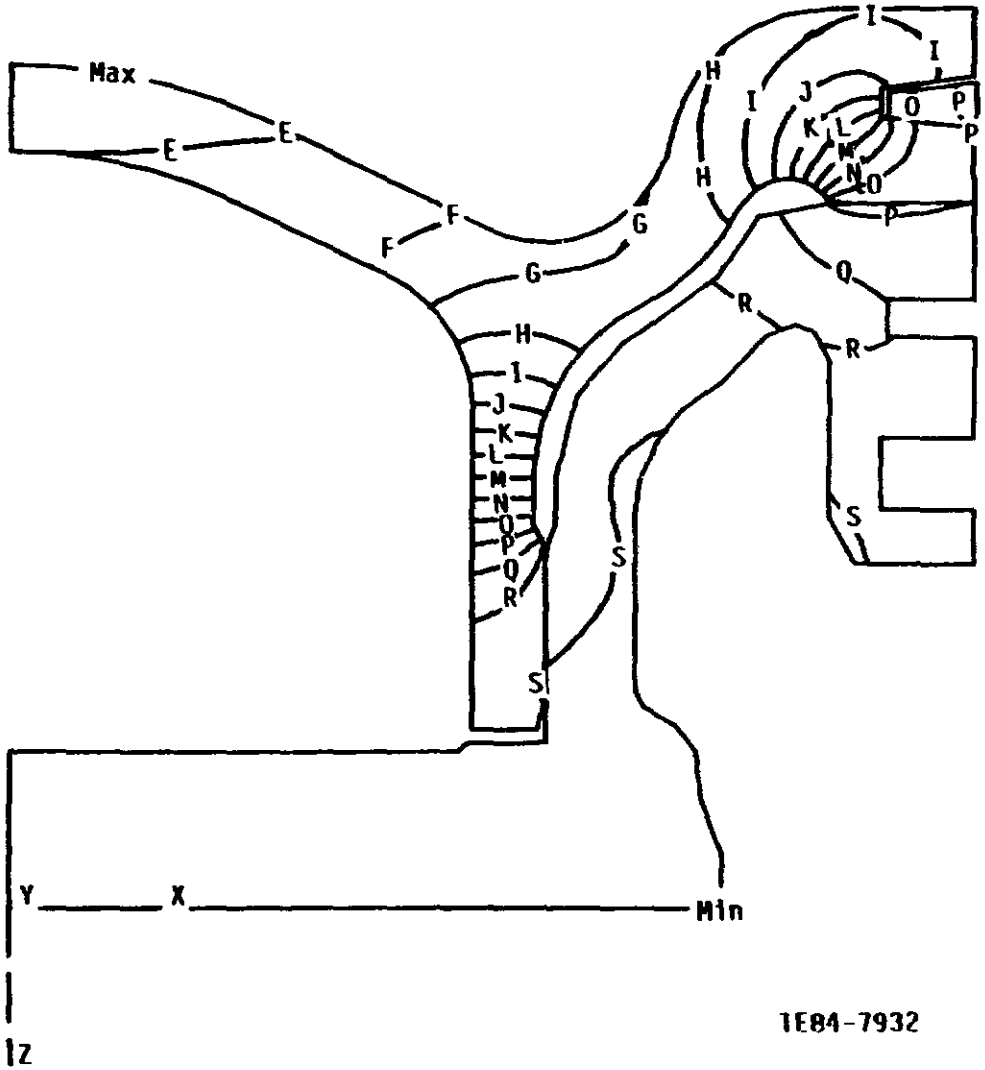

Legend

	°C	°F
A	648.89	1200.0
B	621.11	1150.0
C	593.33	1100.0
D	565.56	1050.0
E	537.78	1000.0
F	510.00	950.0
G	482.22	900.0
H	454.44	850.0
I	426.67	800.0
J	398.89	750.0
K	371.11	700.0
L	343.33	650.0
M	315.56	600.0
N	287.78	550.0
O	260.00	500.0
P	232.22	450.0
Q	204.44	400.0
R	176.67	350.0
S	148.89	300.0
T	121.11	250.0
Max	544.57	1012.2
Min	127.93	262.3

Figure 13. Contour plot of temperatures in an uncoated piston.

The TBCs tested in this program were applied to modified components of a LHR engine that operated without water coolant. This approach was chosen because this engine provided a reliable LHR environment in which to evaluate the advanced TBCs. The final heat transfer analysis shows the effect of the TBCs applied to these LHR components. Once an advanced coating has been successfully demonstrated in such an engine, the coating technology can be used in an advanced engine design in which the advantages of the coating's potential can be enhanced.

A detailed review of the final heat transfer analysis reveals several locations in the engine where TBCs could be used to advantage. For example, the analysis of the fire deck showed effects of heat transfer to the intake air charge and from the exhaust gas in the port regions of the head. Thermal barrier treatments to these regions would improve both heat retention in the exhaust gas and volumetric efficiency of the engine.

The heat transfer calculations on the valves revealed that coating the port side of both the intake and the exhaust valves would also improve heat retention in the exhaust gas and volumetric efficiency of the engine. Other possible locations in the engine where TBCs would enhance engine performance and reliability include the cylinder liner and the surfaces outside the combustion chamber. Coating these surfaces would prevent heat transfer from one component to another. For example, the fire deck could be insulated from the upper cylinder head structure and/or the cylinder liner.

The heat transfer analysis results discussed previously describe calculated changes in component temperatures (increased combustion surface temperature and reduced metal temperatures) for a constant engine operating (power) condition. Another approach to the use of TBCs would be to increase the power rating of an engine by increasing fuel flow to a point where the component metal temperatures were equal to those of an uncoated component.

To investigate this approach, an analysis was conducted on the piston used in this program. The results, shown in Figure 14, reveal that if the maximum metal temperature of the piston (about 543°C [1010°F]) was maintained, the engine power rating could be increased 16% (from 205 kW to 239 KW [from 275 hp to 320 hp]). Based on the average crown surface temperature of the piston (about 471°C [880°F]), the engine power rating could be increased 33% (from 205 kW to 273 kW [from 275 hp to 366 hp]).

3.3.3.3 Final Fire Deck Heat Transfer Analysis

The final fire deck heat transfer analysis was accomplished using the engine cycle simulation model in combination with the heat transfer FEM analysis program. Fire deck temperatures were calculated using the 3-D FEM model shown in Figure 5. The 3-D model was necessary because of the nonsymmetry of the part and severe intake-to-exhaust side thermal gradient. The fire deck configuration incorporated the coating system selected for engine testing (Task III). This coating system was comprised of a 1.02 mm (0.040 in.) thick SI pad coated with a 1.52 mm (0.060 in.) thick PS/HYSZ coating (system No. 7 in Table II). The total TBC system thickness is 2.54 mm (0.100 in.). The thermal FEM of the coated fire deck included two additional layers of elements representing the SI pad and the zirconia coating.

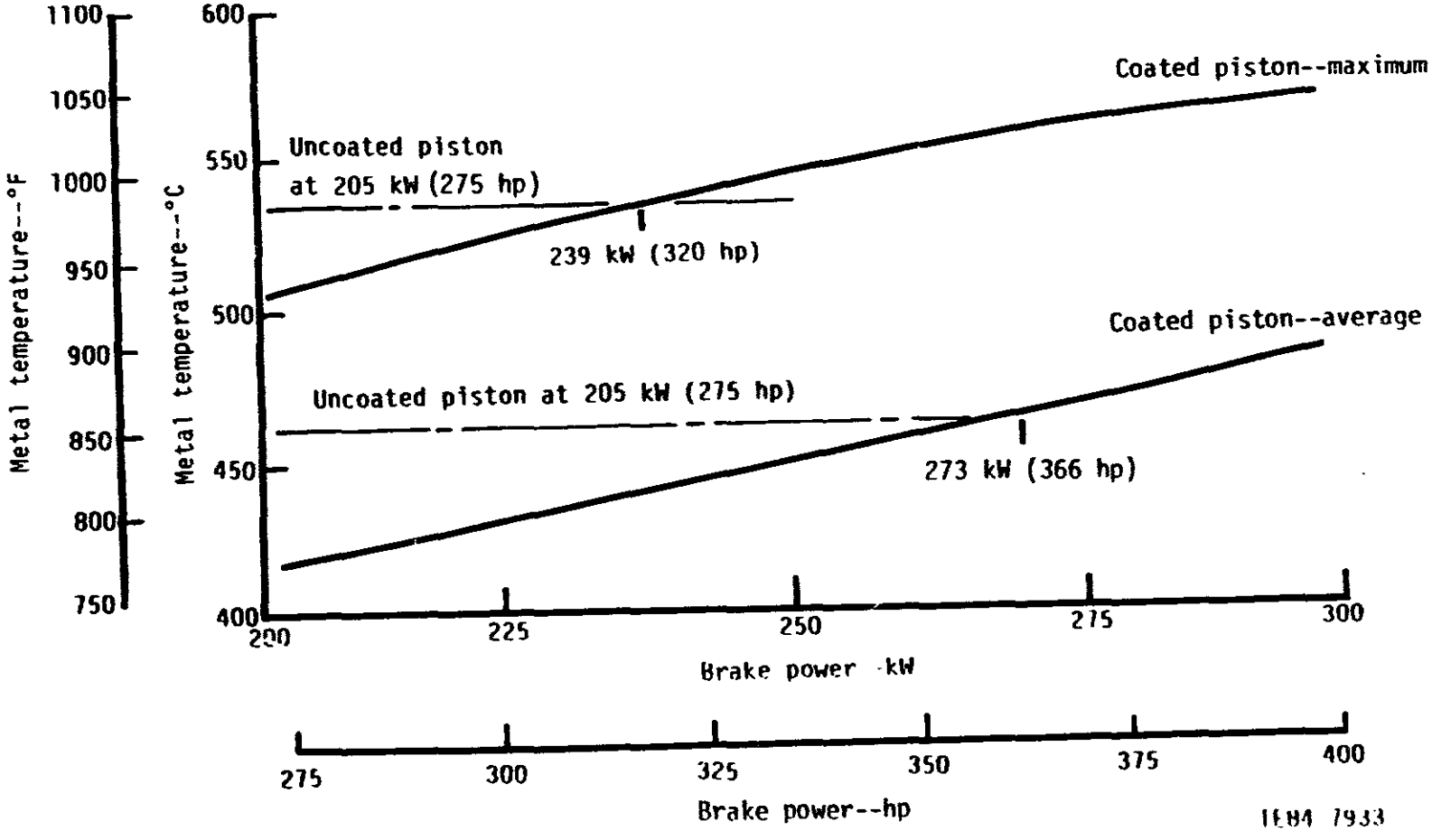

Figure 14. Metal temperatures of the piston versus engine power.

Calculated isotherm lines in the fire deck incorporating the 1.02 mm (0.040 in.) SI/1.52 mm (0.060 in.) PS/HYSZ coating system are shown in Figure 15 and in the uncoated baseline fire deck in Figure 16.

The maximum surface temperature of the coated fire deck and the average temperature of the coated surface were 649°C and 548°C (1201°F and 1018°F), respectively, compared with 597°C and 500°C (1107°F and 932°F), respectively, on the uncoated fire deck. The calculated average temperature drop through the complete coating system (SI pad and coating) was 101°C (181°F), and the heat loss to the coated fire deck was 12.8% less than to the uncoated fire deck. The final fire deck heat transfer analysis results are summarized in Table VIII. The baseline configuration for the thermal effectiveness calculations was the uncoated, uncooled fire deck. The maximum and average metal surface temperatures of the fire deck for the coated and uncoated fire deck are shown in Table IX. Maximum and average surface temperatures of the fire deck are reduced 43°C and 53°C (77°F and 95°F), respectively, with the 2.54 mm (0.100 in.) thick SI-PS/HYSZ coating system applied.

Table VIII.
Summary of the final fire deck heat transfer analysis results.

Configuration	Average surface temperature--°C (°F)	Heat loss--kW (Btu/min)	Thermal effectiveness--%
Uncooled, uncoated (baseline)	500 (932)	0.77 (43.94)	--
2.54 mm (0.100 in.) SI-PS/HYSZ coating (tested configuration)	548 (1018)	0.67 (38.30)	12.8

Table IX.
Reduction in the metal temperatures of the fire deck due to TBCs.

Condition	Metal Temperatures--°C (°F) Maximum	Average
Uncoated fire deck	597 (1107)	500 (932)
2.54 mm (0.100 in.) SI-PS/HYSZ coating (tested configuration)	554 (1030)	447 (837)

The exhaust-to-intake side thermal gradient is shown in the isotherm plots for both fire decks (Figures 15 and 16). The maximum surface temperature occurs between the exhaust ports on the combustion surface. At a similar location on the intake side, the surface temperature was approximately 280°C (500°F) lower.

3.3.3.4 Final Intake and Exhaust Valve Heat Transfer Analysis

The final heat transfer analysis was conducted on coated intake and exhaust valves and on standard, uncoated metal intake and exhaust valves using the engine cycle simulation model in combination with the FEM heat transfer analysis program. Valve FEM models, shown in Figure 7, were used in the final heat transfer analysis. The coating system modeled (and tested in Task III) on the valves was a 1.52 mm (0.060 in.) thick (tapered to 0.51 mm (0.020 in.) on the intake valves and 0.76 mm (0.030 in.) on the exhaust valves) PS/HYSZ coating (system No. 6 in Table II).

Calculated isotherm lines in the coated and uncoated intake valves are shown in Figure 17 and in the exhaust valves in Figure 18. The isotherm lines show the effect on valve temperatures of the varied thicknesses of the coatings and on the intake air flow and exhaust gas flow on the reverse side of the valves.

The average combustion surface temperature increased 95°C (167°F) on the coated intake and 69°C (124°F) on the coated exhaust valves. The maximum combustion surface temperature increased 110°C (198°F) on the intake valve and 57°C (103°F) on the exhaust valve in the region where the full 1.52 mm (0.060 in.) thick coating existed. The heat lost to the intake and exhaust valves was reduced 15.8% and 21%, respectively, by the TBC. The heat transfer analysis results for both valves are summarized in Tables X and XI.

Table X.
Summary of the final intake and exhaust valve heat transfer analysis results.

Configuration	Average surface temperature--°C (°F)	Heat loss--kW (Btu/min) for two valves	Thermal effectiveness--%
Intake valve			
Uncoated	380 (717)	0.47 (26.6)	
1.52 mm (0.060 in.) PS/HYSZ coating	451 (844)	0.39 (22.4)	15.8
Exhaust valve			
Uncoated	502 (936)	0.28 (16.2)	
1.52 mm (0.060 in.) PS/HYSZ coating	571 (1060)	0.23 (12.8)	21.0

3.3.3.5 Summary of Results of Final Heat Transfer Analysis

The results of the final heat transfer analyses of the coated piston, fire deck, and valves are summarized in Table XII.

Application of the TBCs to the piston and fire deck of the LHR test engine increased the average combustion surface temperature by 62°C and 48°C (111°F and 86°F), respectively, and decreased the average metal temperature 45°C and 53°C (81°F and 95°F), respectively. The thermal effectiveness of the coating on the piston was 20% and on the fire deck, 12.8%.

Table XI.
Reduction in the metal temperatures of the valves due to TBCs.

Condition	Metal Temperatures--°C (°F) Maximum	Average
Intake valve		
Uncoated	382 (720)	380 (717)
1.52 mm (0.060 in.) PS/HYSZ coating	382 (719)	371 (700)
Exhaust valve		
Uncoated	566 (1050)	538 (1000)
1.52 mm (0.060 in.) PS/HYSZ coating	510 (950)	502 (936)

Table XII.
Summary of the final heat transfer analysis on the piston, fire deck, and valves.

Component	Average combustion surface temperature --°C (°F)	Average increase in combustion surface temperature --°C (°F)	Average metal temperature reduction °C (°F)	Average Coating temperature drop-- °C (°F)	Thermal effectiveness --%
Piston	536 (996)	61.7 (111)	45.0 (81)	106.7 (192)	20.0
Fire deck	548 (1018)	47.8 (86)	52.8 (95)	100.6 (181)	12.8
Intake valve	451 (844)	70.6 (127)	9.4 (17)	80.0 (144)	15.8
Exhaust valve	571 (1060)	68.9 (124)	35.6 (64)	33.3 (60)	21.0

The operating temperatures of the intake and exhaust valves are substantially influenced by the heat transfer occurring on the port (reverse) side of the valves. The average metal temperature at the coating/metal interface in the intake valve remains nearly constant because of the cooling effect of the 47°C (115°F) intake air charge although the combustion surface average temperature increased 71°C (127°F) with the application of the TBC. The coating reduced the heat loss to the intake valves combustion surface by 15.8%.

The exhaust valve experienced heat input on the port (reverse) side from the hot exhaust gas. Note in Figure 16 that the point of maximum temperature in the uncoated exhaust valve is in the valve stem region and not on the combustion surface. Application of the TBC increased the average coating/metal interface temperature by 36°C (64°F) and increased the average combustion surface temperature by 69°C (124°F). The coating reduced the heat loss to the exhaust valves combustion surface by 21.0%.

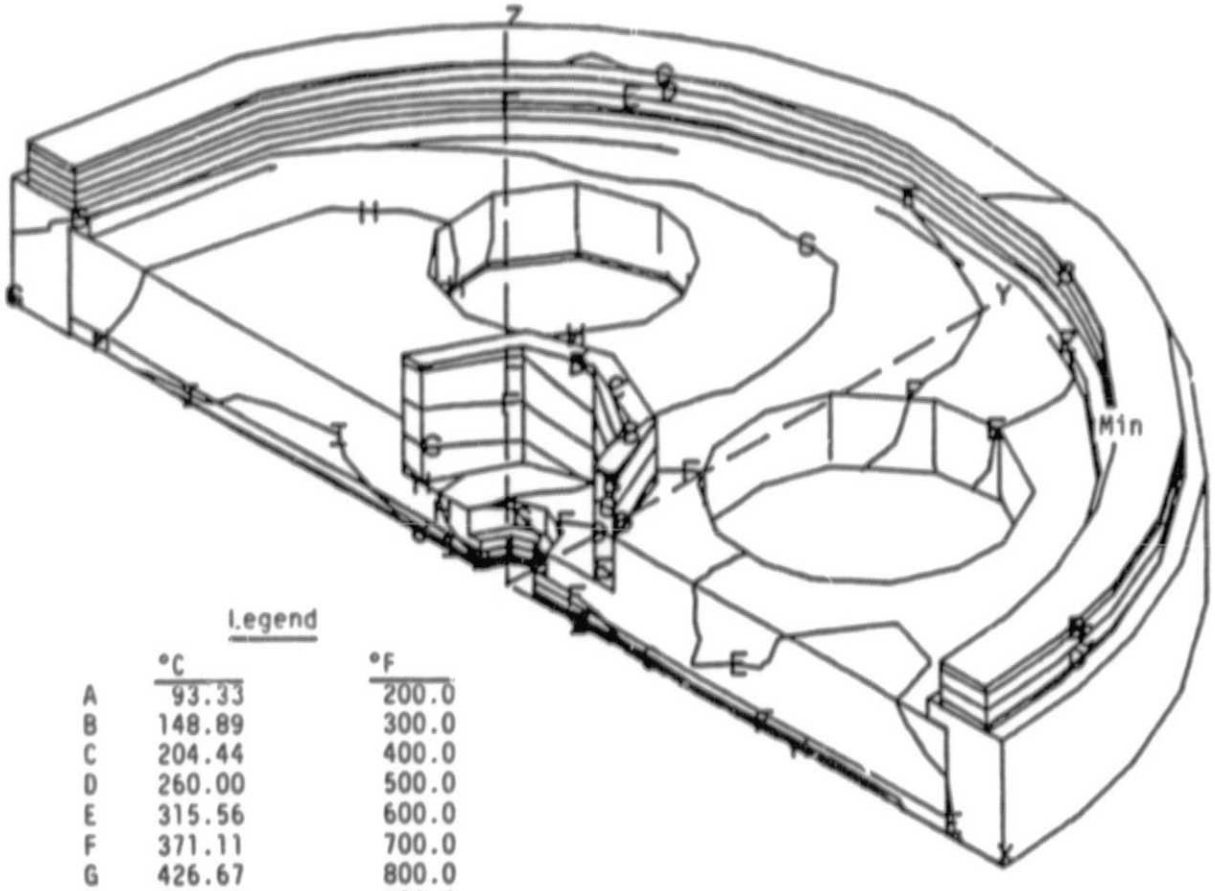

Legend

	°C	°F
A	93.33	200.0
B	148.89	300.0
C	204.44	400.0
D	260.00	500.0
E	315.56	600.0
F	371.11	700.0
G	426.67	800.0
H	482.22	900.0
I	537.78	1000.0
J	593.33	1100.0
K	648.89	1200.0
L	704.44	1300.0
*Max	649.32	1200.8
Min	110.41	230.7

*Denotes hidden

TE84-7934

Figure 15. Contour plot of temperatures in a coated low heat rejection fire deck.

ORIGINAL PAGE IS
OF POOR QUALITY

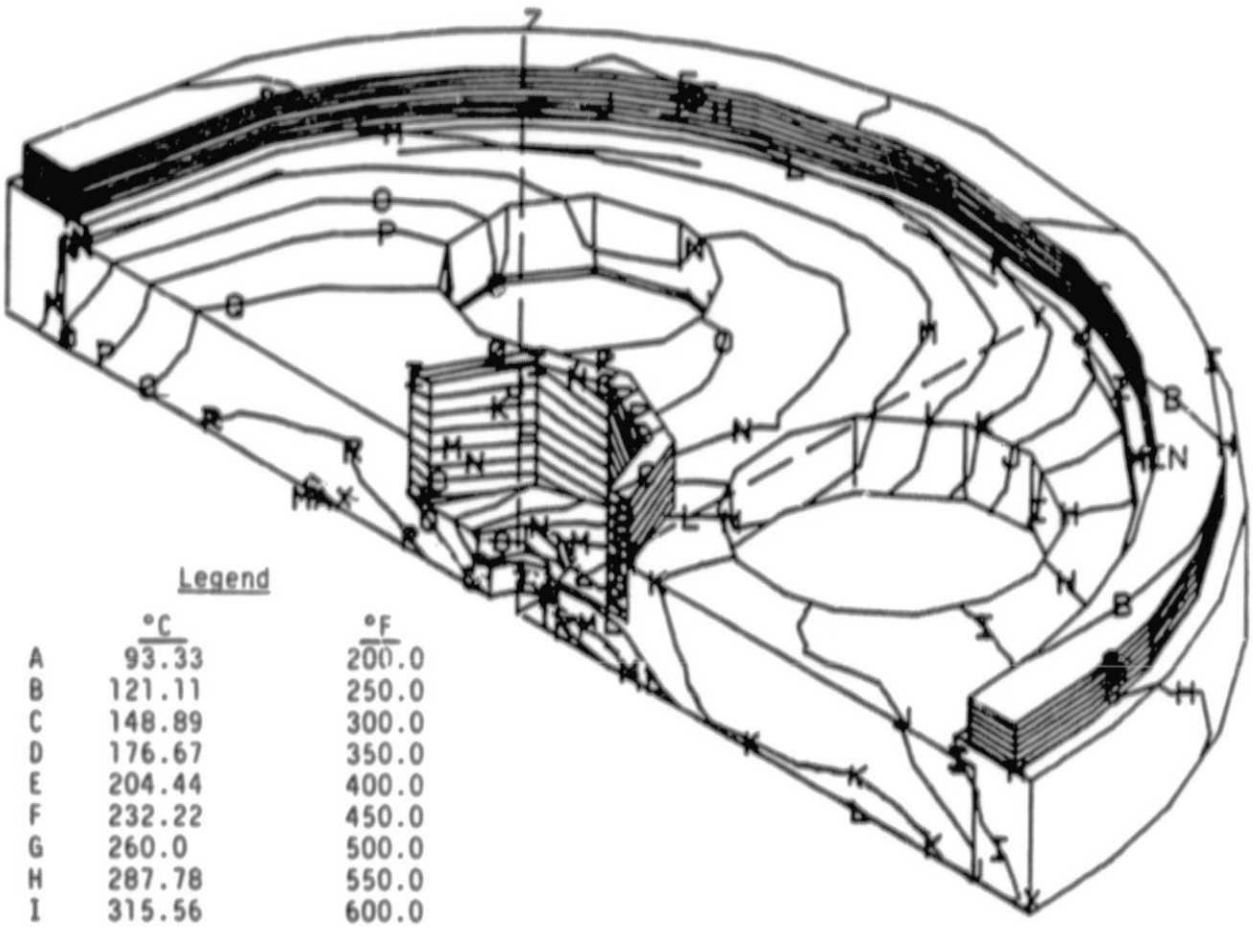

Legend

	°C	°F
A	93.33	200.0
B	121.11	250.0
C	148.89	300.0
D	176.67	350.0
E	204.44	400.0
F	232.22	450.0
G	260.0	500.0
H	287.78	550.0
I	315.56	600.0
J	343.33	650.0
K	371.11	700.0
L	398.89	750.0
M	426.67	800.0
N	454.44	850.0
O	482.22	900.0
P	510.00	950.0
Q	537.78	1000.0
R	565.56	1050.0
S	593.33	1100.0
T	621.11	1150.0
Max	597.02	1106.6
Min	111.45	232.6

TE84-7935

Figure 16. Contour plot of temperatures in an uncoated low heat rejection fire deck.

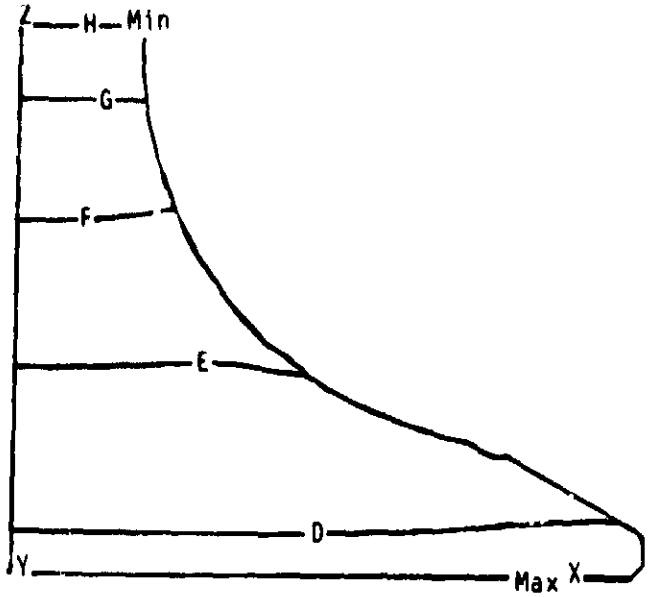

a. Uncoated

Legend

	°C	°F
A	471.11	880.00
B	437.77	820.00
C	404.44	760.00
D	371.11	700.00
E	337.77	640.00
F	304.44	580.00
G	271.11	520.00
H	237.77	460.00
I	204.44	400.00
J	171.11	340.00
Max	381.75	719.16
Min	249.20	480.56

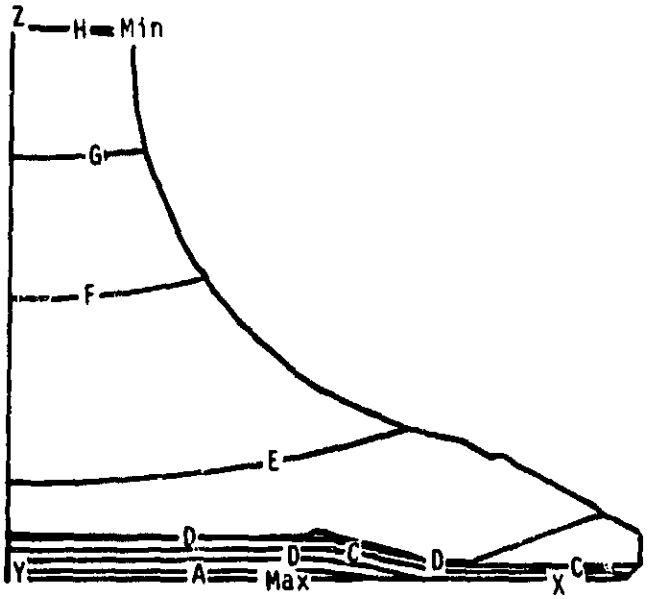

b. PSZ coated

Legend

	°C	°F
A	471.11	880.00
B	437.77	820.00
C	404.44	760.00
D	371.11	700.00
E	337.77	640.00
F	304.44	580.00
G	271.11	520.00
H	237.77	460.00
I	204.44	400.00
J	171.11	340.00
Max	491.83	917.29
Min	236.99	458.58

TE84-7936

Figure 17. Temperatures of uncoated (top) and plasma-sprayed zirconia coated (bottom) intake valves.

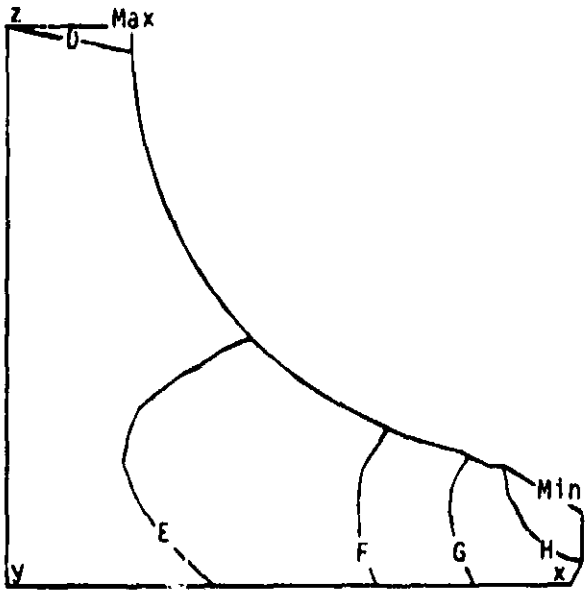

Legend	°C	°F
A	648.89	1200.00
B	621.11	1150.00
C	593.33	1100.00
D	565.56	1050.00
E	537.78	1000.00
F	510.00	950.00
G	482.22	900.00
H	454.44	850.00
I	426.67	800.00
J	398.89	750.00
K	371.11	700.00
L	343.33	650.00
M	315.56	600.00
Max	567.69	1053.84
Min	429.54	805.17

a. Uncoated

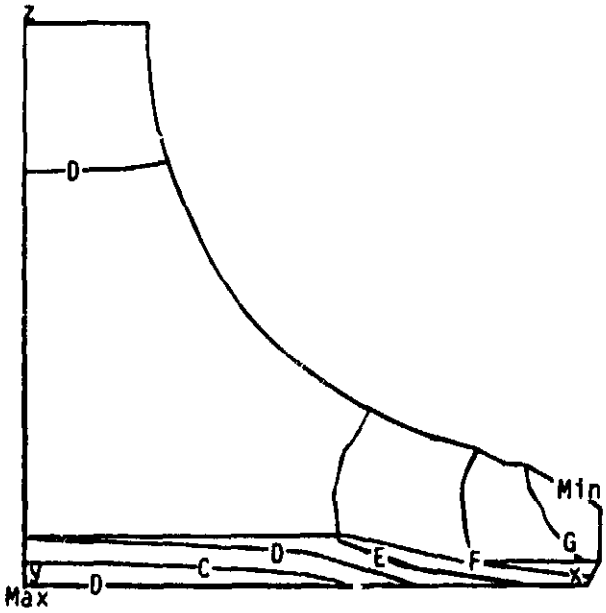

Legend	°C	°F
A	648.89	1200.00
B	621.11	1150.00
C	593.33	1100.00
D	565.56	1050.00
E	537.78	1000.00
F	510.00	950.00
G	482.22	900.00
H	454.44	850.00
I	426.67	800.00
J	398.89	750.00
K	371.11	700.00
L	343.33	650.00
M	315.56	600.00
Max	623.18	1153.73
Min	465.17	869.30

b. PSZ coated

TE84-7937

Figure 18. Temperatures of uncoated (top) and plasma-sprayed zirconia coated (bottom) exhaust valves.

3.4 SI PAD CONFIGURATION

A goal of this program was to evaluate an SI pad element in a diesel engine environment. This was the first application of an SI pad in a diesel engine operating at high power (1.17 MPa [170 lb/in.^{2}] BMEP). The function of the SI element is to provide a compliant layer between the ceramic coating and the metallic substrate to absorb the shear strain caused by mismatch between the coating and the substrate due to thermal expansion. This unique feature may be esssential in advanced capability TBC systems. In this program, the flat and rigid uncooled fire deck assembly is an excellent opportunity to evaluate the SI pad in an LHR diesel engine environment.

The SI pad selected for evaluation in the coating system screening tests and the engine test was a Brunsbond®* sintered fiber metal pad. The Brunsbond pad is fabricated from an oxidation resistant Hoskins 875 (iron, chromium, aluminum) alloy. Low density (20% to 35%) versions of this pad material have been used to enhance ceramic coating durability in nondiesel applications where cyclic high pressure loading does not occur. The SI pad density was increased to 50% for the fire deck application in this program to withstand the high gas pressure loading in the cylinder (13.8 MPa [2000 lb/in.^{2}]). The thermal conductivity of the 50% dense pad is three times that of the 35% dense pad and 10 times that of the PSZ coating.

Vendor recommended thickness for the SI pad was 1.52 mm (0.060 in.). However, the preliminary heat transfer analysis (subsection 3.3.2) showed that a 32% improvement in the overall coating system thermal effectiveness would result by reducing the thickness of the SI to 1.02 mm (0.040 in.). The 1.02 mm (0.040 in.) thickness was deemed the minimal acceptable thickness to maintain the strain relief function because of braze allowance considerations, metal wire diameters, and manufacturing capabilities. (The braze material wicks into the pad approximately 0.38 mm [0.015 in.] and the bond coat penetrates about two wire diameters, leaving about 0.64 mm [0.025 in.] thickness to function as an SI.)

The physical characteristics of the SI pad evaluated in screening tests and engine tests are shown in Table XIII.

This SI configuration was evaluated in combination with the Allison PS/HYSZ coating, the Allison 80/20 SYSZ/Eccosphere coating, and the vendor coating A in Task II of this program.

*Brunsbond is a registered trademark of Brunswick Technetics.

Table XIII.
Physical characteristics of the SI pad for diesel applications.

Material	Hoskins 875 alloy (iron, chromium, aluminum)
Pad thickness	1.02 mm (0.040 in.)
Pad density	50%
Thermal conductivity	3.82 W/m °C (2.21 Btu/hr-ft-°F) at 23°C (73°F)
	5.05 W/m °C (2.92 Btu/hr-ft-°F) at 300°C (572°F)
	7.21 W/m °C (4.17 Btu/hr-ft-°F) at 600°C (1112°F)
Compressive modules	1.72 MPa (250,000 lb/in.^{2}) at 21°C (70°F)
	0.38 MPa (55,000 lb/in.^{2}) at 816°C (1500°F)
Maximum operating temperature	982°C (1800°F)

IV. TASK II--BENCH TEST EVALUATION

The purpose of this task was to determine the heat transfer characteristics of the TBC systems being investigated and to evaluate, through a series of laboratory test rigs, the thermal and mechanical durability characteristics of these coating systems. The results of these tests formed the basis from which coating systems were selected for application to the piston, fire deck and valves of a single-cylinder research diesel engine. These coated components were engine tested, as described in Task III, to evaluate the coating's performance in an actual operating engine environment.

Bench test evaluation of the coating system's performance was based on the following experimentally collected data:

- o thermal conductivity
- o erosion resistance
- o corrosion/oxidation resistance
- o thermal shock/fatigue resistance

4.1 COATING SYSTEM MORPHOLOGY

The critical examination of coating structures provides one means for determining the potential suitability of the system to fulfill the desired objectives. In the case of the TBC for the diesel engine, the following two significant characteristics are desired:

- o the distributed porosity of the coating, which enables the coating to absorb the strain imposed by thermal expansions
- o the closed pore porosity, which retains the strain relief features and, at the same time, closes the surface and subsurface to migratory paths of contaminant ingression, which are believed to be detrimental to coating survival

The structure of the TBCs was examined by SEM for record purposes as well as to correlate the morphology with subsequent test results, particularly those concerned with corrosion/oxidation and thermal shock.

A vendor-supplied coating, designated as vendor coating A, is shown in Figures 19 and 20. This coating consists of PS YSZ. Figure 19a is an overall view of the coating system. The surface of this coating appears to be more dense than the interior, as shown in Figure 19b, which may help prevent contaminant ingression. Figure 19c shows that the coating does not exhibit much porosity, although there are isolated regions of large open cavities. Of particular interest are the views of the SI pad shown in Figure 20. In Figure 20a, the PS coating is shown infiltrating the topmost layer of the pad. Foreign material located about the third fiber layer down is believed to be abrasive grit that was trapped in the pad following the grit blast preparation for the PS process. It is virtually impossible to dislodge this material once it has infiltrated the pad. However, it is not believed to affect the overall compliance of the pad. The braze attachment to the substrate can be readily seen in Figure 20b, where the braze has penetrated the pad to a depth of approximately three fibers.

Vendor coating B is shown in Figure 21. This is a PS coating consisting primarily of calcia-stabilized zirconia. This coating displays a high degree of

ORIGINAL IS
OF POOR QUALITY

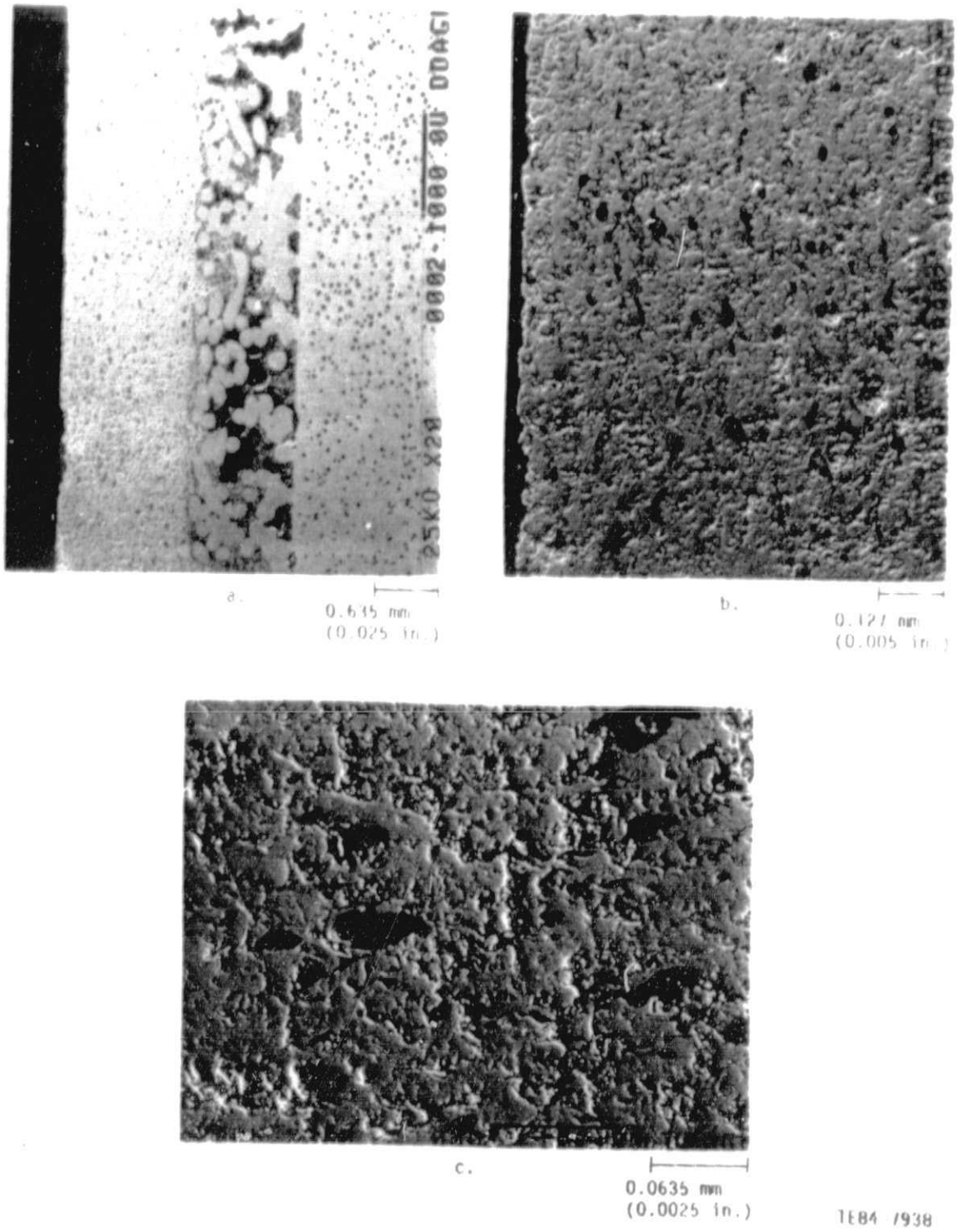

Figure 19. Vendor coating A on strain isolator pad in system 2.

ORIGINAL PAGE IS
OF POOR QUALITY

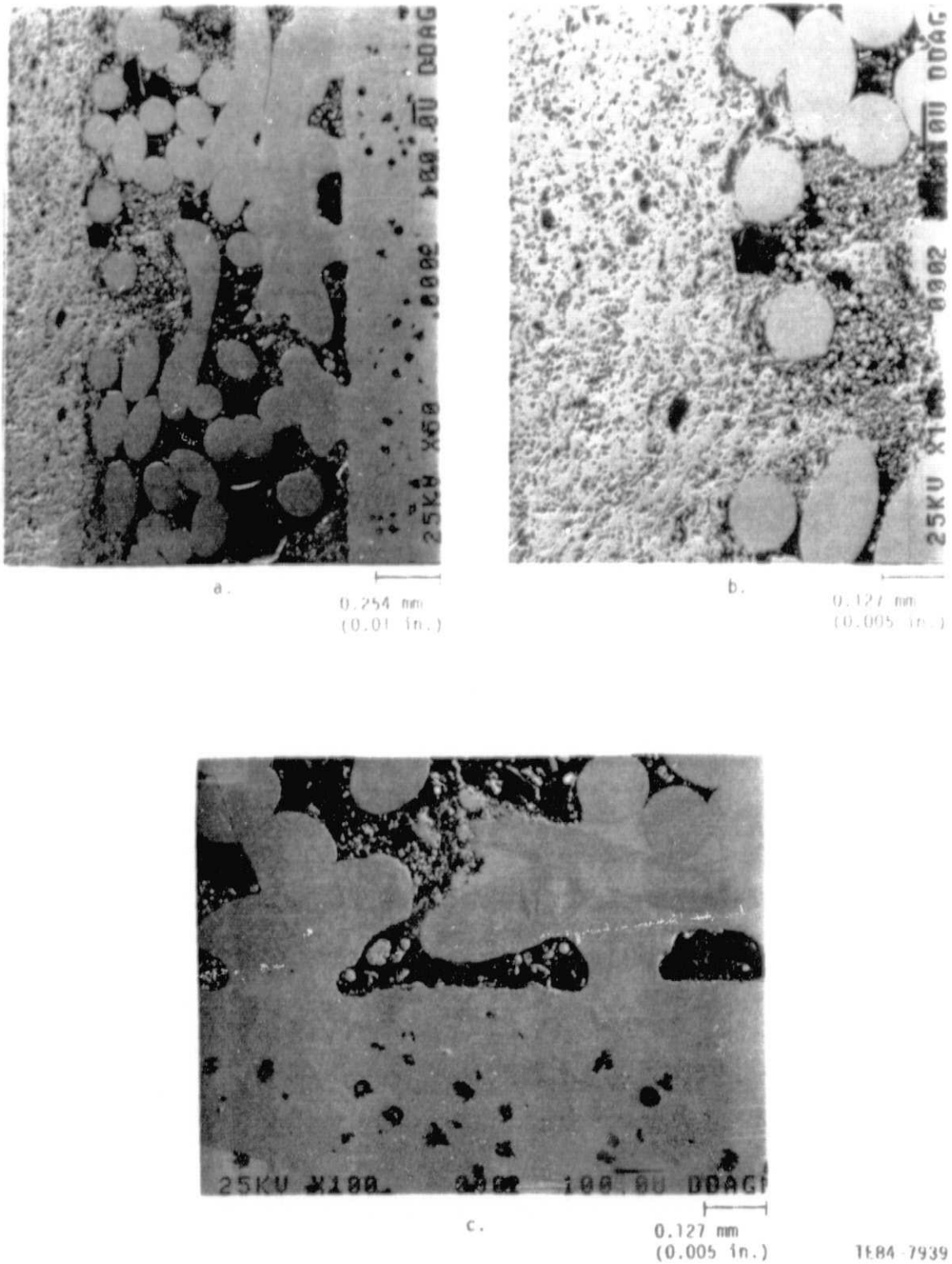

Figure 20. Brazed and coated strain isolator pad.

ORIGINAL PAGE IS
OF POOR QUALITY

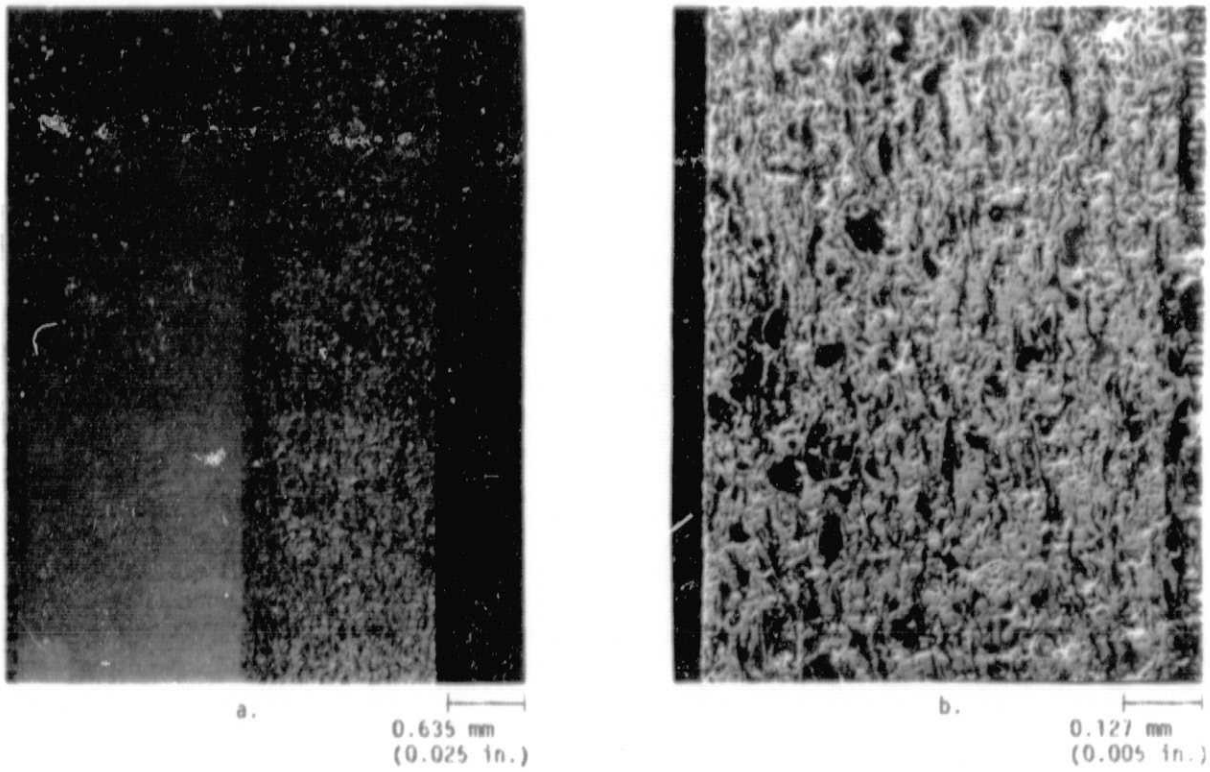

Figure 21. Vendor coating B in system 3.

porosity, as shown in Figures 21b and 21c. However, it appears to have a laminar structure with a high degree of interconnected pores. This presumably could lead to poor performance in terms of contaminant ingression and thermal shock resistance.

The SYSZ/Eccosphere coating system developed by Allison is shown in Figure 22. This is a PS coating in which SYSZ is sprayed simultaneously with Eccosphere. The Eccosphere consists of hollow alumino-silicate particles supplied by Emerson-Cumming. The materials are fed to the PS gun from two separate powder feeders and combined in the plasma efflux. The combined material consists of 80% (by volume) YSZ and 20% Eccosphere. Examination of this coating structure, as shown in Figures 22a and 22b, reveals some of the Eccosphere retained in the structure as hollow particles. The porosity appears randomly distributed with some interconnected paths.

Figure 23 illustrates the partially developed HYSZ coating system. In this particular case, the coating is a combination of the SYSZ powder, which is injected normally through the gun into the plasma stream, and the HYSZ particles, which are injected into the plasma stream through an external feed port. The objective of this procedure is to capture the hollow particles with the molten solid particles and subsequently deposit the resulting mixture onto the substrate, retaining a hollow particle structure as the coating cools. The micrograph of the coating indicated that this objective was partially achieved. Due to program time constraints the decision was made to proceed with this partially developed coating and initiate thermal and mechanical testing. Laboratory development of the hollow particle coating continued as a parallel effort.

4.2 TEST COUPON PREPARATION

Materials typical of diesel engine components were used for test specimens where applicable. These materials are listed in Table XIV. The test coupons were prepared and coated in the exact manner and with the same processes as those planned for an actual engine component using a Plasmadyne SG-1-B gun. The coated surfaces were subsequently processed with a conventional fine-grit grinding wheel or with single-point carbide tooling. All removal of material required shallow cuts and slow feeds and speeds. No coolant was used on any of the ceramic surface finishing. The ceramic surface was ground with conventional 120 grit silicon carbide wheels that removed no more than 0.013 mm (0.0005 in.) per pass.

Single-point carbide machining used surface speeds of 45.7 m/min (150 ft/min) or less and made cuts less than 0.13 mm (0.005 in.) deep. Extremely slow cross-feeds on the order of 0.020 mm/rev (0.0008 in./rev) were used.

4.3 THERMAL CONDUCTIVITY EVALUATION

4.3.1 Approach

Engine component material thermal property data are necessary for accurate engine thermal analysis. Thermal conductivity data were not available for the TBC systems evaluated in this program.

Table XIV.
Single-cylinder diesel engine component materials.

Component	Material
Piston	Ni-Resist Ductile Iron D5B with molybdenum
Fire deck	Waspaloy--AMS 5708
Intake valve	Eaton EMS 1
Exhaust valve	Eaton EMS 235
SI pad	Hoskins 875
Vendor coating A	YSZ
Vendor coating B	Calcia-stabilized zirconia
Allison 80/20 coating	8% YSZ standard spray grade + Emerson and Cuming Eccospheres
Allison PS/HYSZ coating	8% YSZ standard spray grade + Metco HYSZ CE 2198A

A comparative type of thermal conductivity test apparatus was used to experimentally determine the conductivities of the thermal barrier materials and the overall conductances of systems that were tested in this program. Experimental procedures for the in-house thermal conductivity test fixture, built originally to test compliant diesel engine head gaskets and similar thermal barrier materials, were developed to test the rigid ceramic coatings (Reference 2).

Thermal conductivity tests were first conducted on the metallic substrate materials used in the coated engine components to provide data for engine component heat transfer analysis. Waspaloy, the fire deck material, was selected as the substrate material for testing the TBCs because the material was readily available and documentation of Waspaloy material properties is much more extensive than for the other engine component materials.

Tests were conducted on each of the coating system constituent materials applied to Waspaloy coupons. These data were used to calculate thermal conductivity data for complete coating systems and thermal conductivity data for components not easily tested individually in the fixture, such as the SI pad.

To determine the thermal resistance of the SI pad, a system that was composed of a Waspaloy substrate, an SI pad, a thin NiCrAlY bond coat, and a 0.025 mm (0.010 in.) thick layer of PS YSZ was prepared. The thermal resistance of the SI pad was reduced from the overall conductance value by subtracting the conductances of the other system components.

The final step in the test procedure was testing the complete TBC systems for conductance. These data provided thermal resistance information for the TBC system analyzed in the final heat transfer analysis of the engine components.

ORIGINAL PAGE IS
OF POOR QUALITY

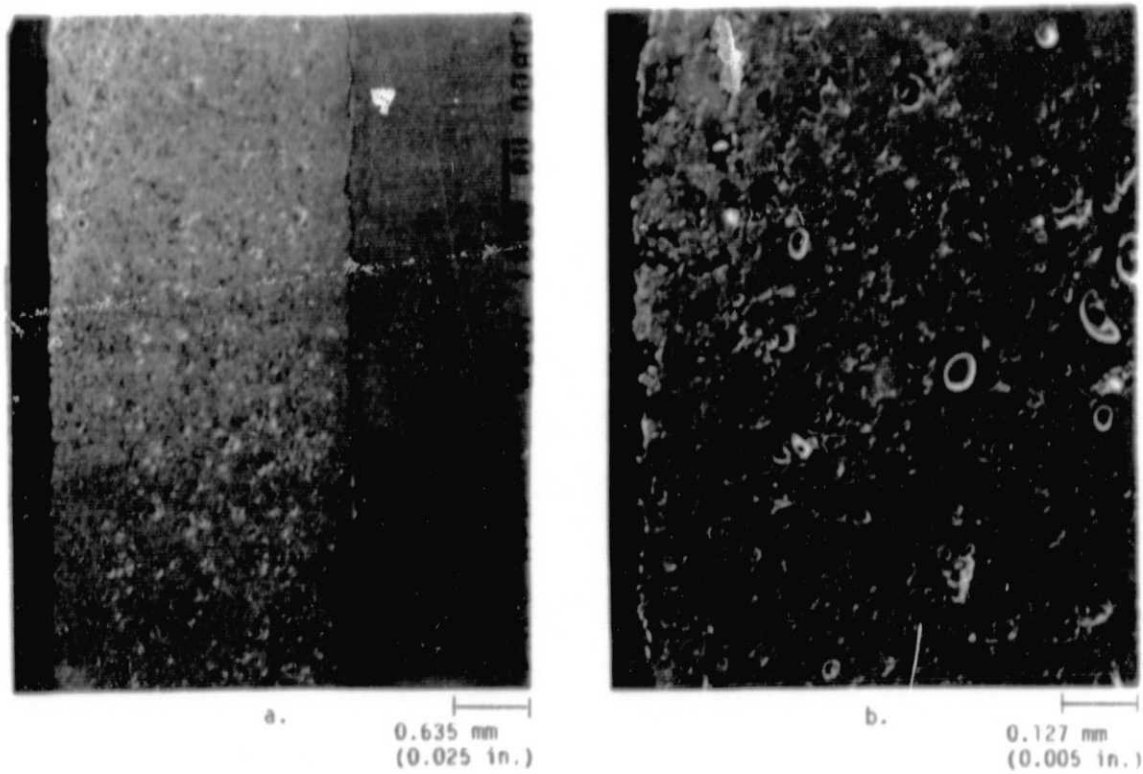

Figure 22. 80/20 SYSZ/Eccosphere coating in systems 4 and 5.

ORIGINAL PAGE IS
OF POOR QUALITY

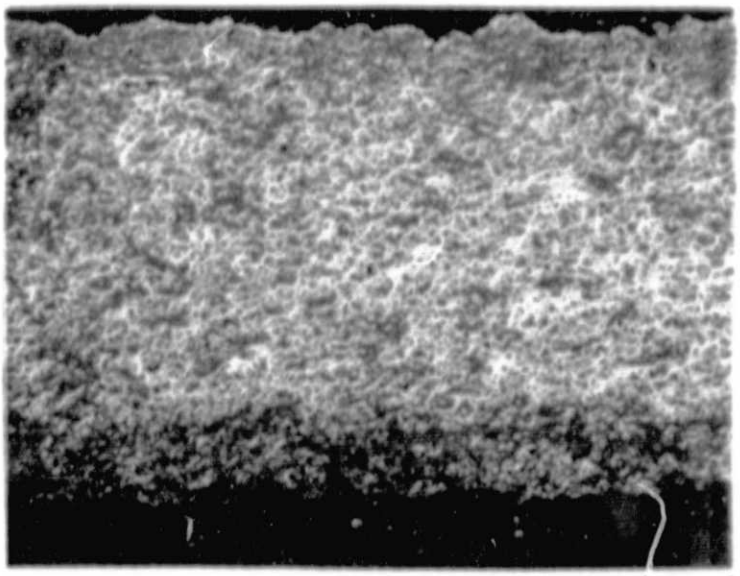

Figure 23. Plasma-sprayed hollow yttria-stabilized zirconia coating developed by Allison.

Test Apparatus Design

A drawing of the thermal conductivity test fixture is shown in Figure 24. The heat source at the base is a 600 W (34.1 Btu/min) washer-type heater. A 250 W (14.2 Btu/min) washer-type guard heater mounted below and separated by a layer of insulation is used to reduce heat loss from the bottom of the main heater.

Two 99.63% pure nickel reference sections, 50.8 mm (2 in.) long each and 24.1 mm (0.95 in.) in diameter, are positioned between the heat source in the base and the cooled heat sink at the top of the fixture. The upper nickel reference section is attached below a hollow cavity in a large steel flange. Air or water can be passed through this cavity to control the temperature of the heat sink. Thermocouples are positioned at 90 deg intervals around both nickel reference sections, as shown in Figure 25. The material sample being tested is placed between the two nickel reference sections.

This test apparatus permits variable mechanical loading of the test sample. A small hydraulic cylinder is mounted between the steel flange containing the cooling cavity and the flange on which it exerts force. The flange with the cooling cavity is free to float and find proper alignment. The top flange is secured to the base with long bolts. The test fixture can impart a unit load up to 27.6 MPa (4000 lb/in.^{2}) on the test sample.

The test section and the heat source section of the fixture are insulated. This minimizes radial heat losses in the nickel comparator bars and protects the operator from exposure to hot surfaces.

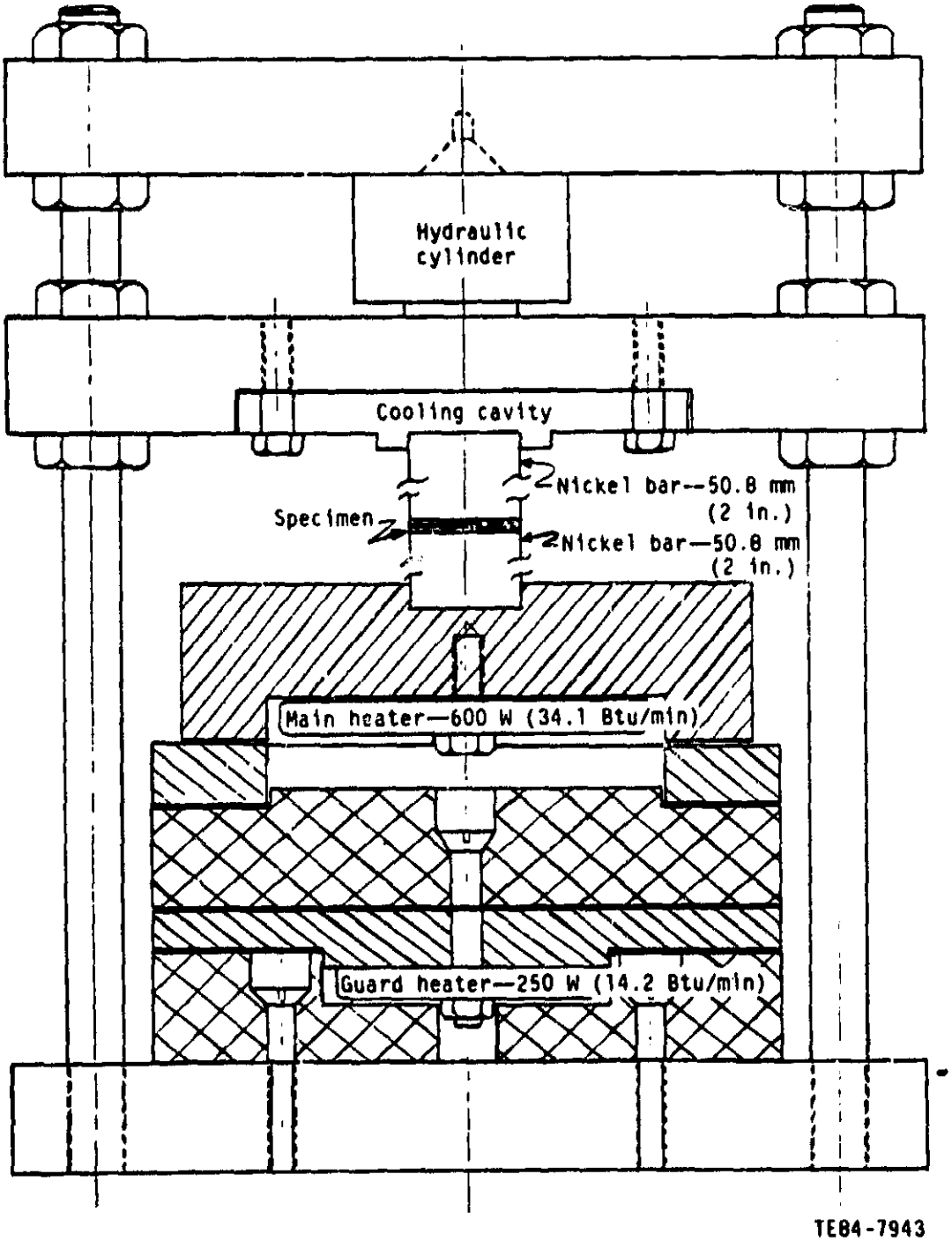

Figure 24. Thermal conductivity measurement fixture.

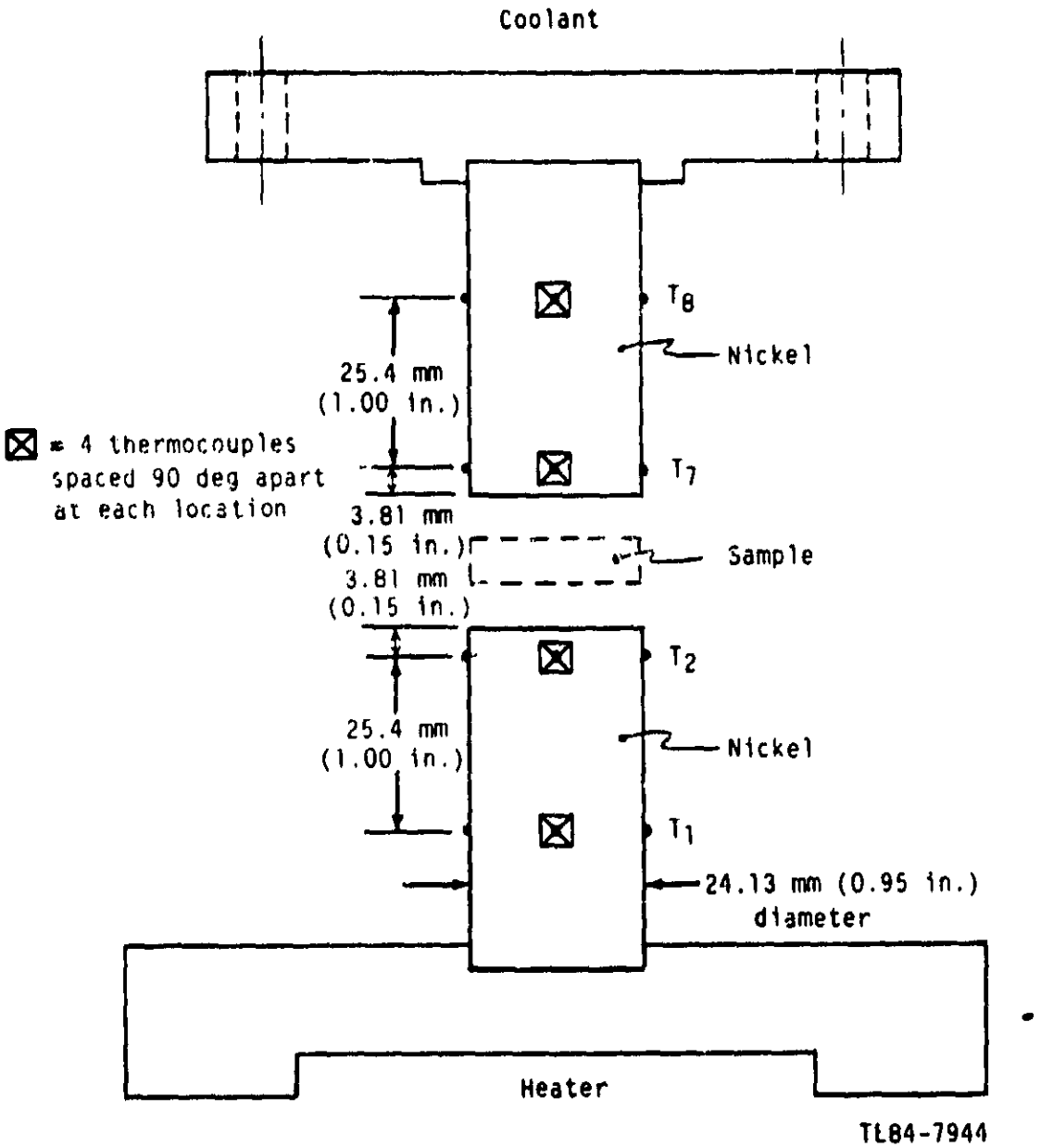

Figure 25. Thermocouple locations in the thermal conductivity measurement rig.

Test Fixture Calibration

Calibration of the test fixture was accomplished by determining the conductivity of the nickel reference section. The nickel reference section was compared with a sample of Inconel 702 material, for which thermal conductivity is well documented.

The Inconel 702 sample was instrumented with thermocouples and run in the test fixture. The heat flux through the instrumented sample was determined, and by assuming that heat losses were negligible in the test section, the assumption was then made that the same amount of heat flux was flowing through the nickel test bars. From this heat flux and the temperature measurements on the nickel base, the conductivity of the nickel comparator sections was calculated.

A FEM analysis of the conductivity test fixture confirmed that radial heat loss was negligible when calibrating the fixture with the Inconel 702 material sample.

Test Procedure

The test sample is placed between the two nickel reference sections and loaded to the specified unit loading. Essentially 1-D heat transfer is established through the fixture by applying power to the electric heat source at the fixture base and supplying cold air or water to the cold sink heat exchanger at the top. The heat flux is determined by measuring the temperature gradient in each reference section and multiplying those gradients by the calibrated nickel conductivity at the reference section mean temperatures. The heat flux in the sample is taken as the mean value of that of the reference sections. The temperatures at the top and bottom of the sample are established by extrapolating the temperature gradient in each nickel reference section to the test section sample surface. The test sample surface temperatures are then used to calculate the sample's conductance or conductivity.

Uncoated Waspaloy test samples were tested with several techniques to ensure that a low contact resistance was maintained between the test sample and the nickel reference sections in the test fixture. A 0.076 mm (0.003 in.) thick soft copper shim placed between the sample and the reference sections was found to provide consistant low contact resistance and all subsequent testing used copper shims on both surfaces of the sample with the ceramic surface facing the heat source. The test sample systems without SI pads were tested at 27.6 MPa (4000 lb/in.^{2}) unit loading while the samples incorporating an SI were tested at 13.8 MPa (2000 lb/in.^{2}) unit loading to avoid deformation of the SI pad and a resultant change in the conductance of the overall system.

The thermal conductivity of the ceramic coating was determined by the temperature drop (ΔT) across the ceramic coating, the ceramic coating thickness, and the heat flux passing through it. To determine the ceramic coating ΔT, the Waspaloy substrate ΔT (calculated by using measured thermal conductivity, thickness, and heat flux) is subtracted from the total sample ΔT. The same technique was used to calculate the thermal conductivity of the SI pad. In that instance, the ΔT across the SI pad is determined by subtracting calculated ΔTs of the Waspaloy substrate plus the other coating system constituents from the total sample ΔT.

4.3.2 Results of Thermal Conductivity Tests

Thermal conductivity was measured on the four diesel engine component materials to which TBCs would be applied and on 12 Waspaloy coupon samples coated with partial or complete TBC systems. The thermal conductivity of the SI pad was calculated using thermal conductivity data obtained in these tests.

The following engine component materials were evaluated:

- o Waspaloy--fire deck (cylinder head)
- o Ni-Resist D5B--piston crown
- o EMS 1--intake valves
- o EMS 235--exhaust valves

Table XV lists the 12 coated test coupon samples on which thermal conductivity was measured.

The tested thermal conductivity of the Waspaloy sample and published data are shown in Figure 26. As shown in the figure, close agreement between tested and published values was obtained. This agreement provided additional verification of the calibration of this test fixture.

Tested thermal conductivity data for Ni-Resist D5B, EMS 1, and EMS 235 materials are shown in Figure 27. The Waspaloy material has the lowest thermal conductivity of the four metals, Ni-Resist D5B the next lowest, and the thermal conductivity of the valve materials (EMS 1 and EMS 235) is slightly higher. These data were used in the final heat transfer analysis of the engine components.

Table XV.
Thermal conductivity test plan.

Sample No.	TBC system	Component layer makeup
1	--	Waspaloy + bond coat
2	--	Waspaloy + bond coat + 1.52 mm (0.060 in.) SYSZ
3	--	Waspaloy + bond coat + 1.52 mm (0.060) in. HYSZ
4	--	Waspaloy + bond coat + 1.52 mm (0.060 in.) SYSZ/ Eccosphere
5	--	Waspaloy + SI + bond coat + 0.254 mm (0.010 in.) SYSZ
6	1	Vendor coating A on Waspaloy
7	2	Vendor coating A/SI on Waspaloy
8	3	Vendor coating B on Waspaloy
9	4	Waspaloy + bond coat + 0.254 mm (0.010 in.) SYSZ + SYSZ/Eccosphere
10	5	Waspaloy + SI + bond coat + 0.254 mm (0.010 in.) SYSZ + SYSZ/Eccosphere
11	6	Waspaloy + bond coat + 0.254 mm (0.010 in.) SYSZ + HYSZ
12	7	Waspaloy + SI + bond coat + 0.254 mm (0.010 in.) SYSZ + HYSZ

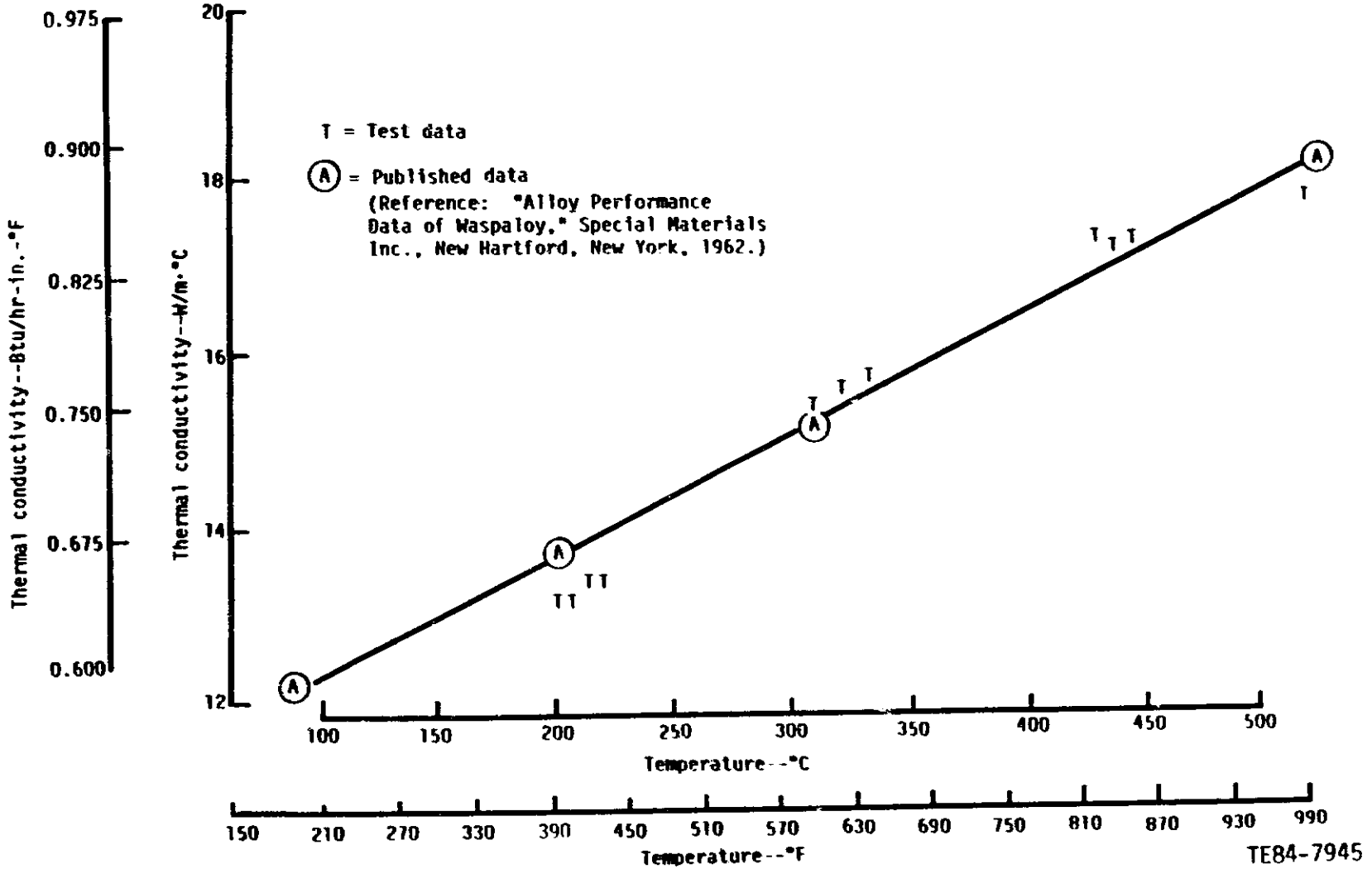

Figure 26. Waspaloy thermal conductivity.

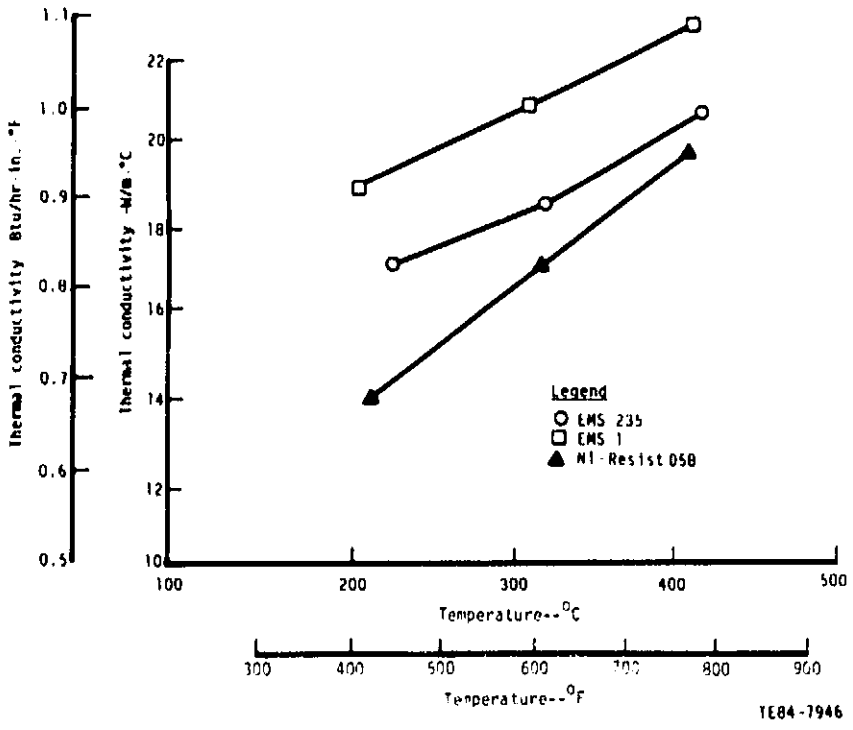

Figure 27. Measured thermal conductivity of Ni-Resist D5B, EMS 1, and EMS 235.

As noted in Table XV, the thermal conductivity tests of the TBC constituents were conducted with Waspaloy as the metal substrate. The thermal conductivity of the Waspaloy coupon (sample 1) with and without a NiCrAlY bond coat is shown in Figure 28. The intent in testing sample 1 was to determine the thermal conductivity of the bond coat. The bond coat thinness (about 0.102 mm [0.004 in.] after being ground flat) and porosity caused difficulty in testing. The results showed the bond coat thermal conductivity to be near that of the Waspaloy and thus in heat transfer analyses was considered to be thermally identical to the substrate.

Samples 2, 3, and 4 in Table XV provide thermal conductivity measurements of the three coating elements used in the Allison coating systems shown in Table XV (sample numbers 9, 10, 11, and 12).

Thermal conductivity test results for the SYSZ (sample 2), HYSZ (sample 3), and 80/20 SYSZ/Eccosphere coating (sample 4) are shown in Figure 29. Also shown in this figure are data for vendor coating A (sample 6) and vendor coating B (sample 8). The thermal conductivity of all of the coating samples except vendor coating B are similar. The difference in conductivity between vendor coating A and vendor coating B is attributed to variations in the constituents and densities of the two coatings. The conductivity of the 80/20 SYSZ/Eccosphere coating is nearly as high as the SYSZ coating because of the high conductivity of the Eccosphere (6.05 W/m °C [3.5 Btu/hr-ft-°F] compared to 1.04 W/m °C [0.6 Btu/hr-ft-°F] for 100% YSZ) which offsets the increased porosity of the 80/20 composite. The conductivity of the HYSZ coating is less than the SYSZ coating, as expected, but not greatly different. The HYSZ coating was undergoing development when the thermal conductivity tests were conducted. The tested HYSZ sample incorporated hollow YSZ particles and an Aremco 542 cement

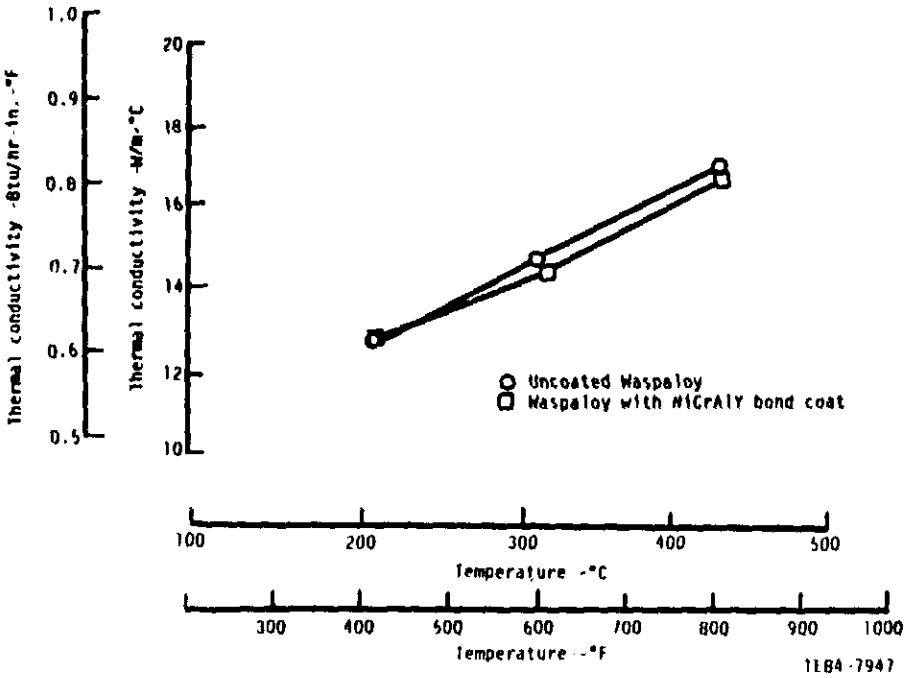

Figure 28. Thermal conductivity of Waspaloy with and without a bond coat.

to maintain the morphology of the hollow particle zirconia powder. The presence of the cement increased the coating density and may have slightly affected its conductivity.

As a point of reference, the tested thermal conductivity of a sample of toughened structural monolithic zirconia, produced by the AC Spark Plug Divison of General Motors, is shown in Figure 29 to point out the low thermal conductivity of all of the tested ceramic coatings.

The thermal conductivity of the SI pad was calculated by measuring the overall thermal barrier system conductance and substracting the known conductivities of its individual constituents. The resulting thermal conductivities are shown in Figure 30. Published thermal conductivity data for a 50% dense SI pad are also shown in Figure 30. The values at 300°C and 390°C (571°F and 731°F) are

comparable to data published by the vendor. Variability in the calculated conductivity stems from the following factors:

- o the amount of braze wicking into the pad
- o the amount of bond coat infiltrating the pad
- o the effective thickness and density of the pad
- o variations in thickness and conductivity of other components in the system
- o actual average temperature of the pad and other components

These results validate the data provided by the vendor and, therefore, the published data were used for analyses of the coating systems.

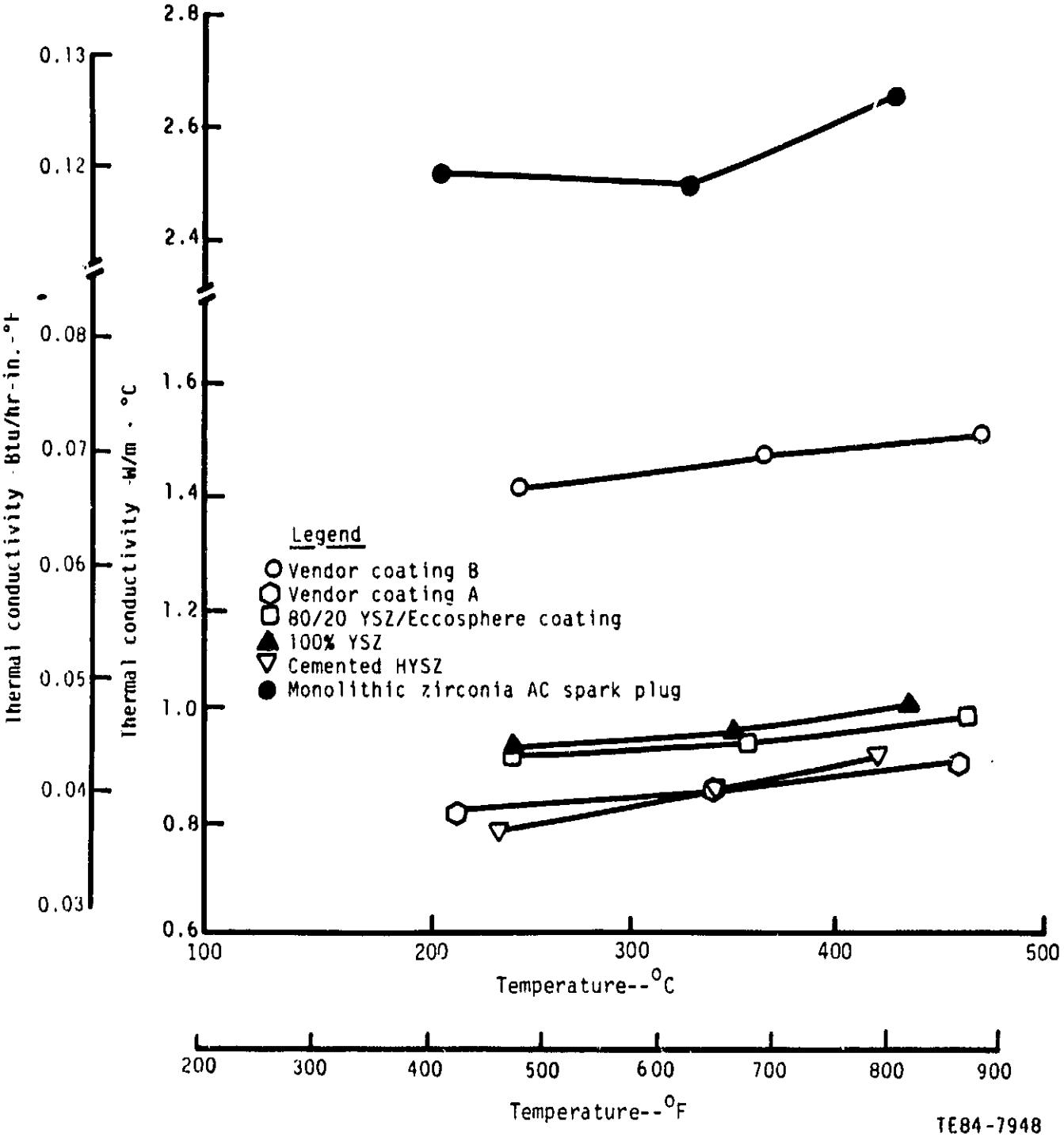

Figure 29. Conductivity versus temperature for ceramics.

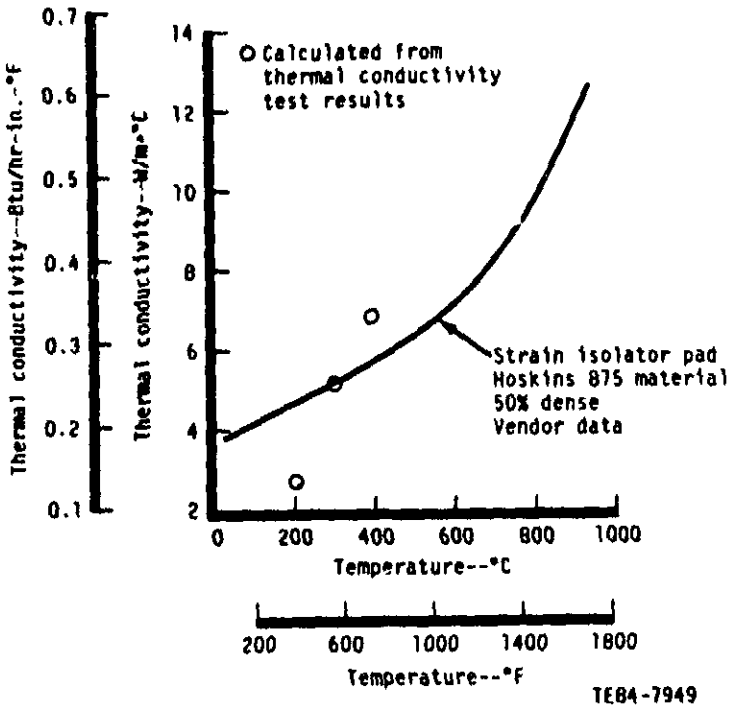

Figure 30. Thermal conductivity of a strain isolator pad.

The measured thermal conductance of complete TBC systems comprised of more than one constituent are shown in Figures 31 and 32. The thermal conductance of the composite coating systems is ranked as expected with the vendor coating A being the lowest of the group. The conductance of the coating systems that incorporate SIs (as shown in Figure 32) is lower than than of the coating systems without SIs because, in addition to relieving strain at the coating/metallic interface, the SI serves as an additional element in the TBC system. The thermal conductivity of the SI pad is less than that of the metal substrate.

In summary, the results of the thermal conductivity tests showed the following:

- o the thermal conductivity of the PSZ coatings is low--one third to one half of that of monolithic zirconia
- o the thermal conductivity of the PS/HYSZ coating was 10% less than that of the SYSZ coating
- o all zirconia-based coatings tested, excluding vendor coating B, had thermal conductivities within 11%
- o the thermal conductivity of vendor coating B was 60% greater than that of the other zirconia coatings grouped together

The thermal conductivity of the zirconia coatings is 37% of that of the monolithic zirconia; 18% of the SI pad; and 5% of the metallic engine components materials. The low thermal conductivity of the zirconia coatings is compared graphically in Figure 33 with the other ceramic and metallic materials tested in this program.

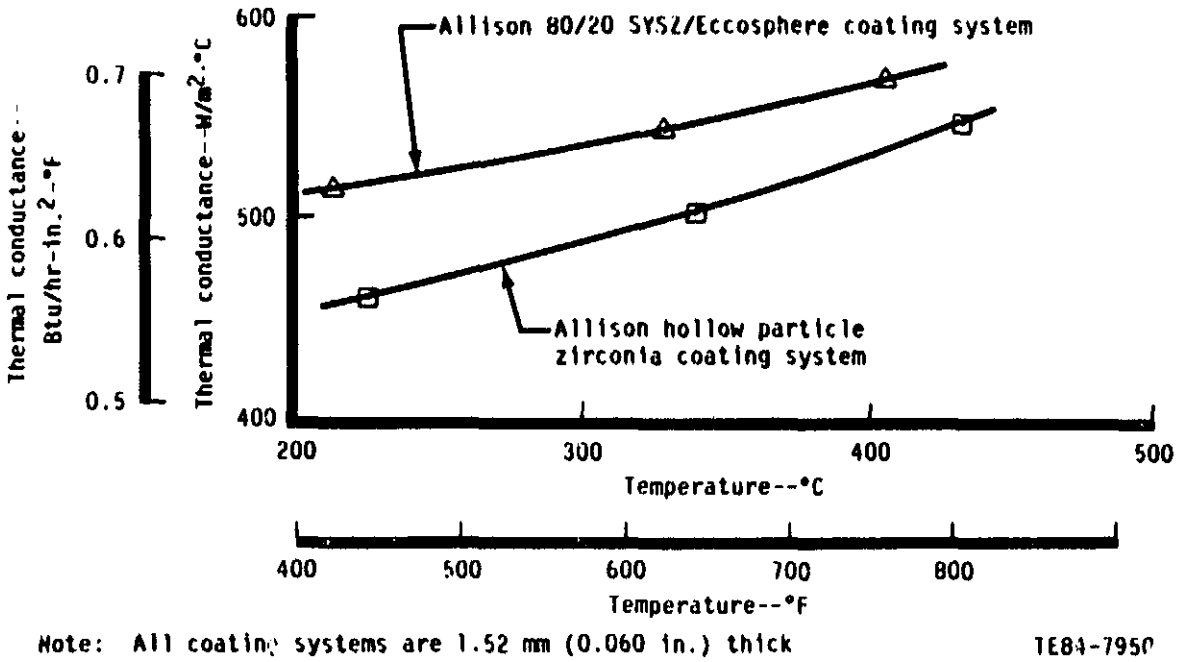

Figure 31. Conductance versus temperature for ceramic systems without strain isolator pads.

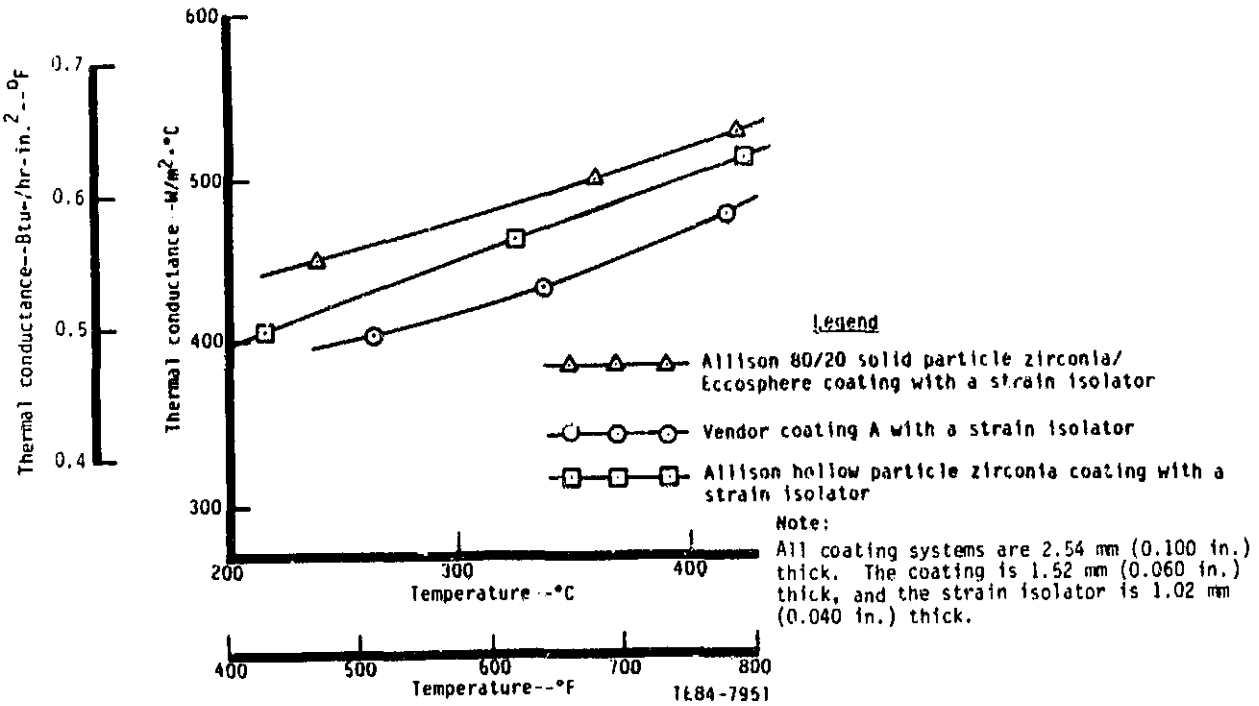

Figure 32. Conductance versus temperature for ceramic systems with strain isolator pads.

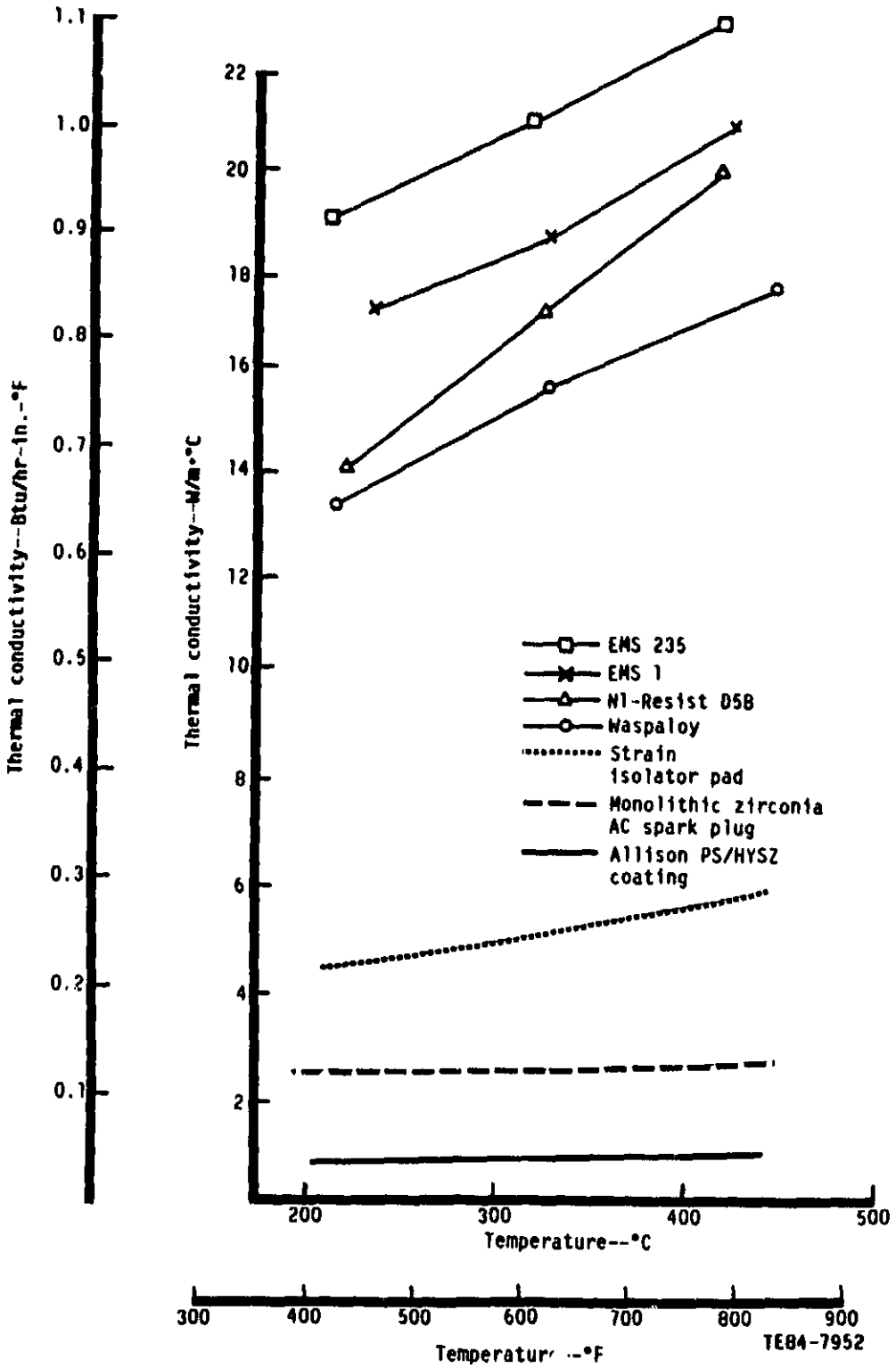

Figure 33. Thermal conductivities of zirconia coatings, monolithic zirconia, strain isolator pad, and metallic engine materials.

4.4 EROSION RESISTANCE

4.4.1 Approach

The resistance of ceramic coatings to diesel erosion in the cylinder cycle is an important parameter that must be considered. The action of fuel impingement from the injector on the ceramic-coated piston is unknown. Similarily, combustion velocities and inlet and exit fuel and air charges result in scrubbing actions on all of the cylinder components in contact with the combustion charge. The erosion test described herein was intended to rank the coatings with respect to each other in terms of erosion resistance to airborne particulate matter. Coarse Arizona road dust is the medium commonly used at Allison for erosion testing. This relative ranking provided one basis for selecting coatings for further evaluation.

The erosion rig, as shown in Figure 34, is a room temperature device that directs a particulate-laden air stream onto the test surface at approximately Mach 0.75. Tests were conducted for 2 hr and the weights of the consumed particulates and sample were monitored. Results of the specific erosion (weight loss in the sample divided by weight of the dust used) are plotted as a function of time. A 15 deg impingement angle, which facilitated comparison with an existing data base, was used for these tests.

4.4.2 Erosion Resistance Test Results

Erosion testing was conducted on the following four basic coatings:

- o vendor coating A
- o vendor coating B
- o 80/20 SYSZ/Eccosphere coating
- o PS/HYSZ coating

Test results are presented graphically in Figure 35, with the specific erosion plotted as a function of exposure time. The specific erosion is defined as the weight loss of the samples divided by the weight of the Arizona road dust particulate consumed in the test. Comparison with similar tests conducted on aircraft gas turbine TBCs shows these results to be similar to those for the aircraft coatings.

Figure 36 shows the eroded coatings at the completion of 2 hr testing. Visual examination of the surfaces shows the pictured damage to reflect the plotted data shown in Figure 35.

Vendor coating B displayed the best erosion resistance of the four coatings tested, followed by the 80/20 system, vendor coating A, and the PS/HYSZ system. Results for the latter two coatings were virtually identical.

4.5 CORROSION/OXIDATION RESISTANCE

4.5.1 Approach

In a high temperature gas turbine environment, clean fuels, such as kerosene, are used extensively and contamination of the coating due to fuel impurities

ORIGINAL PAGE IS
OF POOR QUALITY

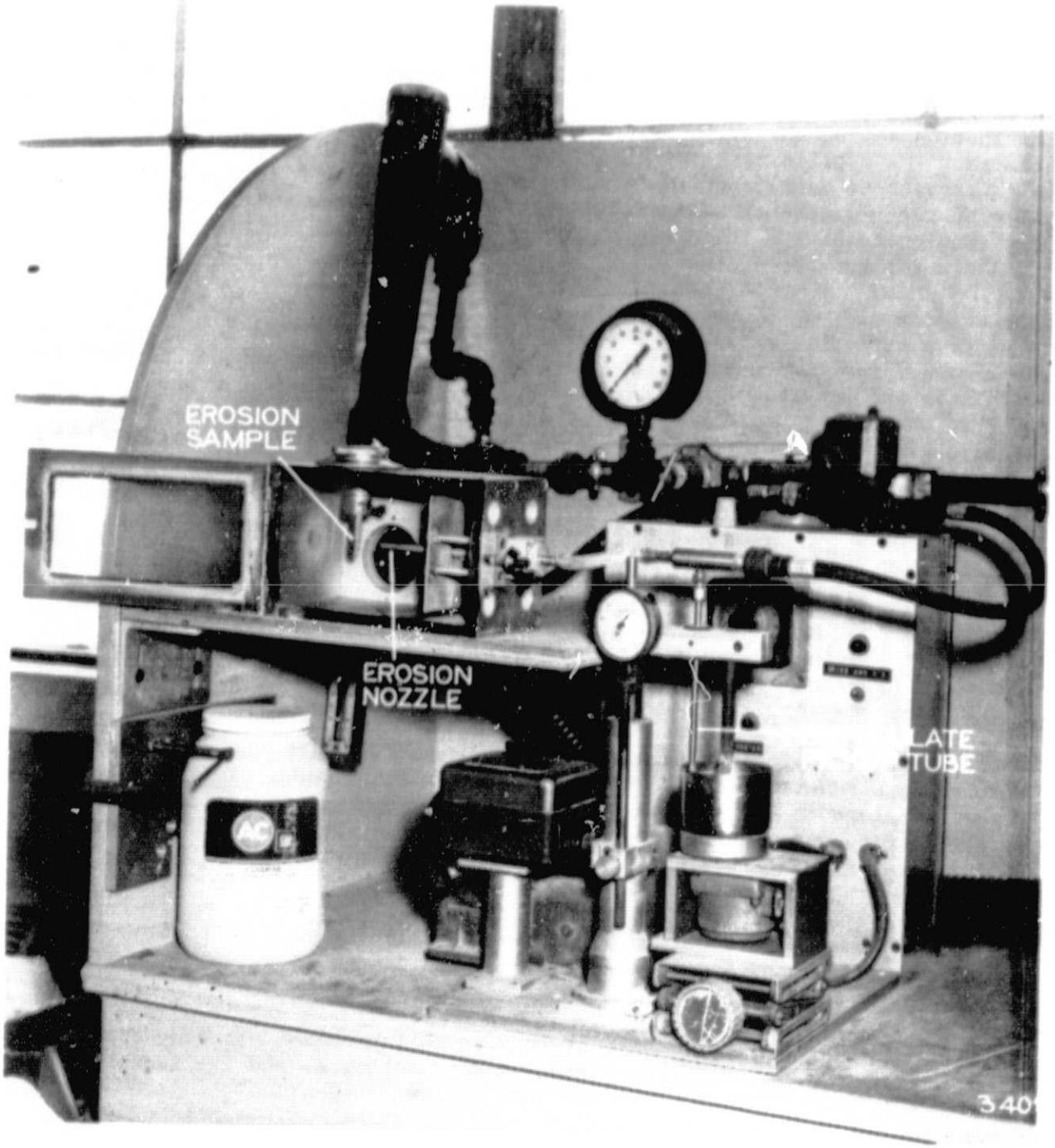

Figure 34. Erosion test fixture.

TE84-7953

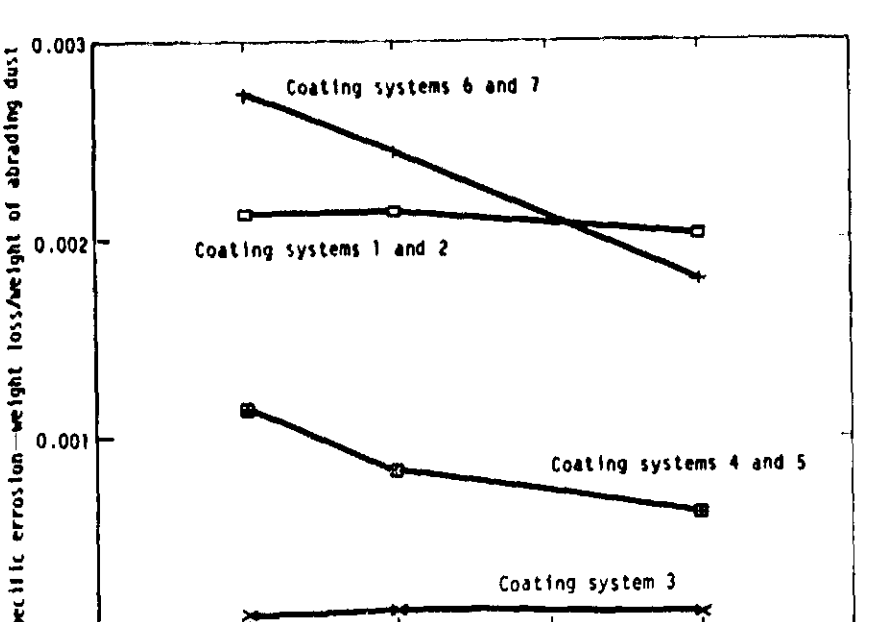

Figure 35. Erosion test results.

is rare. In these high temperature applications, failure of the coating generally occurs at the YSZ/bond coat interface and is a result of bond coat oxidation. This effect has been substantially reduced by the use of a high chromium NiCrAlY bond coat. In a diesel engine application, the nature of the fuel being used is entirely different. Diesel fuels are notoriously dirty and may contain many contaminants, such as sodium or vanadium compounds. It has been speculated that these contaminants may penetrate the coating system along the paths provided by the inherent porosity within the coating structure. The thermal gradient which occurs in the YSZ layer probably places the dew point of these impurities somewhere within the TBC. As temperature changes occur in the cylinder due to changes in the operating mode, phase changes of the contaminants can take place and possibly result in premature failure of the coating. The object of the corrosion/oxidation test was to place the selected TBCs in a typical diesel combustion environment to observe the effects, if any, on the coating subsurface structure.

The 100 hr corrosion/oxidation testing was conducted in a diesel-fuel-fired burner that subjected the samples to burning No. 2 diesel fuel at a chamber temperature of 899°C (1650°F) as shown in Figure 37.

In conducting the tests, the test rig was preheated to 899°C (1650°F). Samples were then inserted on a rotating platform and held so that the combustion gases circulated around the samples prior to being exhausted. The test continued for 24 hr after which the samples were withdrawn from the hot chamber and subjected to fan-blown room temperature air for 45 sec. This reduced the sample temperature to approximately 93°C (200°F). The samples were then reinserted in the chamber, which had been maintained at 899°C (1650°F), for the next 24-hr cycle. In addition to exposure to the burning diesel fuel, the samples were consequently subjected to a small number of thermal shock cycles.

ORIGINAL PAGE IS
OF POOR QUALITY

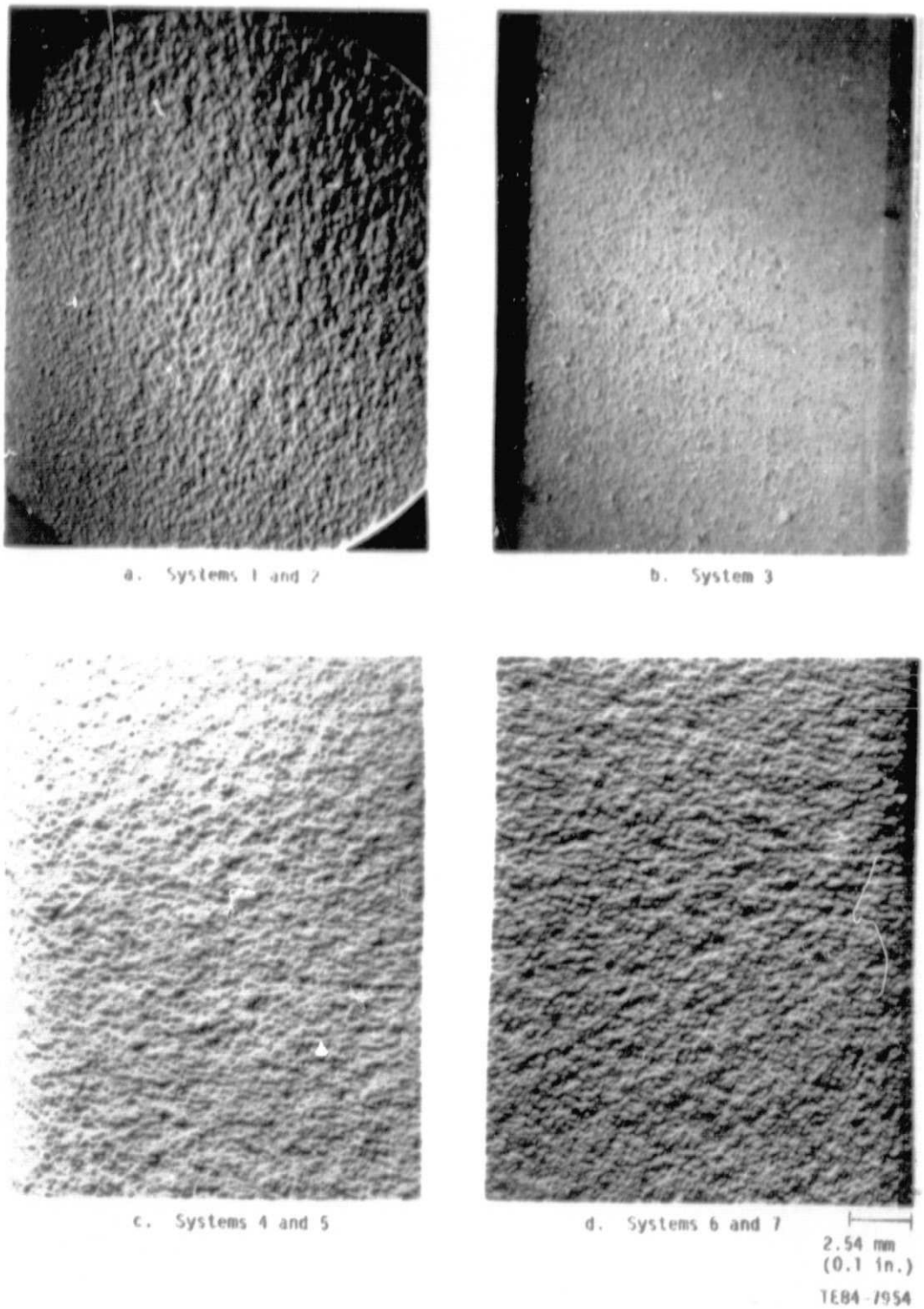

Figure 36. Systems 1-7 2 hr after the erosion test.

ORIGINAL PAGE IS
OF POOR QUALITY

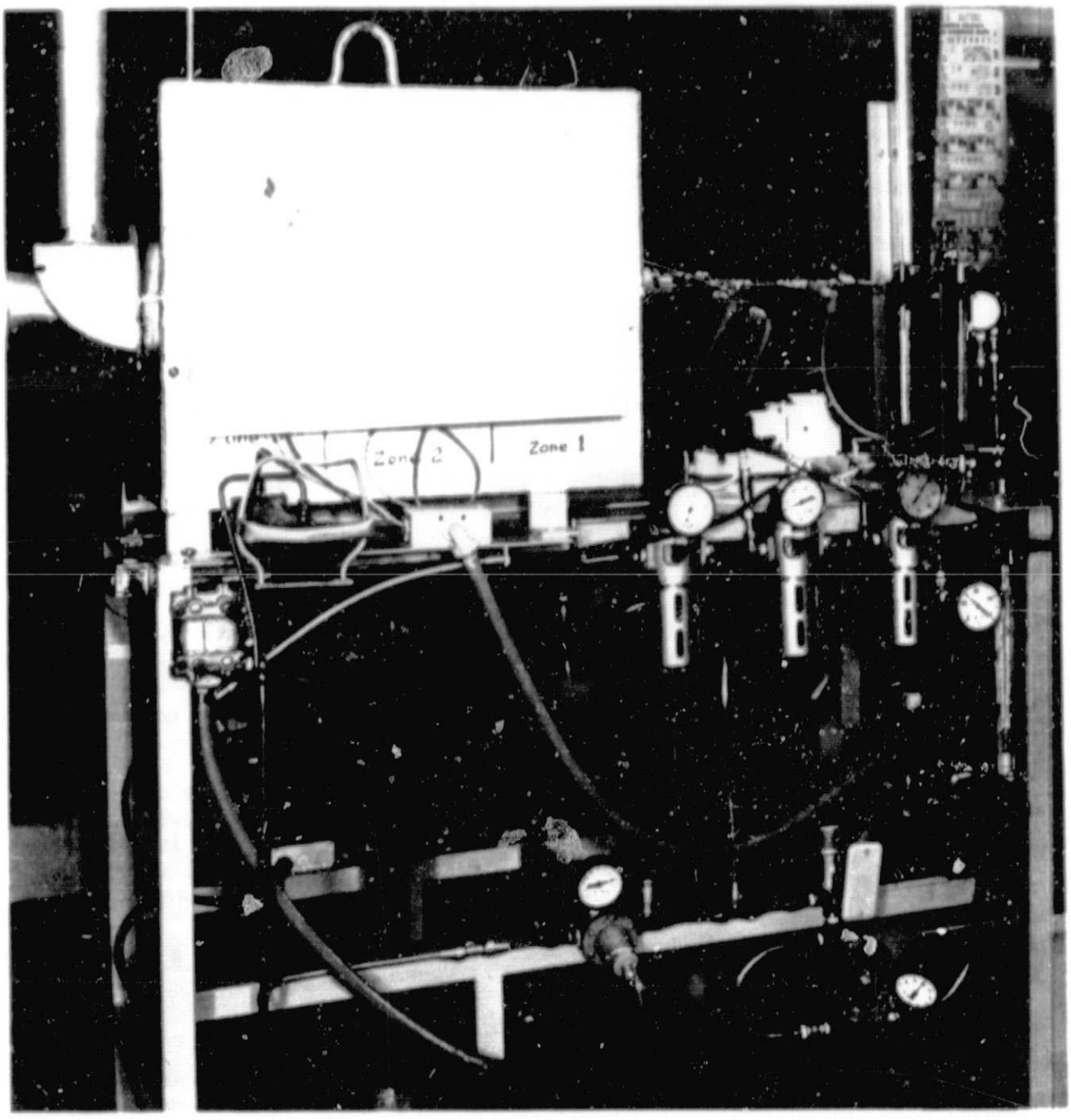

TE84-7955

Figure 37. Corrosion/oxidation test fixture.

4.5.2 Corrosion/Oxidation Resistance Test Results

The corrosion test was conducted on the diesel-fuel-fired combustion rig at temperatures of 899°C (1650°F) for a total of 100 hr. This time was accumulated in four 24-hr cycles. The following three ceramic coatings were subjected to the corrosion test:

- o vendor coating A
- o vendor coating B
- o 80/20 SYSZ/Eccosphere coating

In addition, an Allison research coating was tested. This coating was a cemented hollow particle system in which the hollow zirconia powders were cemented together instead of being plasma sprayed. This coating was developed to investigate the thermal conductivity of a more nearly ideal hollow particle structure in which most of the particles were closed pore-hollow spheres. The cemented structure was included in the corrosion test due to the unavailability of a plasma-sprayed system.

At the completion of the 100-hr test period, two of the four coating specimens, vendor coating B and the cemented HYSZ specimen, had separated from the substrates. It could not be determined when during the 100 hr test period this separation occurred. The separated pieces could not be located in the test chamber. Visual examination of vendor coating A and the 80/20 SYSZ/Eccosphere coating specimens showed no obvious damage to the surfaces as a result of the testing. Pretest and posttest specimens are shown in Figure 38. SEM examination of the tested structures, as shown in Figure 39, and comparison with similar specimens examined prior to testing (Figures 19 and 22, respectively) reveal no obvious alterations to the microstructure or any penetration of contaminants below the surface. Semiquantitative X-ray energy dispersion analysis (XEDA) of specimens before and after testing reveals basically the same chemistry with no diesel fuel-supplied contamination, e.g., sulfur or sodium compounds, being present.

No definite conclusions could be made regarding the susceptibility of the coating systems to damage by subsurface contamination. It was apparent that gaseous diesel fumes did not affect the integrity of the coating, at least for the period tested. It has not been determined whether liquid fuel will penetrate the coating and subsequent to that, undergo a phase change which could initiate a damaging fracture.

4.6 THERMAL SHOCK/FATIGUE RESISTANCE

4.6.1 Approach

The thermal shock/fatigue test was used as a primary method for ranking the performance of the coatings. In the studies performed in this program, TBC thicknesses up to 1.52 mm (0.060 inch) were investigated.

In the thermal shock test fixture, shown in Figures 40 and 41, eight test specimens were mounted on a rotating carousel. Surrounding the carousel were four gas/oxygen burners spaced 90 deg apart. Interspaced between each burner was a cooling air nozzle. The carousel rotated 45 deg at a time, stopping with the test specimen exposed to either a gas flame or a cooling air jet for a

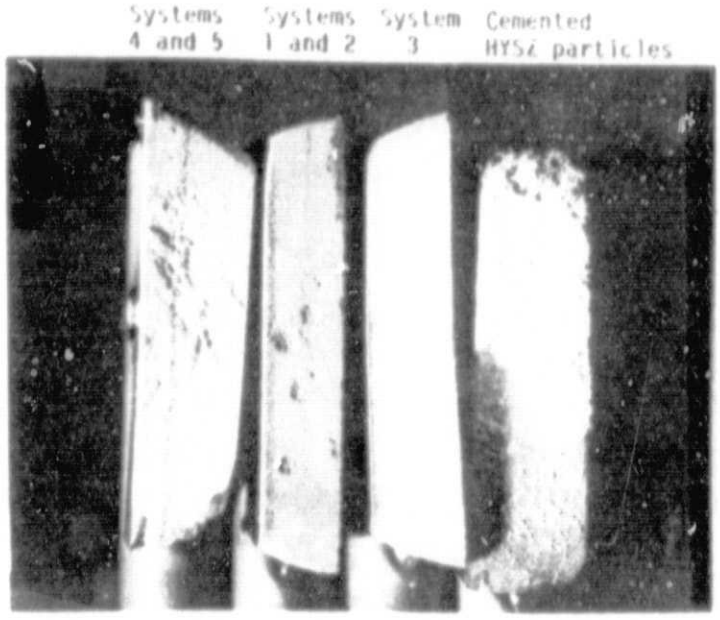

a. Pretest samples

ORIGINAL PAGE IS
OF POOR QUALITY

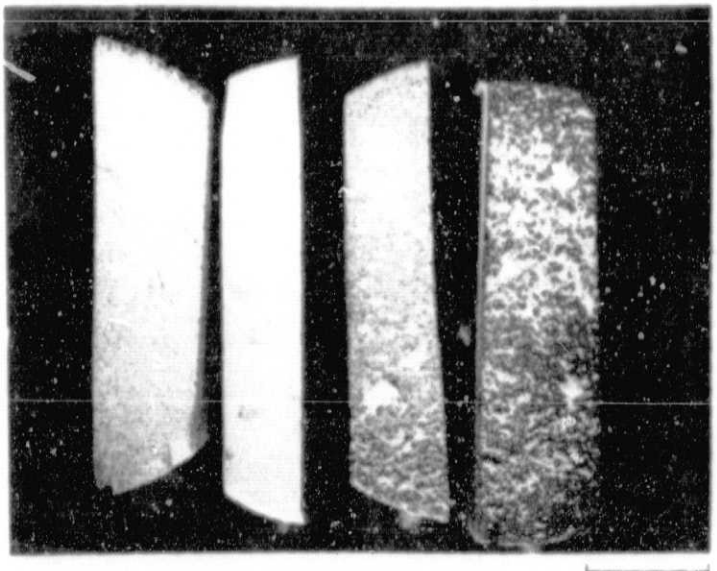

b. Posttest samples

6.35 mm
(0.25 in.)
TE84-7951

Figure 38. Corrosion/oxidation test samples.

ORIGINAL PAGE IS
OF POOR QUALITY

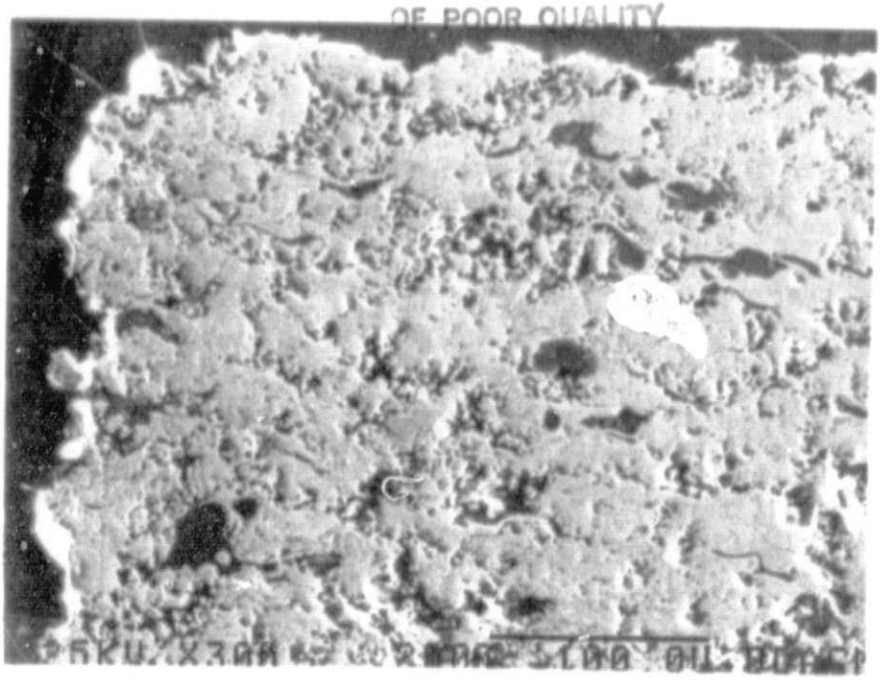

a. Systems 1 and 2

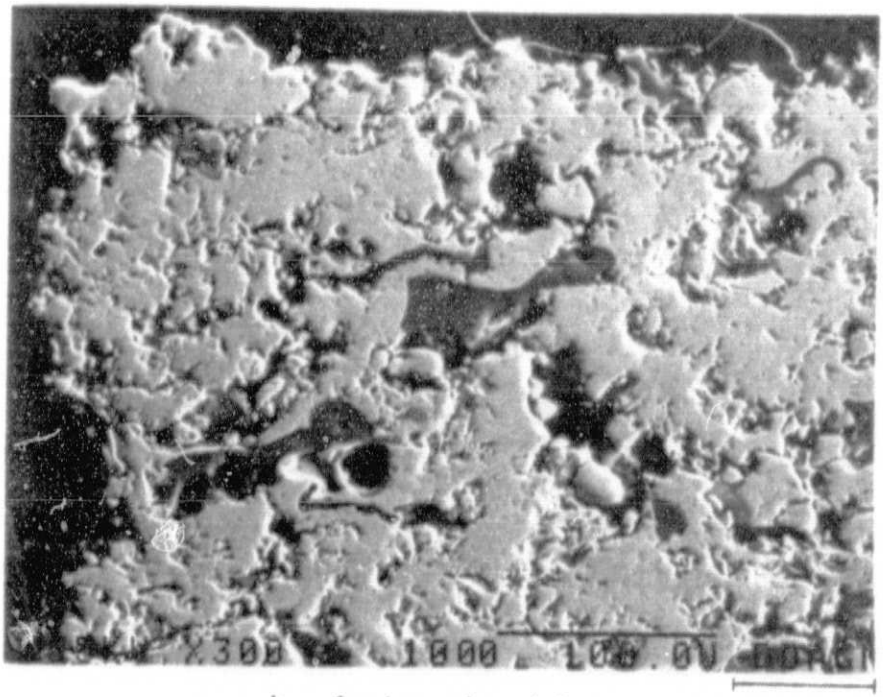

b. Systems 4 and 5

0.0635
(0.0025 in.) TE84-7958

Figure 39. Corrosion test results as seen through a scanning electron microscope.

ORIGINAL PAGE IS
OF POOR QUALITY

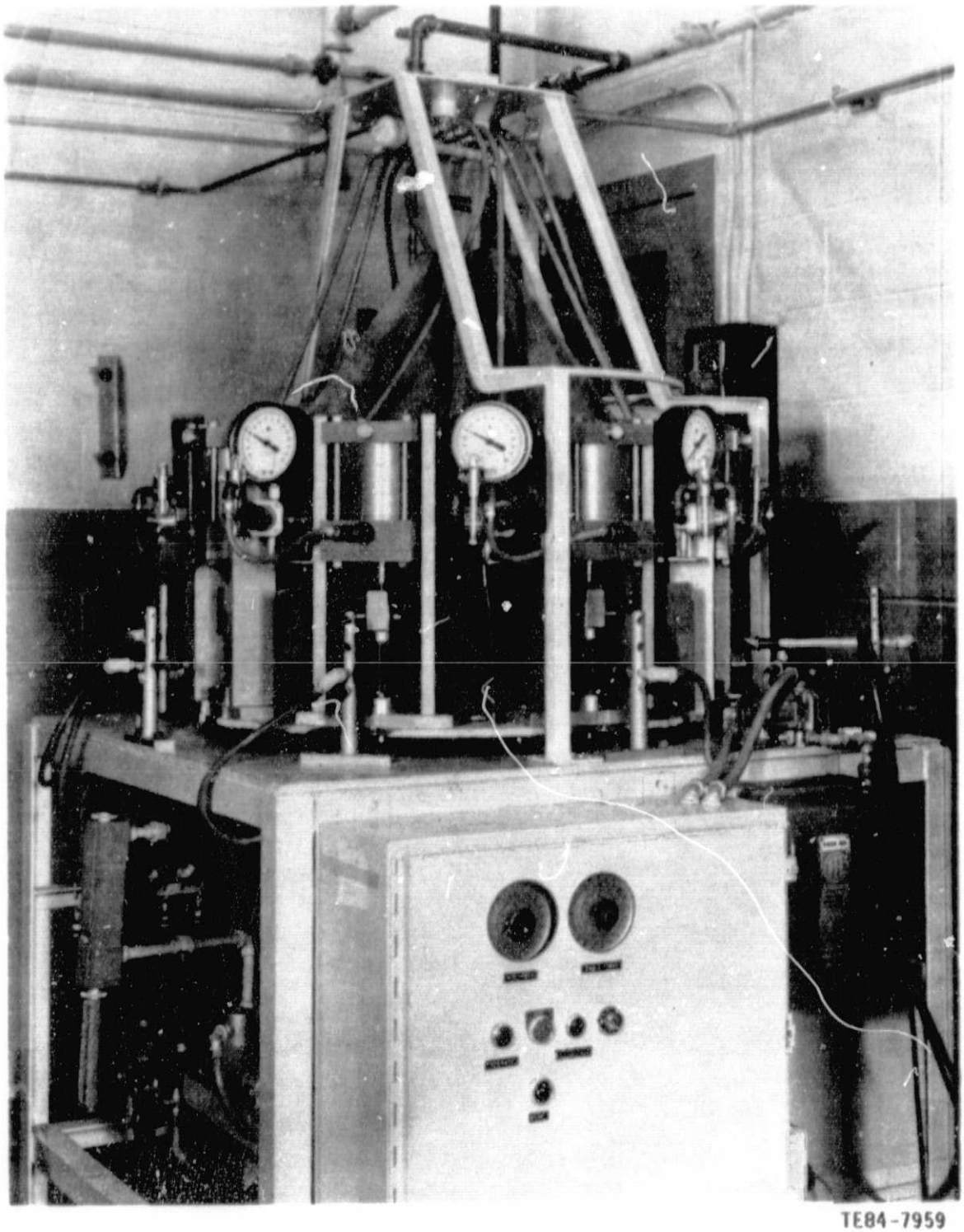

TE84-7959

Figure 40. Overall view of the thermal shock test fixture.

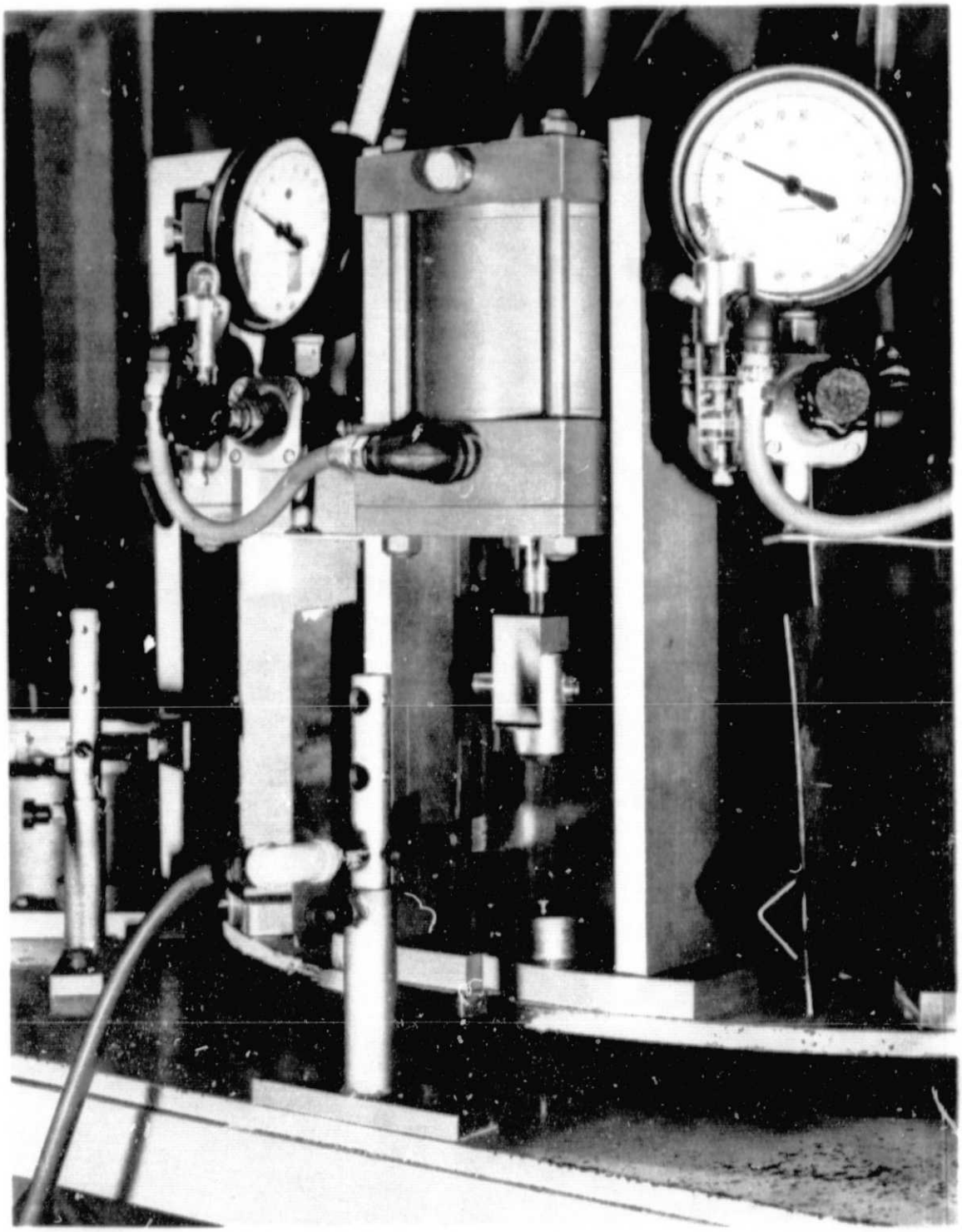

TE84-7960

Figure 41. Burner station of the thermal shock test rig.

ORIGINAL PAGE IS
OF POOR QUALITY

preset period. For this test, each sample was heated and cooled approximately 225 times each hour. Each test specimen was sequentially exposed to all of the burners and cooling jets, thereby eliminating the effects of slight nonuniformities between each burner and cooling jet station.

The sample surface temperature was monitored with a radiation thermometer. Emissivity of the sample surface was selected as 0.52 for purposes of presetting the thermometer. This value is based on NASA test data of similar TBCs (Reference 3).

4.6.2 Thermal Shock Resistance Test Results

Thermal shock testing was conducted on the carrousel rig described in subsection 4.6.1. A full complement of eight specimens were initially loaded into the test rig. As the test progressed and early failures occurred, additional specimens were added. Figure 42 shows a typical test cycle. The surface temperature of each of the coating specimens was monitored by the radiation thermometer during the heating portion of the cycle. Temperatures measured at the coating surface varied between 732°C and 816°C (1350°F and 1500°F). This variation in the surface temperature of the coatings is probably due to differences in the thermal conductivity of each of the systems and minute differences in the emissivity of the surface.

Testing was considered to be completed with the achievement of 25,260 cycles, which is equivalent to 112 hr of cyclic variations. Table XVI lists the complete series of coatings tested. Included are three additional coating system samples identified as IA, IA_1, and IIIA in Table XVI. These samples were added to stations that became available as a result of early failures of other coating systems.

Four coating systems completed the 25,260-cycles test successfully, as listed in Table XVI. Although these four coatings remained firmly adhered to their respective substrates, there was thermal cracking present at the surface of the coatings. These cracks were primarily located in the region of the flame impingement on the coating surface and are believed to be a direct result of the unusually high heat flux associated with this particular method of testing. This characteristic is not believed to be present during actual diesel cycle operation.

The performance of each of the coating systems is described in order of system number (refer to Table XVI) and followed by a summary and discussion of significant results.

System I--Vendor Coating A without an SI Pad

Three samples of vendor coating A were evaluated in the thermal shock test fixture, Nos. I, IA, and IA_1 in Table XVI. Figure 43 shows sample I before the test and the spall that occurred after 20 thermal cycles at midthickness in the coating system. This spall may have been precipitated by an existing subsurface crack in the sample. This sample had a translucent appearance during heating not seen in other test specimens, suggesting an interruption in heat flux by a subsurface layer crack. Two additional vendor coating A specimens incurred coating/bond coat interface separations. Sample IA, shown in Figure 44, completed 6,723 thermal cycles and sample IA_1, shown in Figure 45, completed 192 thermal cycles.

Table XVI.
Thermal shock test results.

System number	Coating/substrate description	SI pad	Cycles completed	Remarks
I	Vendor coating A/EMS 235	No	20	Shear failure in coating
II*	Vendor coating A/Waspaloy	Yes	25,260	No failure
III	Vendor coating B/Ni-Resist D5B	No	17	Delamination at coating/bond coat surface
IV*	80/20/Waspaloy	No	25,260	No failure
V	80/20/Waspaloy	Yes	24,350	Delamination at coating/bond coat surface
VI*	PS/HYSZ/Waspaloy	No	25,260	No failure
VII*	PS/HYSZ/Waspaloy	Yes	25,260	No failure
IA	Vendor coating A/Ni-Resist D5B	No	6,723	Delamination at coating/bond coat surface
IA_1	Vendor coating A/Waspaloy	No	192	Delamination at coating/bond coat surface
IIIA	Vendor coating B/EMS 235	No	0.5	Delamination at coating/bond coat surface

*Four coating systems completed 112 hr (25,260 cycles) of thermal shock testing

System II--Vendor Coating A with an SI Pad

The test specimen of this coating system completed the 25,260 cycle test with the coating firmly attached to the substrate. Surface mud flat cracking occurred in this sample, as seen in Figures 46 and 47. This same phenomenon was observed in varying degrees in other coating specimens that survived large numbers of thermal cycles. Figure 47 also shows an edge crack present at the coating/SI interface. Details of the SI pad are not clearly seen due to smearing of the pad in the specimen cutting process.

System III--Vendor Coating B without an SI Pad

Two specimens of this coating system, samples III and IIIA in Table XVI, were tested for thermal shock resistance. Sample III, as shown in Figure 48, delaminated at the coating substrate interface after 17 thermal cycles. Sample IIIA separated at the same location during the first heating cycle. Figure 49

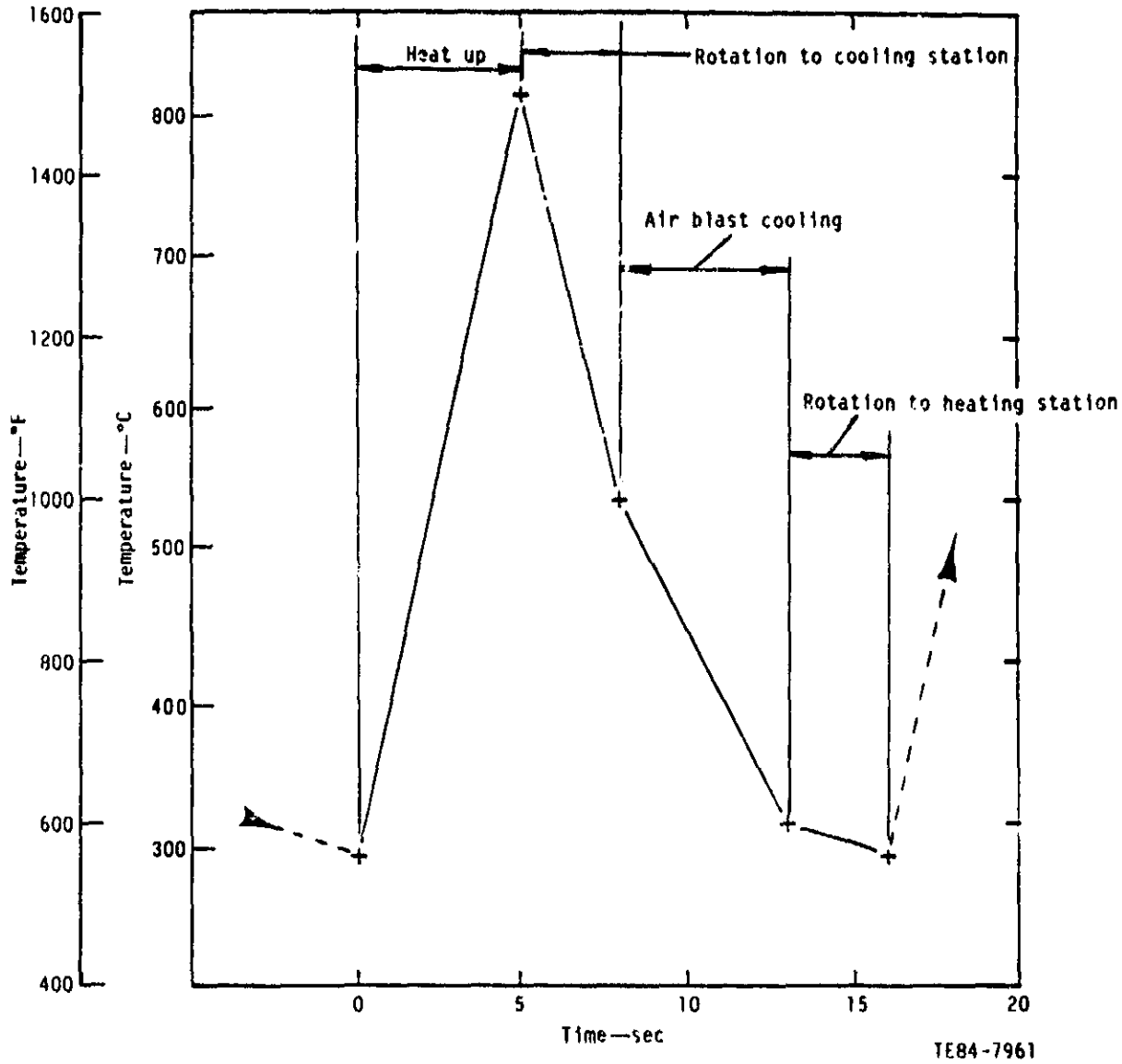

Figure 42. Typical thermal shock test cycle.

ORIGINAL PAGE IS
OF POOR QUALITY

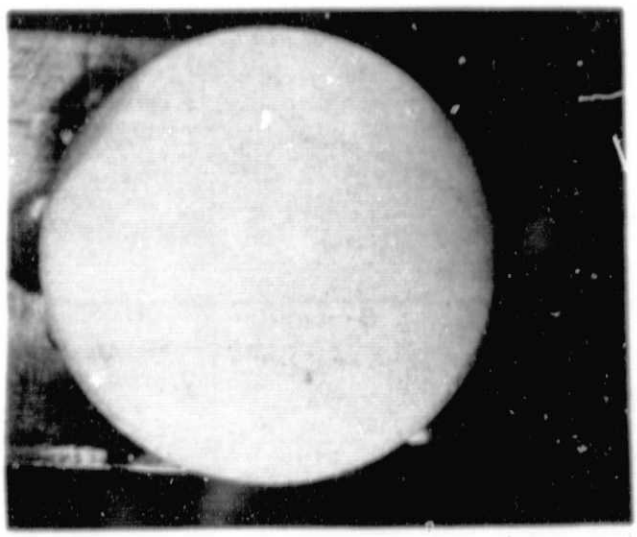

a. Pretest

6.35 mm
(0.25 in.)

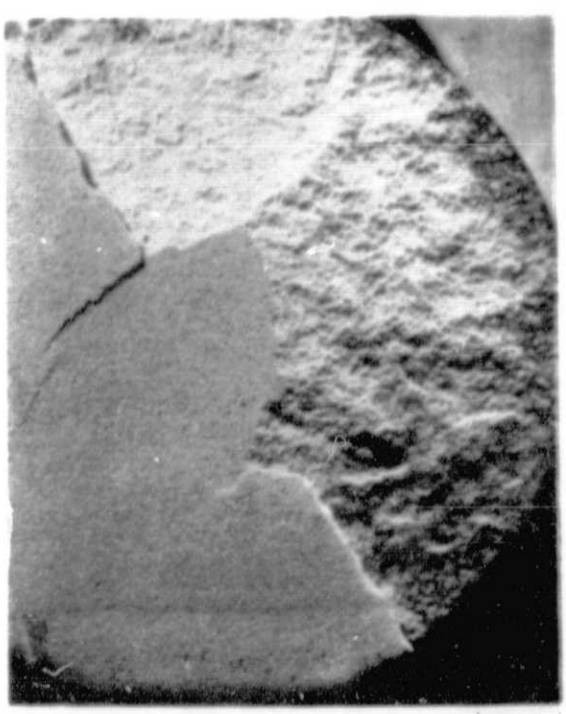

2.54 mm
(0.1 in.)

2.54 mm
(0.1 in.)

b. Posttest

1E84-7962

Figure 43. Thermal shock testing to system 1--vendor coating A without a strain isolator pad; substrate of EMS 235; 20 cycles to failure.

ORIGINAL PAGE IS
OF POOR QUALITY

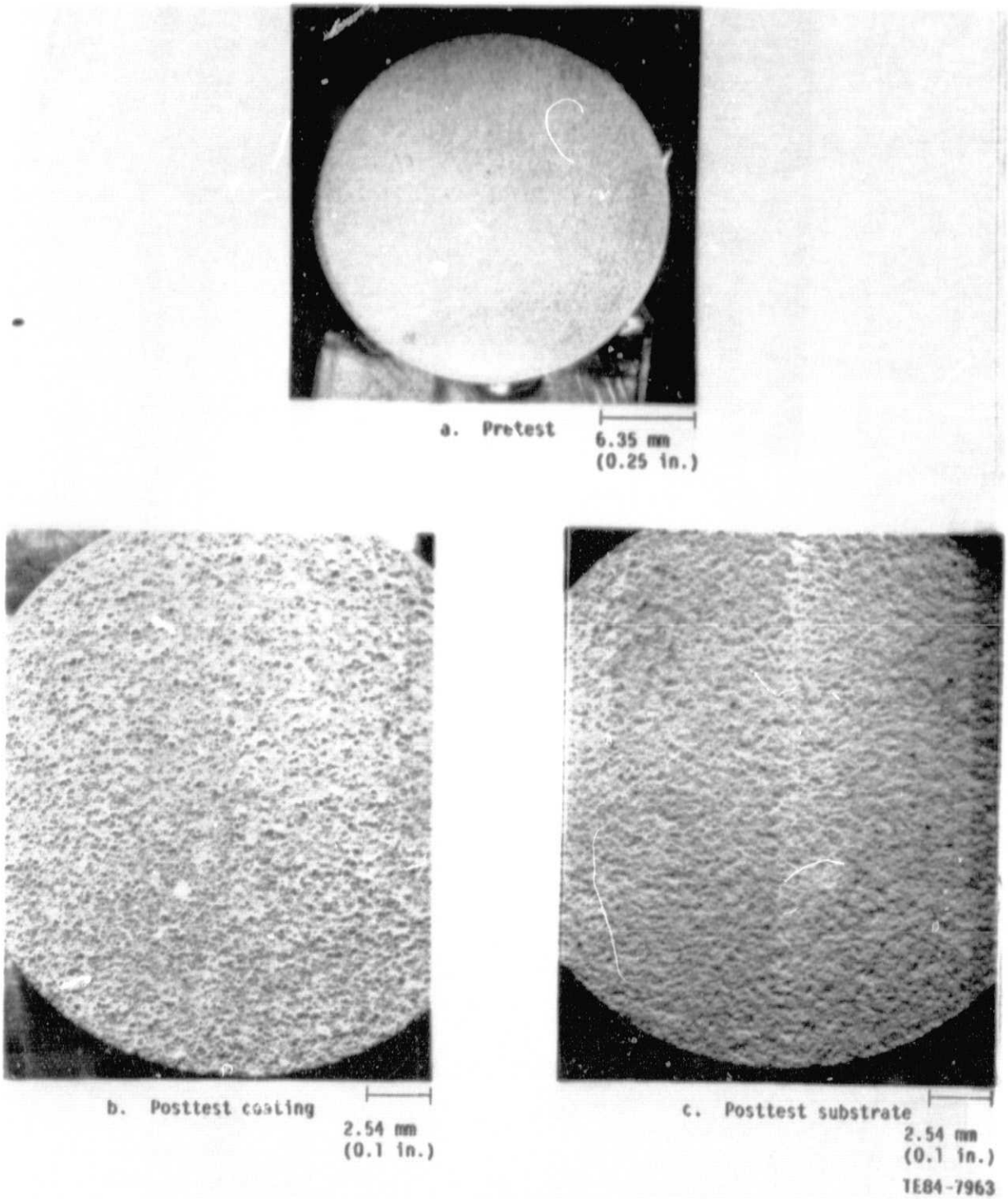

Figure 44. Thermal shock testing to system 1--vendor coating A without a strain isolator pad; substrate of D5B; 6723 cycles to failure.

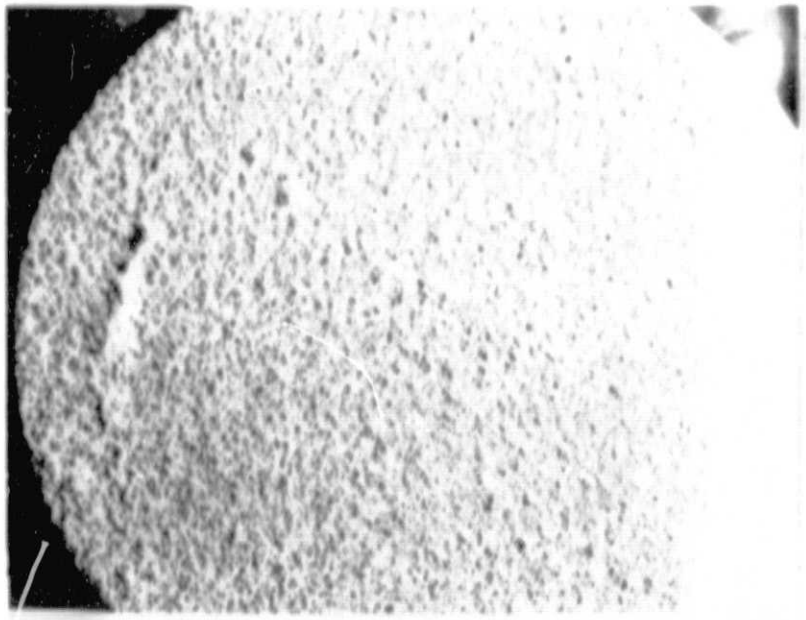

a. Posttest substrate

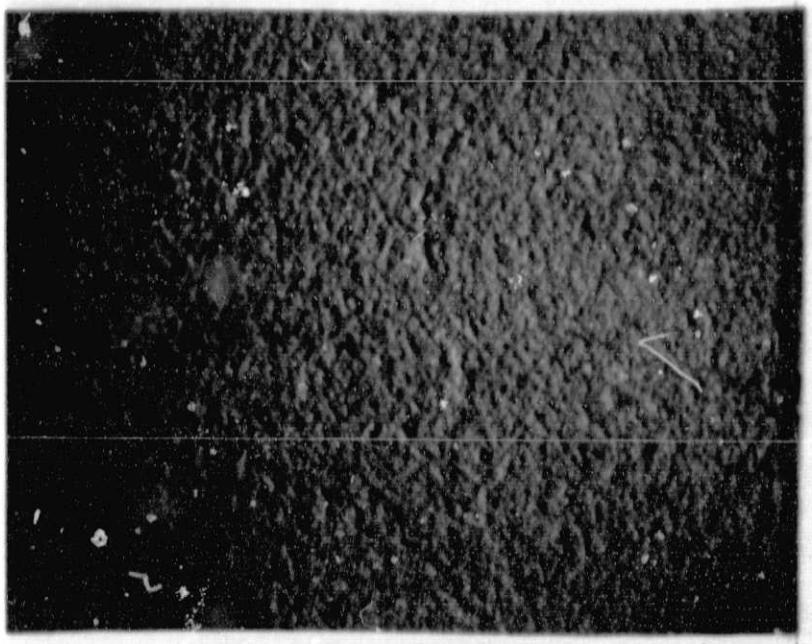

b. Posttest coating

2.54 mm
(0.1 in.)

TE84-7964

Figure 45. Thermal shock testing to system 1--vendor coating A without a strain isolator pad; substrate of Waspaloy; 192 cycles to failure.

ORIGINAL PAGE IS
OF POOR QUALITY

ORIGINAL PAGE IS
OF POOR QUALITY

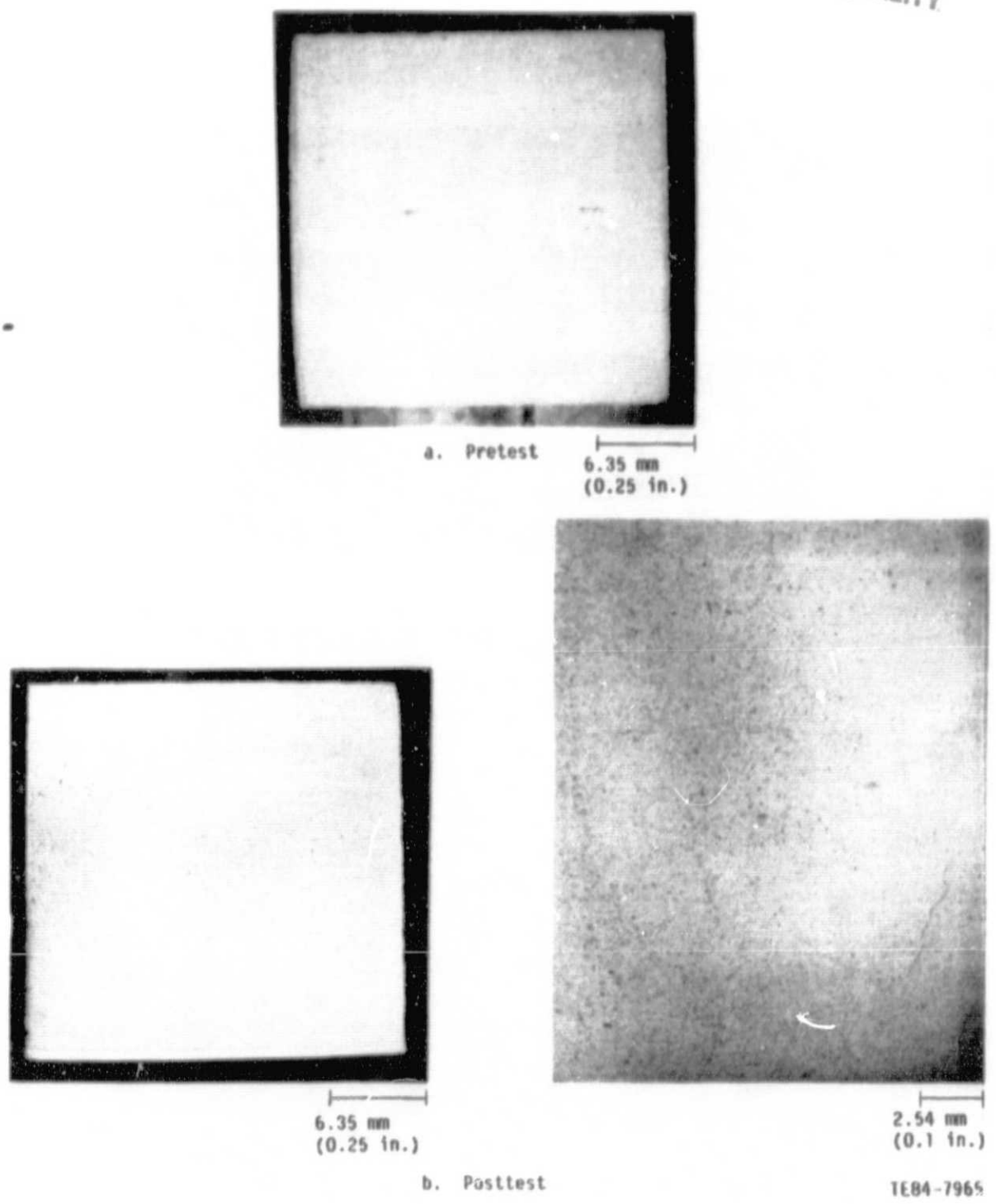

Figure 46. Thermal shock testing to system 2--vendor coating A with a strain isolator pad; substrate ot Waspaloy; completed 25,260 cycles without failing.

ORIGINAL PAGE IS
OF POOR QUALITY

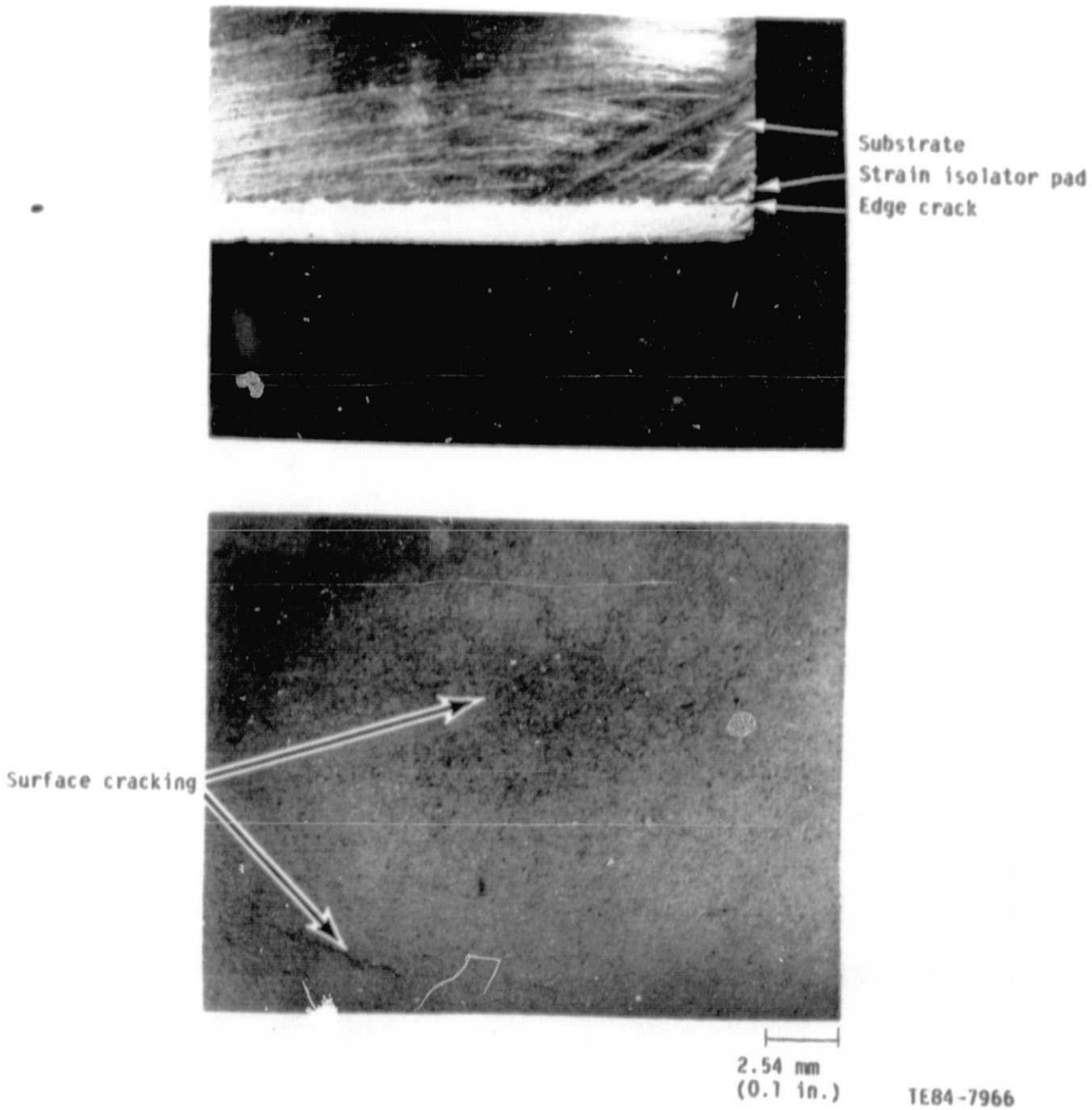

Figure 47. Results of thermal shock testing to system 2--vendor coating A with a strain isolator pad on a Waspaloy substrate after the completion of 25,260 cycles without failing.

ORIGINAL PAGE IS
OF POOR QUALITY

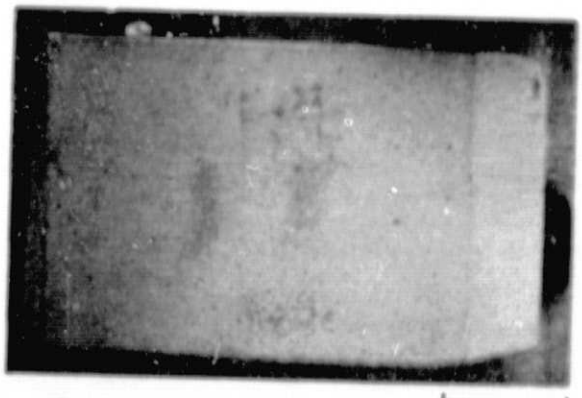

a. Pretest

6.35 mm
(0.25 in.)

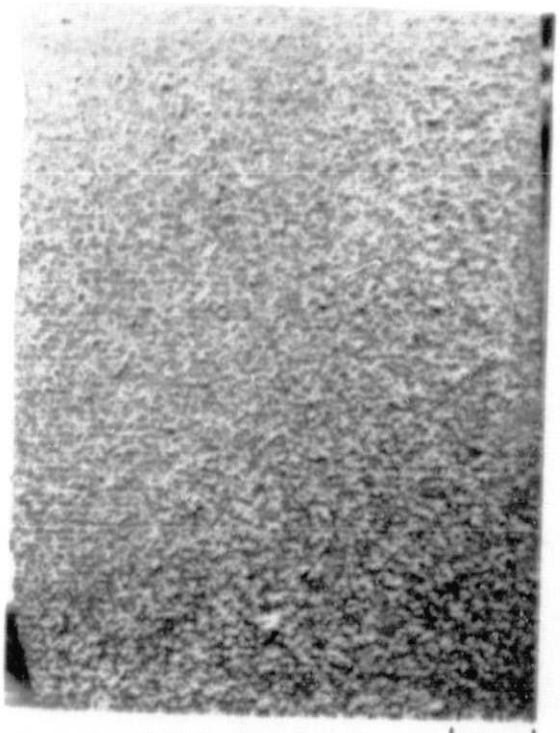

b. Posttest substrate

2.54 mm
(0.1 in.)

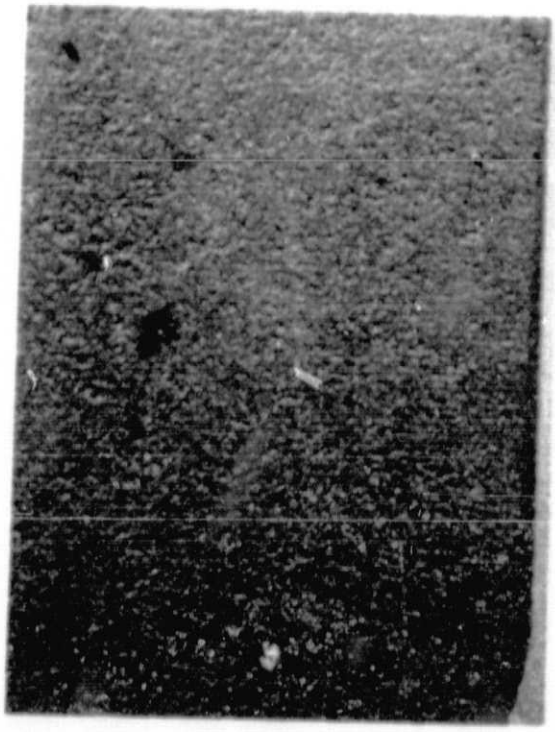

c. Posttest coating

2.54 mm
(0.1 in.)

TE84-7967

Figure 48. Thermal shock testing to system 3--vendor coating B without a strain isolator; substrate of D5B; 17 cycles to failure.

ORIGINAL PAGE IS
OF POOR QUALITY

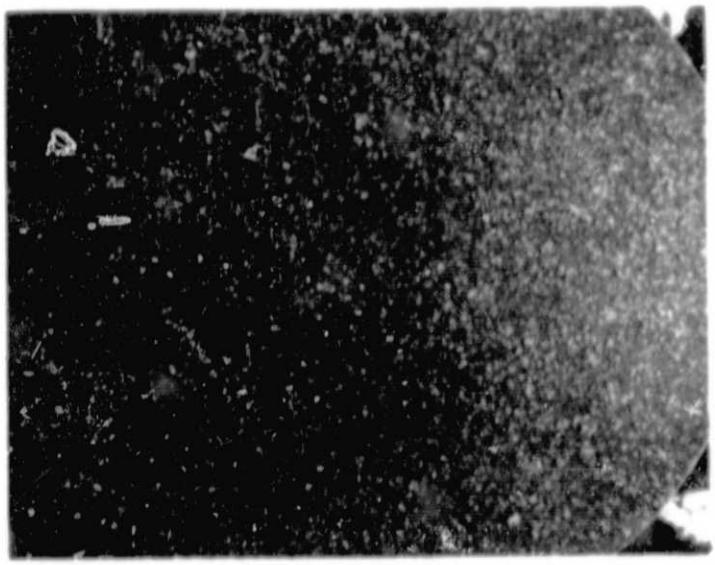

a. Posttest substrate

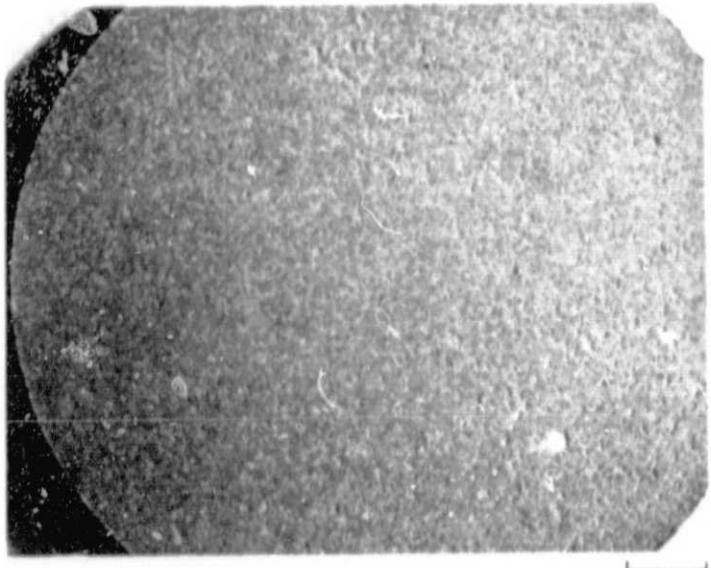

b. Posttest coating

2.54 mm
(0.1 in.)

1E84-7968

Figure 49. Thermal shock testing to system 3--vendor coating B without a strain isolator pad; substrate of EMS 235; 0.5 cycles to failure.

shows the separated sample IIIA. Vendor coating B was not available in combination with an SI pad.

System IV--80/20 SYSZ/Eccosphere Coating without an SI Pad

The 80/20 coating test specimen completed the 25,260 thermal cycle testing with the coating attached to the substrate. Figure 50 shows the test specimen before and after the thermal shock test. Mud flat cracking, shown in Figure 51, occurred in the 80/20 specimen to a greater degree than in vendor coating A and the PS/HYSZ coating (systems VI and VII) described hereafter. Figure 51 shows an edge crack that virtually encircled the periphery of the specimen and that is clearly located in the ceramic portion of the coating. The edge crack in the 80/20 specimen was considered more severe than that observed in the vendor coating A specimen.

System V--80/20 SYSZ/Eccosphere Coating with an SI Pad

The 80/20 coating specimen incorporating an SI pad completed 24,350 thermal shock cycles before it suffered a coating delamination in the same location of the edge crack that was observed in the 80/20 specimen without the SI pad. Figure 52 shows the pretest appearance of the 80/20 SI specimen and both surfaces of the coating at the plane of delamination.

System VI--PS/HYSZ Coating without an SI Pad

The PS/HYSZ coating system completed the 25,260 cycle thermal shock test with the coating firmly attached to the substrate. Figure 53 shows the appearance of the coating before and after thermal shock testing. The surface cracks in the PS/HYSZ specimen, shown in Figures 53 and 54, were less severe than those observed in vendor coating A and the 80/20 coating specimens. Figure 54 also shows a minor localized edge crack near the coating/substrate interface.

System VII--PS/HYSZ Coating with an SI Pad

The PS/HYSZ specimen completed the 25,260 cycle thermal shock test with the coating system firmly attached to the substrate. Figure 55 shows the condition of the test specimen after testing. The PS/HYSZ SI coating, like its sister PS/HYSZ coating in system VI, had moderate surface (mud flat) cracking. Figure 55 also shows the edge of the coating specimen where no edge cracking was observed in the coating structure or at the coating/SI interface.

4.6.3 Summary of Thermal Shock Test Results

Four test specimens completed the 25,260 cycle (112 hr) thermal shock test. Ranked in order of observed resistance to surface (mud flat) cracking and edge or intercoating laminar cracking, they were:

- o PS/HYSZ coating with an SI pad
- o PS/HYSZ coating
- o vendor coating A with an SI pad
- o 80/20 SYSZ/Eccosphere coating

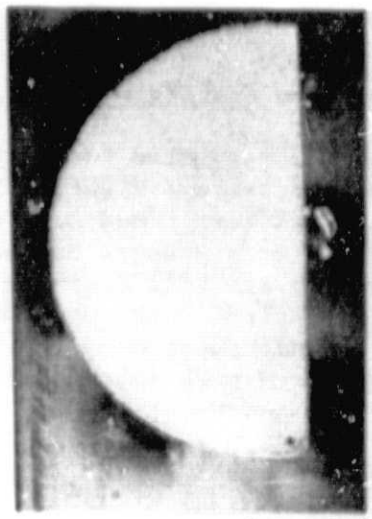

6.35 mm
(0.25 in.)

a. Pretest

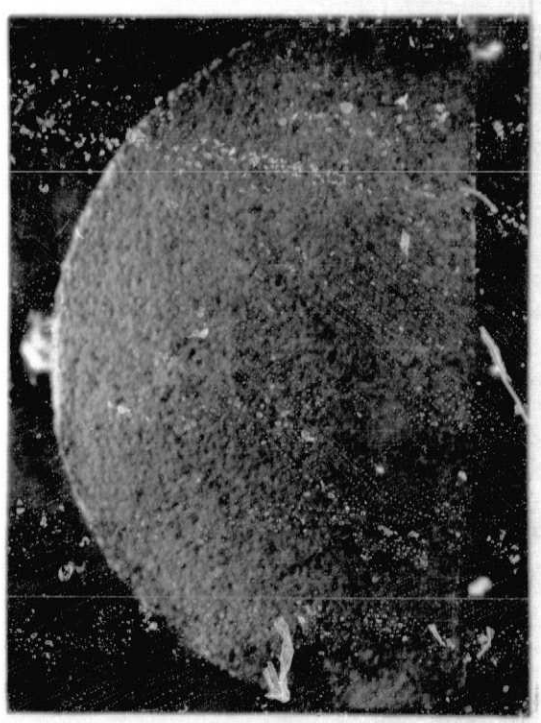

6.35 mm
(0.25 in.)

2.54 mm
(0.1 in.)

b. Posttest

TE84-7969

Figure 50. Thermal shock testing to system 4--80/20 SYSZ/Eccosphere coating without a strain isolator pad; substrate of Waspaloy; completed 25,260 cycles without failing.

ORIGINAL PAGE IS
OF POOR QUALITY

ORIGINAL PAGE IS
OF POOR QUALITY

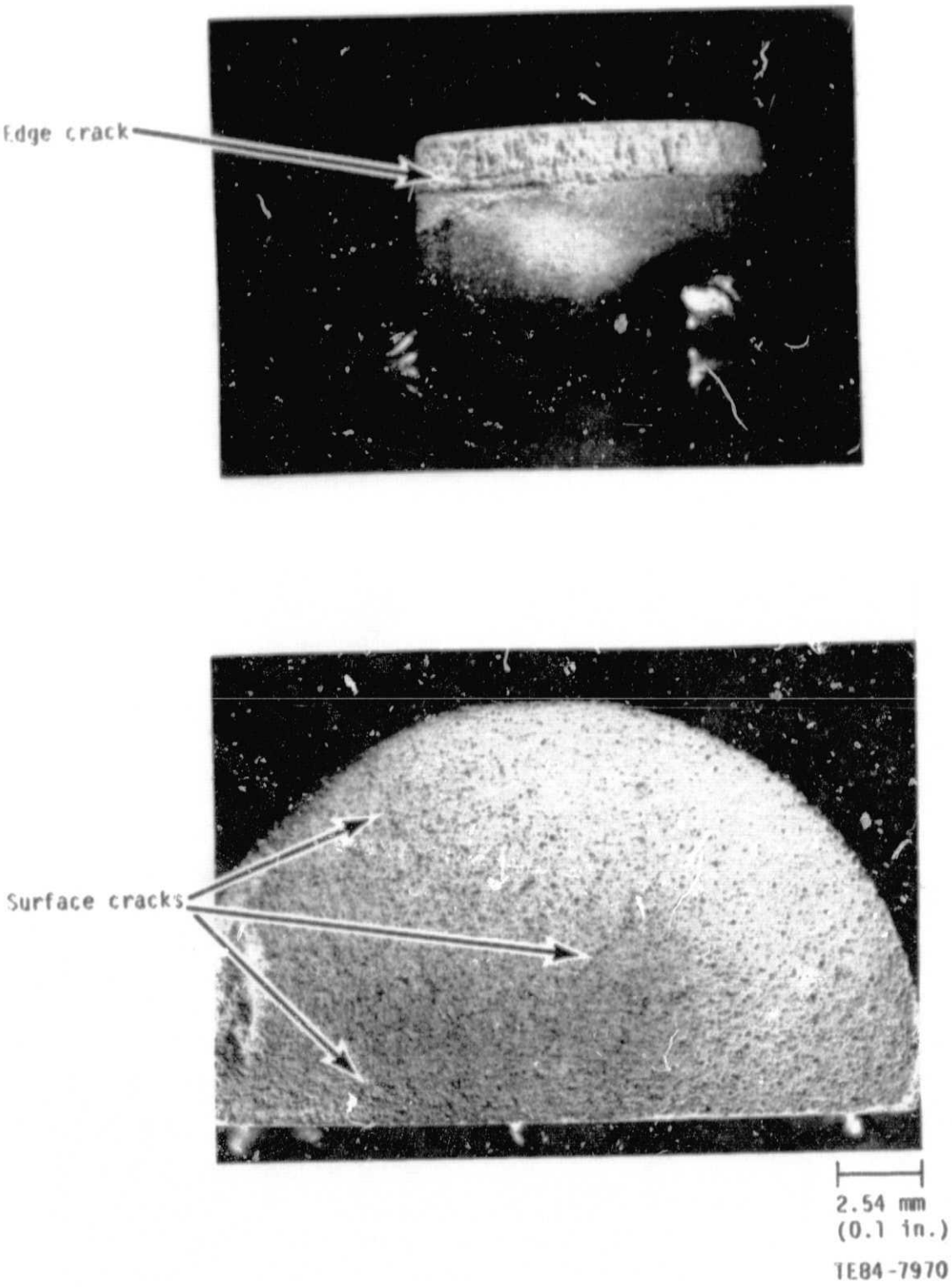

Figure 51. Results of thermal shock testing to system 4--80/20 SYSZ/Eccosphere coating without a strain isolator pad on a Waspaloy substrate atter the completion of 25,260 cycles without failing.

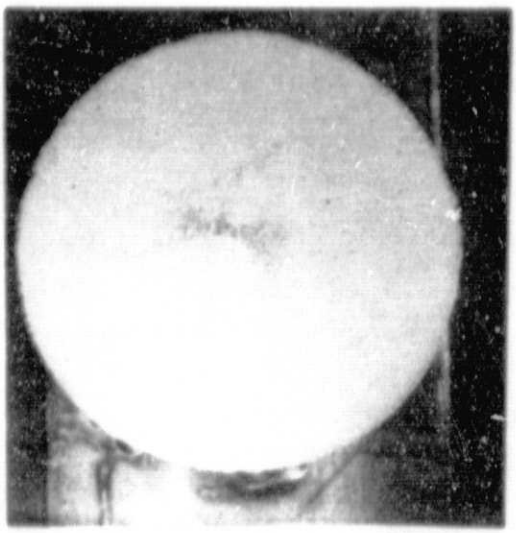

a. Pretest

6.35 mm
(0.25 in.)

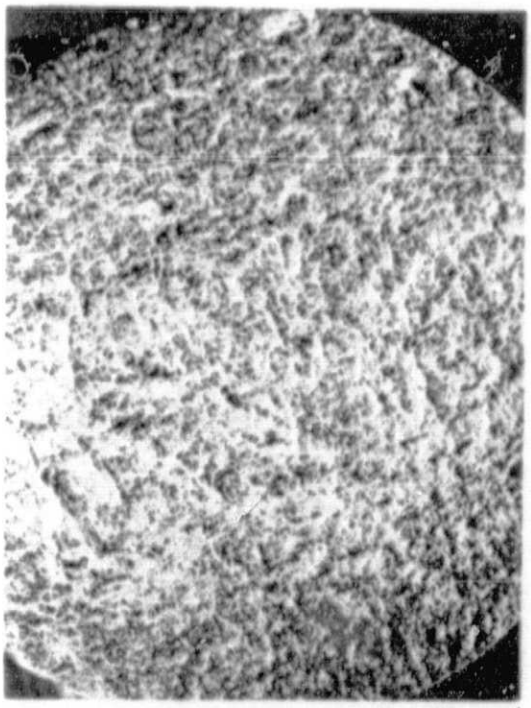

b. Posttest substrate

2.54 mm
(0.1 in.)

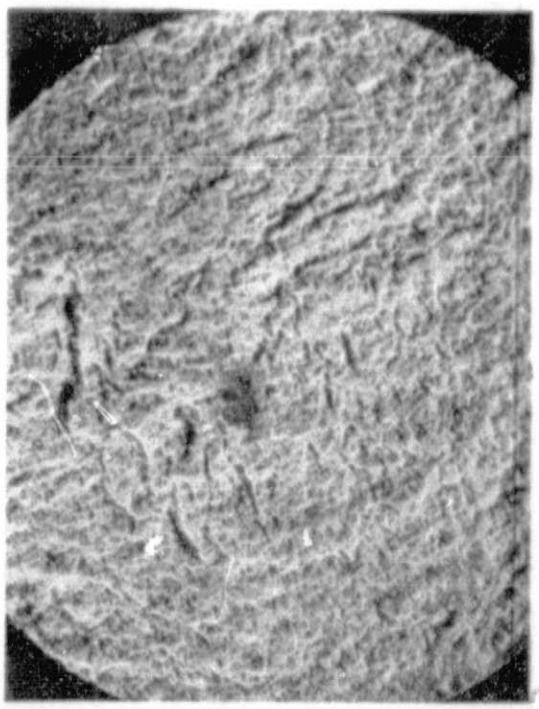

c. Posttest coating

2.54 mm
(0.1 in.)

TE84-7971

Figure 52. Thermal shock testing to system 5--80/20 SYSZ/Eccosphere coating with a strain isolator pad; substrate of Waspaloy; 24,350 cycles to failure.

ORIGINAL PAGE IS
OF POOR QUALITY

ORIGINAL PAGE IS
OF POOR QUALITY

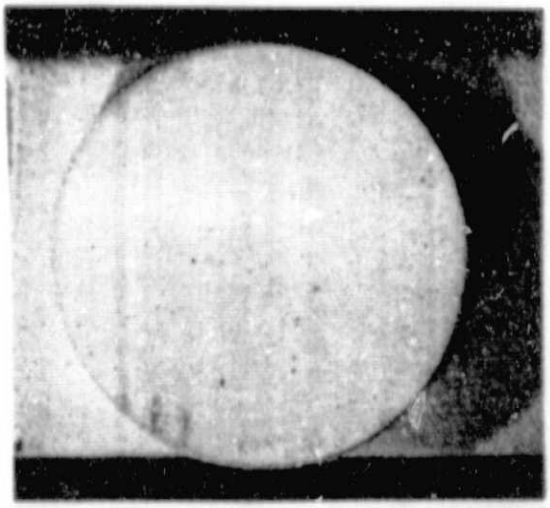

a. Pretest

6.35 mm
(0.25 in.)

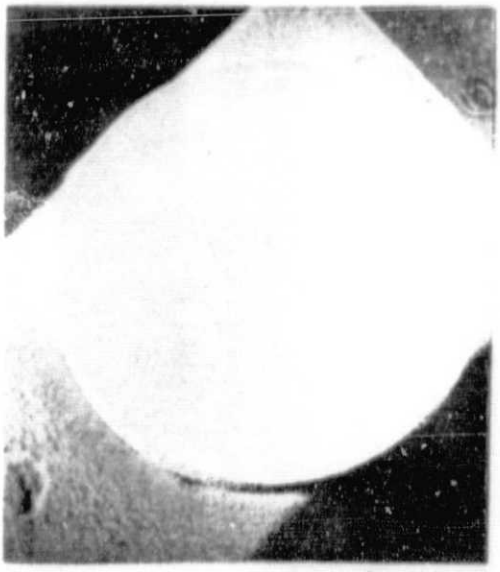

6.35 mm
(0.25 in.)

2.54 mm
(0.1 in.)

b. Posttest

TE84-7972

Figure 53. Thermal shock testing to system 6--PS/HYSZ coating without a strain isolator pad; substrate of Waspaloy; completed 25,260 cycles without failing.

ORIGINAL PAGE IS
OF POOR QUALITY

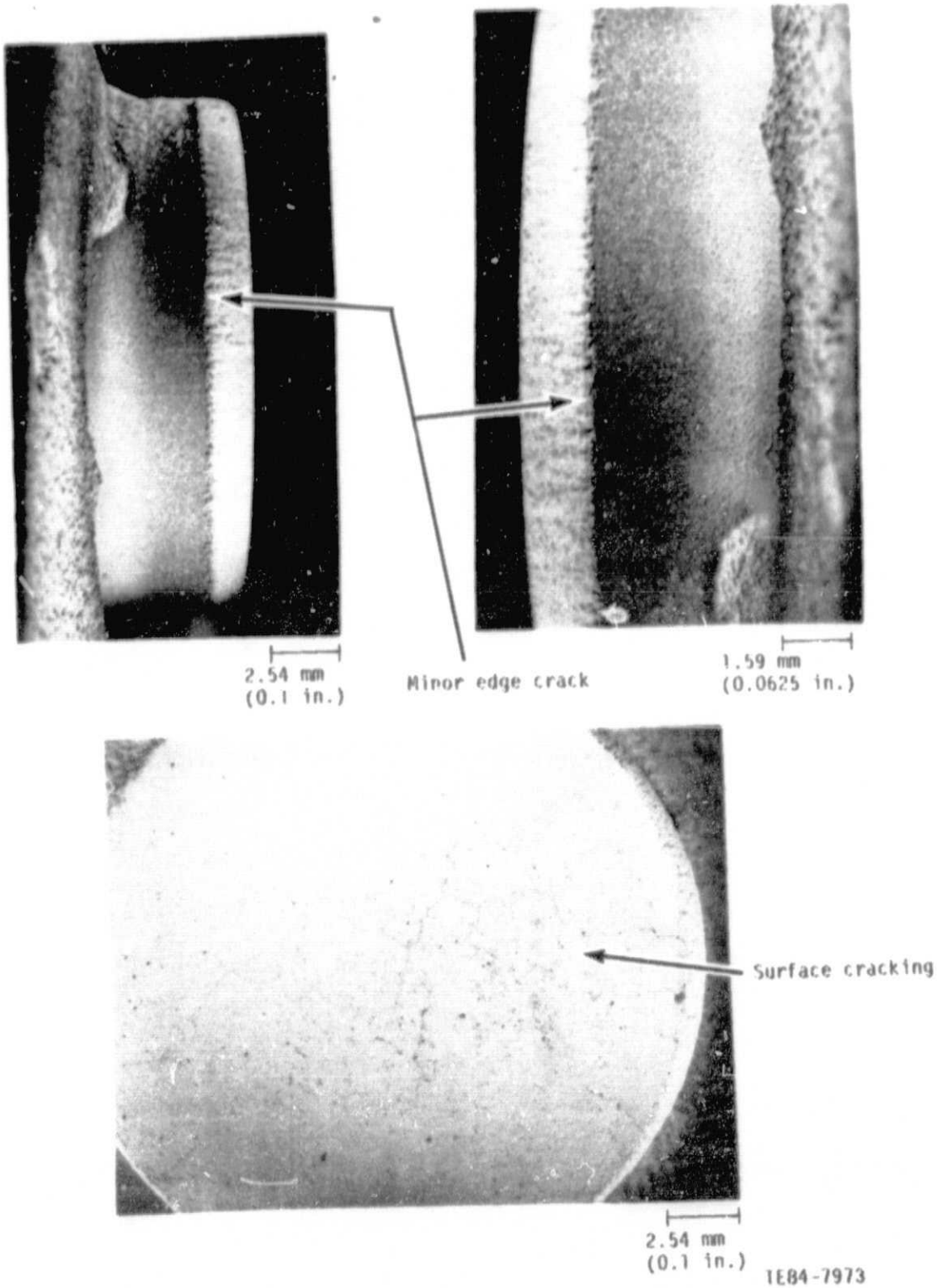

Figure 54. Results of thermal shock testing to system 6--PS/HYSZ coating without a strain isolator pad on a Waspaloy substrate after completion of 26,250 cycles without failing.

OF POOR QUALITY

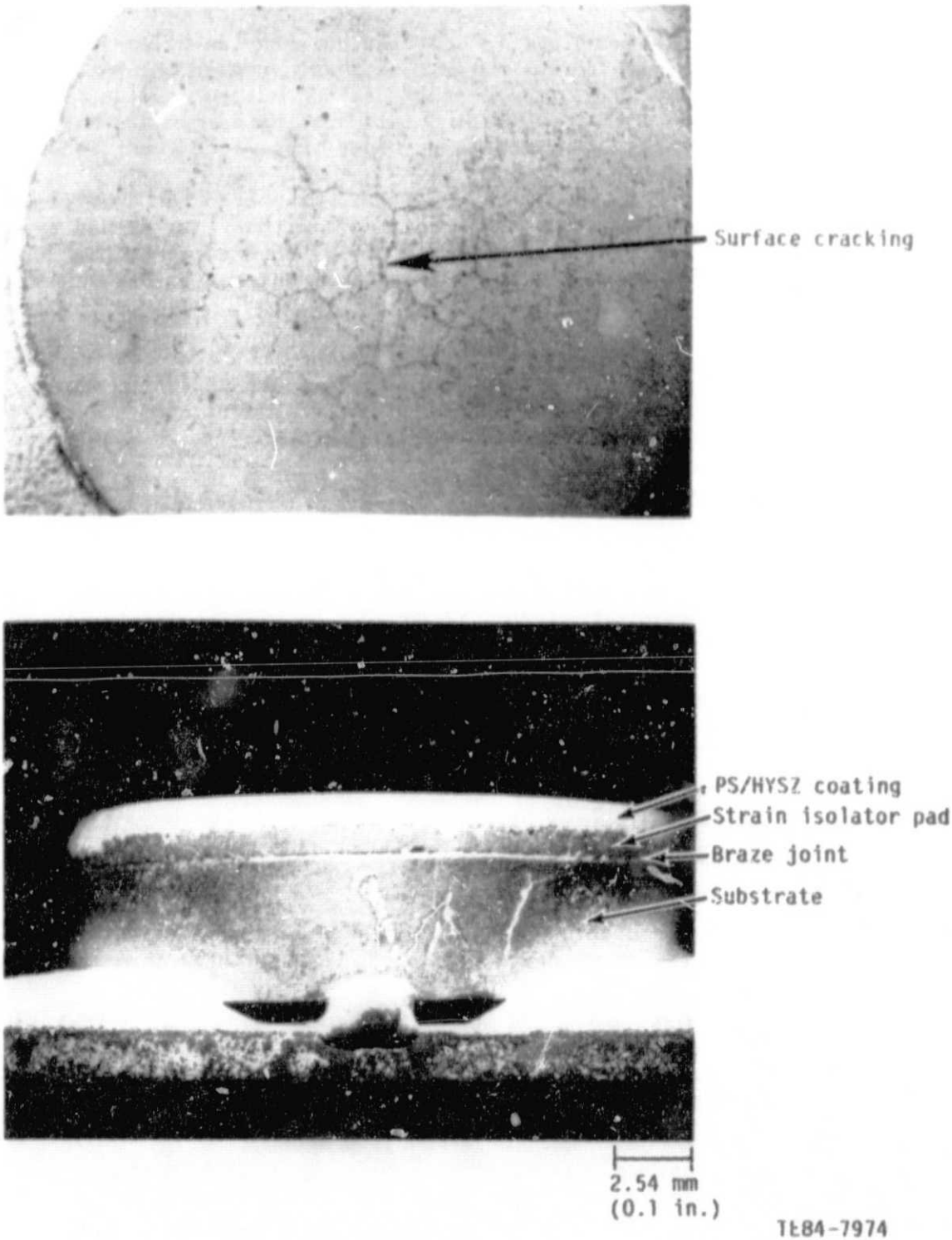

Figure 55. Results of thermal shock testing to system 7--PS/HYSZ coating with a strain isolator pad on a Waspaloy substrate after the completion of 25,260 cycles without failing.

4.6.4 Discussion of Thermal Shock Test Results

The 80/20 SYSZ/Eccosphere coating, in combination with the SI, nearly completed the thermal shock testing before a delamination occurred in the interior of the coating. The similar 80/20 SYSZ/Eccosphere coating without the SI pad exhibited a similar characteristic, suggesting this coating system may have reduced durability compared to the PS/HYSZ coating under these test conditions.

Vendor coating A, in combination with an SI pad, completed the thermal shock testing whereas three samples of Vendor coating A without the SI pad separated from their substrates early in the test sequence. This suggests that the SI pad element corrects a deficiency in the mechanism which attaches vendor coating A to its substrate.

The majority of coating separations occurred during the first few heating cycles of the test fixture daily start-up. These start-up cycles were probably the most severe in terms of thermal shock to the coating system and would be very similar to the cold start-up of a diesel engine.

4.7 COATING SELECTION FOR ENGINE TESTING

4.7.1 Approach

The selection of a TBC for engine testing was based primarily on the results of the four static screening tests. The ranking of the coating specimens in each test and a synopsis of test results follows.

Thermal Conducting Test

The samples were ranked as follows:

1. vendor coating A
2. PS/HYSZ coating
3. 80/20 SYSZ/Eccosphere coating
4. vendor coating B

The thermal conductivities of the first three coatings were closely grouped. The thermal conductivity of vendor coating B was 60% greater than that of the first three coatings.

Erosion Test

The samples were ranked as follows:

1. Vendor coating B
2. 80/20 SYSZ/Eccosphere coating
3. vendor coating A
4. PS/HYSZ

All coatings had specific erosion rates comparable to coatings evaluated in other programs. The specific erosion of vendor coating A and the PS/HYSZ coating were virtually identical.

Erosion/Oxidation Test

The samples were ranked as follows:

1,2 vendor coating A and 80/20 SYSZ/Eccosphere coating

Only the two ranked coatings completed this test. A sample of vendor coating B failed during testing and was lost. A sample of the PS/HYSZ coating was not available for testing.

XEDA of the two ranked samples showed no fuel contamination of either coating following the test.

Thermal Shock Test

The samples were ranked as follows:

1. PS/HYSZ coating with an SI
2. PS/HYSZ coating without an SI
3. vendor coating A with an SI
4. 80/20 SYSZ/Eccosphere coating without an SI

The four ranked coating system samples completed the 25,260 cycle test. The first three samples clearly were in better condition than the forth ranked sample. No samples identical to the ranked samples failed in the test. Samples of vendor coating B failed early in the test sequence.

A review of the results of the four screening tests showed that the thermal shock test results should be given the greatest weight due to the following reasons:

- o The thermal shock test gave a greater measure of coating durability under severe test conditions.
- o The thermal shock test was the only screening test in which the primary SI pad function (strain relief) could be evaluated.
- o The thermal conductivities of the coatings were comparable.
- o The erosion test results were also comparable and no absolute value of acceptable specific erosion is known for the diesel engine environment.
- o The corrosion/oxidation test results were inconclusive.

Further, it was reasoned that only the coating systems that did complete the thermal shock test satisfactorily were qualified to be considered for engine testing.

4.7.2 Coating Selection

The PS/HYSZ coating with and without the SI pad was selected to be engine-tested on the piston, fire deck, and valves.

The fact that the PS/HYSZ coating functioned satisfactorily in the thermal shock tests with and without an SI pad implied that it may have superior durability over vendor coating A, which survived the test only when combined with an SI.

A goal of this program was to evalute an SI pad in a diesel engine environment. Based on the results of the thermal shock tests (and structural analysis of the SI pad) the PS/HYSZ coating system with an SI pad was selected for application to the fire deck.

The coating system on the piston and valves would not include a an SI pad. The scope of this program did not include development of the technology necessary to fabricate and attach an SI pad to the complexly shaped piston crown. In the case of the valves, space limitations on the coating system envelope permitted use of the SI pad only in a small region in the center of the valves. This limited application on the valves was deemed impractical.

The fact that the PS/HYSZ coating performed well in the thermal shock test without the SI made it the best choice for use on the piston and valves because an SI would not be used on these components.

A secondary reason for using the same (PS/HYSZ) coating on all components was that the engine test would provide a direct comparison of the coating with and without the SI pad in the same engine environment.

V. TASK III--ENGINE COMPONENT TESTING

In the preceeding tasks of this effort, analytical and material property data for TBC systems have been assembled and the coating systems have been ranked according to the static screening tests. The resulting rank order permitted the selection of a coating system for application to engine components and for testing in a diesel engine environment. Analysis of the engine components coated with the selected system was conducted to calculate estimated component temperatures.

In this task, the engine components were modified and coated with the selected TBC system. These components were tested individually and collectively for a total of 24 hr each at power levels from 0.83 MPa to 1.17 MPa (from 120 lb/in.^{2} to 170 lb/in.^{2}) BMEP.

5.1 APPROACH

The engine in which the TBC coated components were tested was a LHR single-cylinder research diesel engine that had been used in an LHR diesel engine program funded by General Motors. The engine has the research workhorse configuration of a heavy-duty direct-injection diesel engine with a bore of 130 mm (5.118 in.) and a stroke of 139 mm (5.472 in.). The scope of this program required testing the coated components in conjunction with other engine development activity. Therefore, this program used components (piston, valves, and fire deck) that were interchangeable with ceramic components being tested in this engine. This approach required moderate compromise in the design of the coated components as described in the following subsections.

The maximum test condition for the coated components was defined as 34.3 kW (46 hp) at 1900 rpm under simulated turbocharged conditions. This condition converts to a BMEP of 1.17 MPa (170 lb/in.^{2}). The uncoated piston, fire deck, and valves of the subject engine were designed and have been tested at approximately 25% greater power levels. Thus, the basic design of the components possessed an adequate safety margin to allow a moderate amount of material to be removed and replaced by a TBC, which provided no structural strength to the components. The same PS/HSYZ coating system was applied to all components. The TBC system on the fire deck also included an SI.

5.2 ENGINE COMPONENT DESIGN

5.2.1 Piston Design

The piston selected to be modified for application of the TBC was a patented all-metal LHR design with demonstrated reliability in the in-house LHR engine program (References 4 and 5).

Initial concern about how to add a 2.54 mm (0.100 in.) coating to the top surface of the piston without reducing its structural integrity was laid aside midway through the program effort with two decisions regarding the coating system to be applied to the piston.

First, one goal of this program was to evaluate an SI concept in a diesel engine environment. The fire deck was chosen as the component on which the SI could be evaluated with the least risk. The fire deck, a flat and rigid component, was an ideal substrate on which to braze the SI pad. Comparison of

the performance of the 1.52 mm (0.060 in.) thick PS/HYSZ coating with and without the SI pad in the same diesel engine environment would enhance the evaluation of the PS/HYSZ coating concept.

Second, review of the complete piston connecting rod assembly design for this engine showed that the connecting rod could be shortened by 1.52 mm (0.060 in.) without causing interference between the crankshaft balance weights and the bottom of the piston assembly. This shortened rod would lower the piston 1.52 mm (0.060 in.) in the cylinder leaving space for the TBC without removal of material from the combustion bowl surface, which would reduce its strength. A decision, therefore, was made to modify the connecting rod to permit application of a 1.52 mm (0.060 in.) thick PS/HYSZ TBC to the piston.

Minor dimensional adjustments were made to the piston bowl shape to decrease the slope of the nearly vertical portion of the bowl to improve application of the coating and to increase the radius of the bowl contour at the transition between the bowl and the outer rim of the piston to improve the durability of the coating. Finally, a 1.52 mm (0.060 in.) wide lip on the metal crown provided a protective rim around the o.d. of the coating.

5.2.2 Fire Deck Design

The fire deck used in the uncooled single-cylinder LHR engine in this program was readily removable from the cylinder head assembly. When assembled on the engine, the fire deck is thermally isolated from the upper cast iron head structure and from the cylinder liner/ block components by insulating rings, as shown in Figure 56. This program used insulating rings consisting of 3.81 mm (0.150 in.) thick 410 stainless steel coated on each side with 1.27 mm (0.050 in.) PS/SYSZ total ring thickness) 6.35 mm (0.250 in.). The rings are shown in Figure 57. It should be noted that both insulating rings supported the head gasket compression seal load imposed by the head bolts, and the fire-deck-to-cylinder-liner insulating ring, in addition, sealed the cylinder compression gas pressure.

Analysis showed that up to 2.54 mm (0.100 in.) of material could be removed from the metal (Waspaloy) fire deck and still maintain structural margin to operate at the conditions defined in this program. This constraint established the total thickness potential of the coating system for the fire deck.

A goal of this program was to evaluate an SI pad concept in a diesel engine environment. (The contract required the SI to be evaluated in the coating system screening tests conducted in Task II.) The SI pad concept could be evaluated at low risk and within the scope of the program on the rigid fire deck assembly.

As described in subsection 3.4, the SI design for this program was defined as a 1.02 mm (0.040 in.) thick, 50% dense, sintered Hoskins 875 metal pad to be brazed to a metallic engine component. The 12.7 mm (0.50 in.) thick Waspaloy fire deck provided a flat and rigid substrate to which the SI pad could be brazed.

A 1.52 mm (0.100 in.) thick PS/HYSZ coating was applied to the SI pad to complete the 2.54 mm (0.100 in.) thick TBC system on the fire deck. The PS/HYSZ coating thickness was identical to that on the piston.

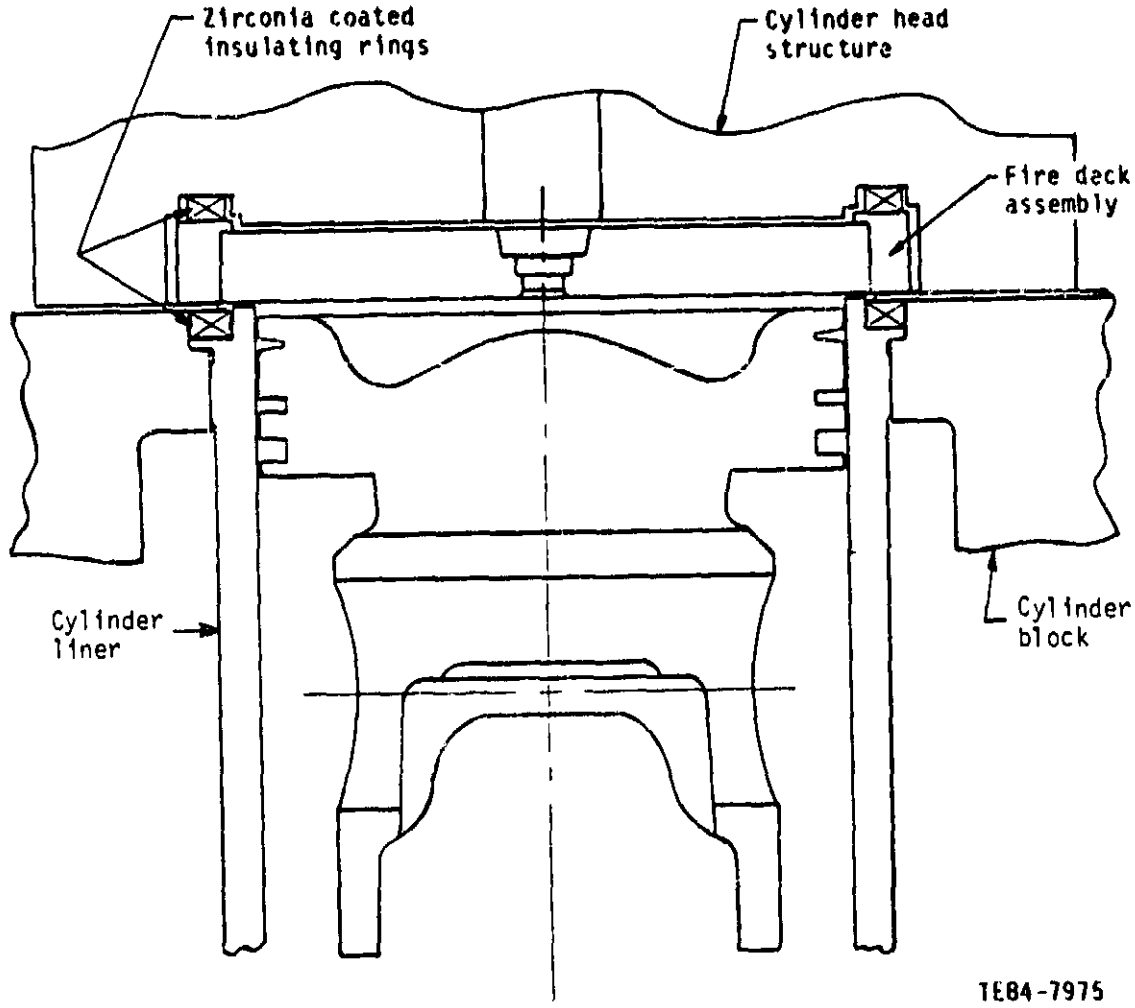

Figure 56. The placement of an assembled fire deck in an engine.

ORIGINAL PAGE IS
OF POOR QUALITY

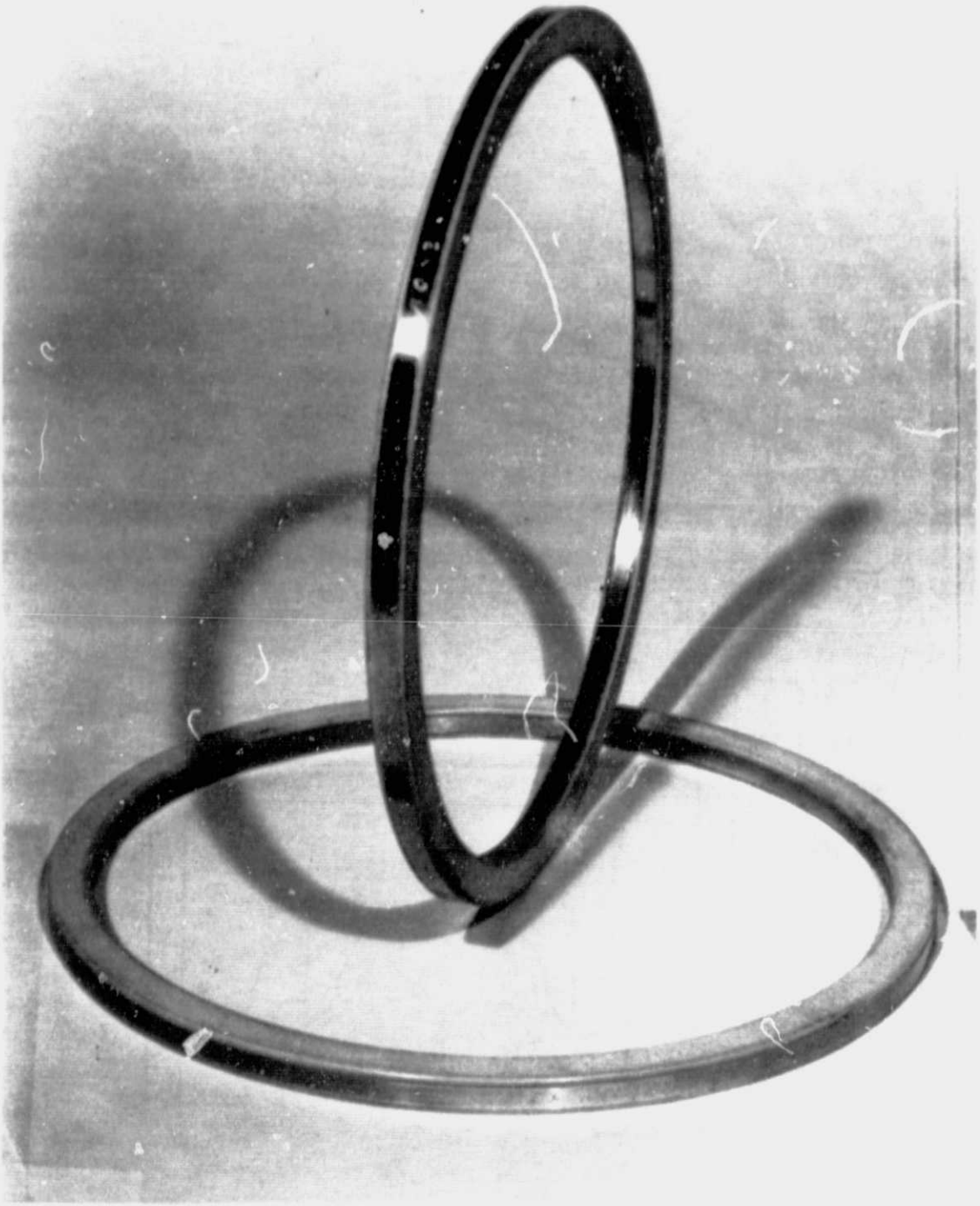

1E84-7976

Figure 57. Fire deck insulating rings.

5.2.3 Valve Design and Analysis

The research diesel engine tested in this program uses four valves--two intake and two exhaust. The valves are geometrically very similar except the intake valves are larger in diameter than the exhaust valves and carry about 20% greater gas pressure load during the combustion process. The TBC valves tested in this program were standard valves modified to accommodate the ceramic coating.

The final design configuration of the coated valves is shown in Figure 58. The coating thickness is 1.52 mm (0.060 in.) to approximately 22.9 mm (0.90 in.) dia and then tapers to 0.76 mm (0.030 in.) over the valve seat area on the exhaust valves and to 0.51 mm (0.020 in.) over the valve seat area on the intake valves. FEM calculations showed that it was necessary to taper the thickness of the coating in the valve seat region so that sufficient metal thickness remained to keep valve head deflections at a minimum and to avoid jeopardizing the durability of the coating.

A summary showing comparisons of the calculated FEM deflections and stresses is given in Table XVII. The deflections of the coated intake valve and the exhaust valve were 0.015 mm and 0.013 mm (0.0006 in. and 0.0005 in.) greater, respectively, than the uncoated valves. This difference resulted in 41 MPa (6000 lb/in.^{2}) higher operating stresses in the intake valve and 63 MPa (9000 lb/in.^{2}) in the exhaust valve. These calculations verified that removing the metal from the valves to add the PS/HYSZ coating would not jeopardize their structural integrity.

An SI pad was not used on the valves because the additional thickness (1.02 mm [0.040 in.]) required in the coating system could be accommodated in only the center of the valves (out to about 1.27 mm [0.50 in.] dia). The effectiveness of a pad over this limited area was not sufficient to justify the added complexity to the part. Further, substitution of the pad in PSZ coating was undesirable because the pad had greater thermal conductivity than the coating.

5.3 FABRICATION OF COATED ENGINE COMPONENTS

Installation of the SI pad to the fire deck as well as deposition of the TBC on the various engine components is discussed in the following sections.

5.3.1 SI Pad

The SI pad is a proprietary design of Brunswick Technetics. The pad fabrication and installation to the fire deck was performed by Brunswick.

The SI pad was brazed to the finish-machined Waspaloy fire deck with AMS 4777 braze material. After brazing, the holes for the valves and fuel injector were finish-machined and the subassembly subjected to final heat treatment. Figure 59 is a photograph of the SI pad brazed to the fire deck and ready for TBC application.

5.3.2 Coating Application

The PS/HYSZ coating developed by Allison was applied to all of the engine components with a Plasmadyne SG-1-B gun using the spray parameters listed in Table XVIII. The coating was deposited automatically by using the apparatus shown

Table XVII.
Summary of deflections and stresses in intake and exhaust valves.

Description	Intake valve		Exhaust valve	
	Coated	Uncoated	Coated	Uncoated
Axial deflection--mm (in.)				
Point A	0.046 (0.0018)	0.031 (0.0012)	0.031 (0.0012)	0.018 (0.0007)
Point B	0	0	0	0
Radial deflection--mm (in.)				
Point C	-0.015 (-0.0006)	-0.008 (-0.0003)	-0.010 (-0.0004)	-0.005 (-0.0002)
Maximum equivalent stress--MPa (lb/in.^{2})	251 (36,400)	210 (30,400)	647 (93,800)	584 (84,700)

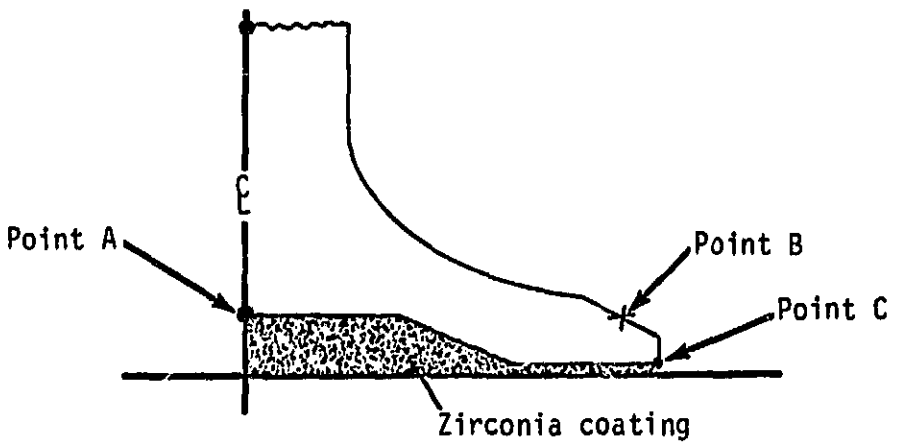

in Figure 60. After proper cleaning and masking of the part, the 0.127-0.175 mm (0.005-0.007 in.) NiCrAlY bond coat was deposited. This was essentially done in one pass/pattern on the stationary component. Following the deposition of the bond coat, a 0.254 mm (0.010 in.) thick SYSZ layer was deposited, followed by the combination SYSZ/HYSZ combination coating. The valves were the simplest components to coat, requiring several straight forward pattern passes to achieve the desired coating thickness of 1.524 mm (0.060 in.), shown in Figure 61. The machined step in the valve seat region can be readily seen through the coating in Figure 61. This step was required to maintain sufficient metal thickness in the valve seat region to keep valve head deflections at an acceptable level. The coating thickness on the valves was 1.524 mm (0.060 in.) from the center to approximately 22.85 mm (0.90 in.) dia and then tapered to 0.762 mm (0.030 in.) over the valve seat area on the exhaust valves and to 0.508 mm (0.020 in.) over the valve seat area on the intake valves.

Table XVIII.
Typical spray parameters for PS/HYSZ coating.

	Layer No.			
	1	2	3	
Coating material	AMI 963 NiCrAlY	8% YSZ	8% YSZ/HYSZ	
Thickness--mm (in.)	0.152 (0.006)	0.254 (0.010)	1.70 (0.067)	
Parameters				
Gun	SG-1-B	SG-1-B	SG-1-B	
Anode/nozzle	SI-3-F	SI-3-F	SI-3-F	
Cathode	SI-3-RW	SI-3-RW	SI-3-RW	
Open circuit voltage	80	80	80	
Arc voltage	38	29	40	
Current--A	360	525	500	
Primary arc gas	Ar	Ar	Ar	
Primary arc gas--m^3/hr (ft^3/hr)	93.4 (55)	101.9 (60)	101.9 (60)	
Line press--kPa (psig)	344.5 (50)	344.5 (50)	344.5 (50)	
Secondary arc gas	--	--	He	
Secondary arc gas--m^3/hr (ft^3/hr)	--	--	33.9 (20)	
Line press--kPa (psig)	--	--	344.5 (50)	
Powder feeder*	#1224	#1250	#1250	#1250
Potentiometer setting	2.5	2.5	1.55	5.2
Powder port	Internal	Internal	Internal	External
Carrier gas	Ar	Ar	Ar	Ar
Carrier gas--m^3/hr (ft^3/hr)	16.9 (10)	16.9 (10)	16.9 (10)	13.6 (8)
Line press--kPa (psig)	344.5 (50)	344.5 (50)	344.5 (50)	344.5 (50)
Spray distance--mm (in.)	63.5 (2.5)	76.2 (3)	88.9 (3.5)	88.9 (3.5)
Spray rate--kg/hr (lb/hr)	1.14 (2.5)	0.99 (2.2)	0.91 (2.0)	3.6 (8.0)

Note: Vapor degrease
60 mesh Al_2O_3 grit blast
Use robot
*In layer No. 3, two powder feeders cosprayed the powder simultaneously.

The piston was coated with an incremental rotational technique that used the translating plasma-gun-holding robot to deposit a transverse pattern across the face of the piston. At the completion of one entire pass, which was a raster pattern consisting of a series of vertically spaced linear passes across the piston crown, the piston was rotated through an incremental angle. This angular indexing between each pass smoothed out irregularities in the coating which might otherwise have been produced by repeated passes of the spray gun as it repeated the same pattern. Approximtely 30 repetitions were required to achieve the desired coating thickness with an incremental rotational angle of 15 deg between each repetition. Coating system thickness was measured on an adjacent coupon and found to be 1.626 mm (0.064 in.). A thinning of the coating in the outer region of the combustion bowl was expected to result as a consequence of the oblique coating surface angle with respect to the PS particle stream path.

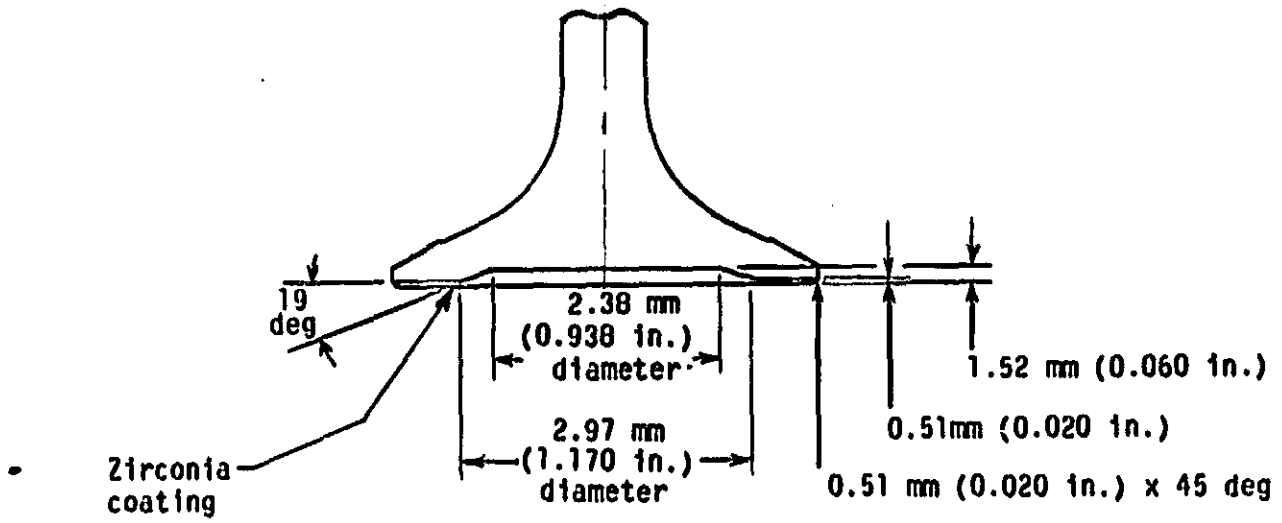

a. Intake valve

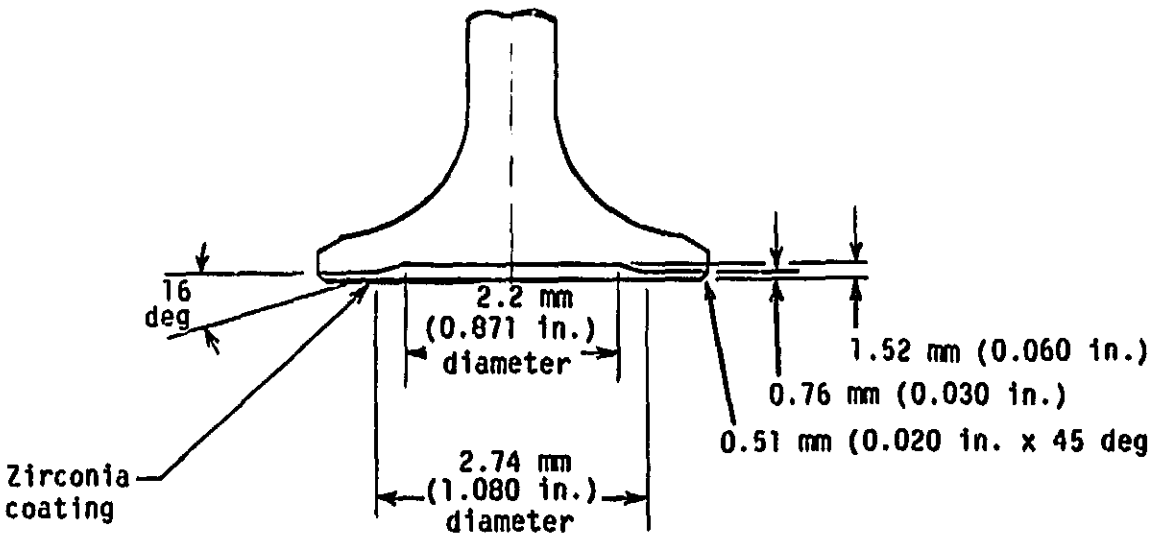

b. Exhaust valve

TE84-7977

Figure 58. Final design configuration of coated valves.

ORIGINAL PAGE IS
OF POOR QUALITY

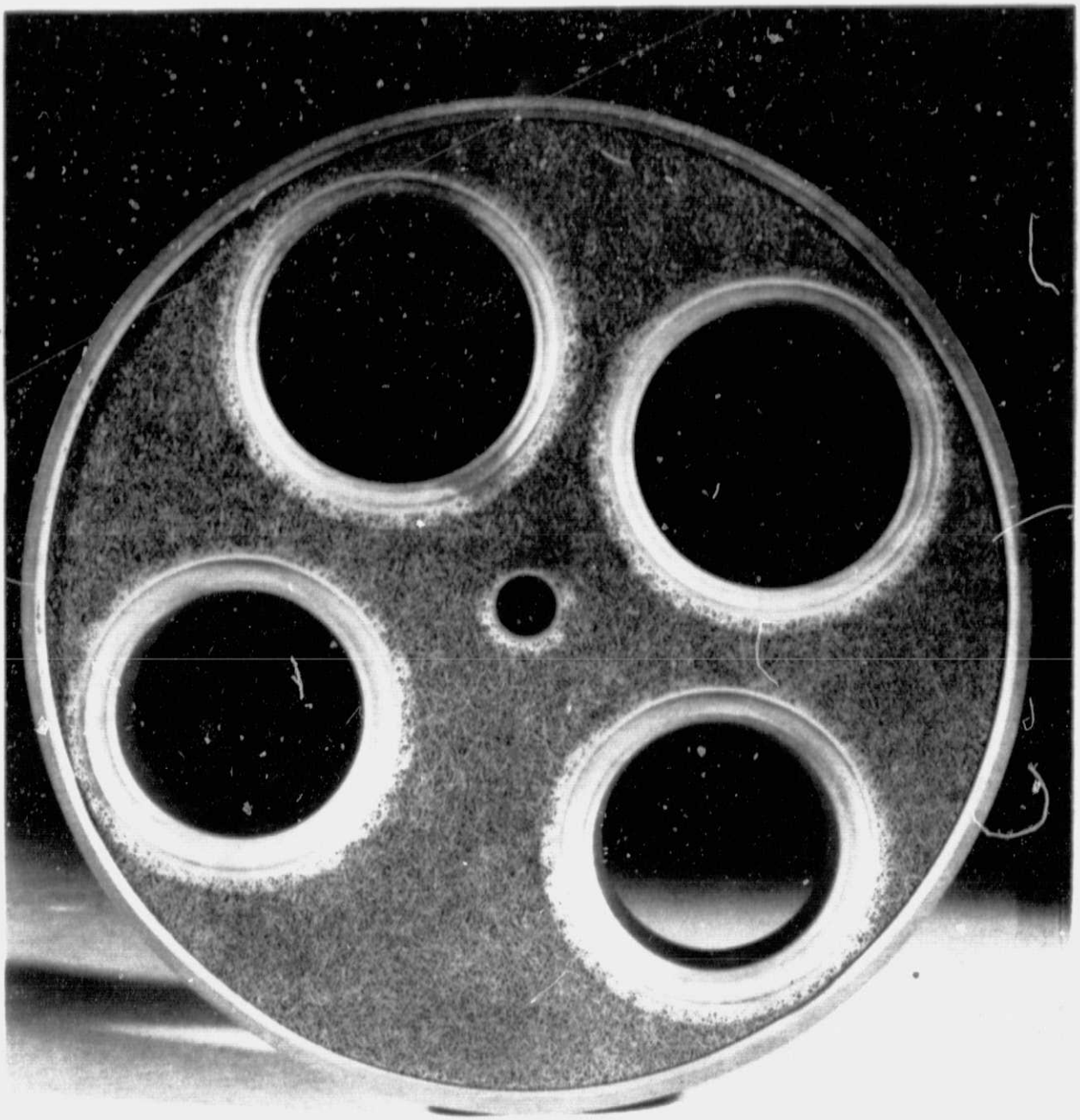

TE84-7978

Figure 59. Strain isolator pad installed on a Waspaloy fire deck.

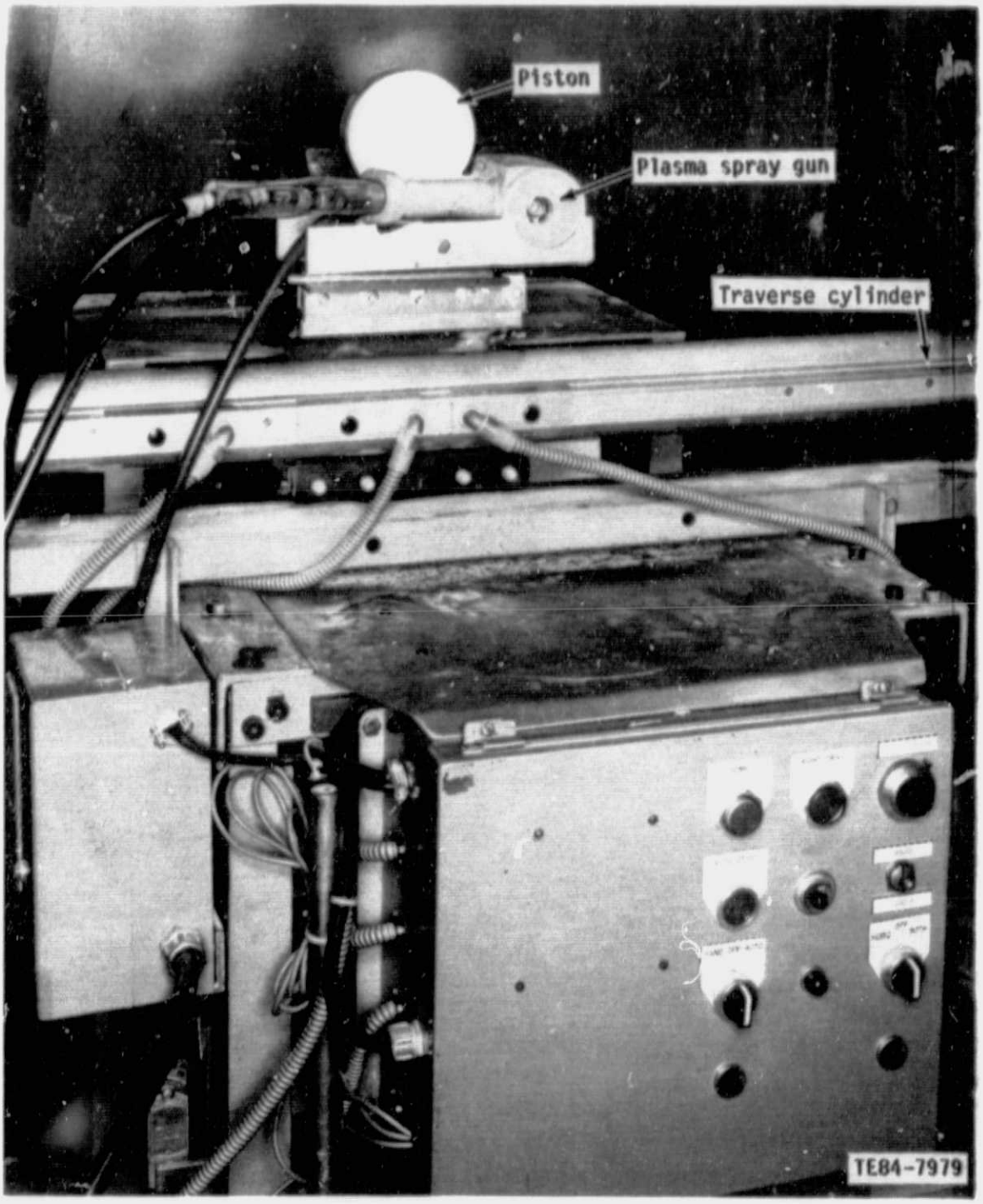

Figure 60. Equipment that applies a plasma-sprayed coating to piston, fire decks, and valves.

ORIGINAL PAGE IS
OF POOR QUALITY

ORIGINAL PAGE IS
OF POOR QUALITY

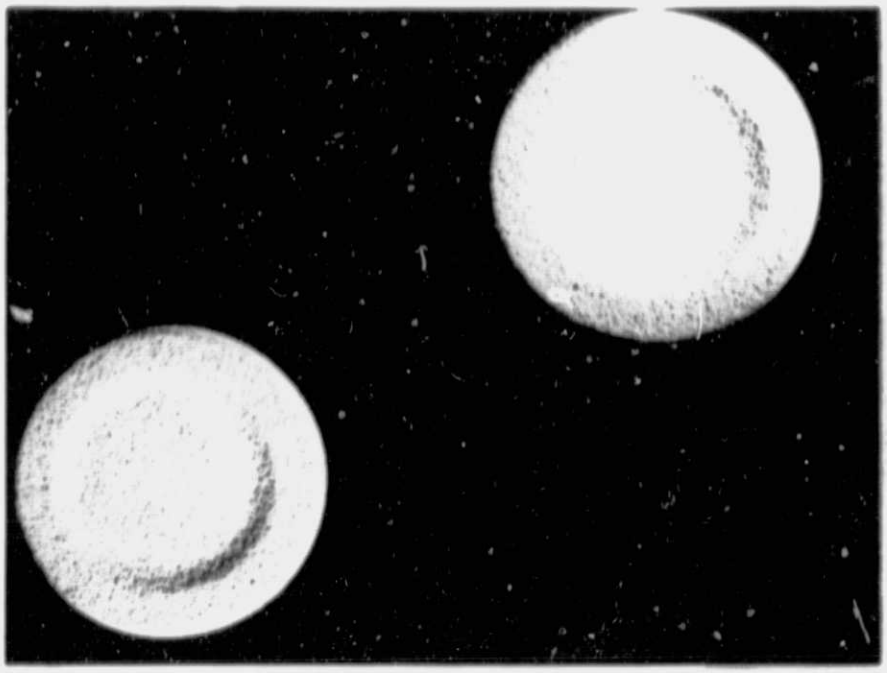

TE84-7980

Figure 61. As-sprayed coated valves.

A topographical contour measurement was made of both the uncoated and coated piston crowns to determine the actual thickness of the deposited coating. As a result of these measurements, it was determined that the coating was extremely thin at the outer extremities of the bowl, where the sidewalls meet at 60 deg angle with the axis of the piston. This angle is undesirable for proper spray deposition and the decision was made to strip the coating from the piston and modify the plasma gun setup to rectify this problem. The gun was manually repositioned during the spray process so that the bowl wall was sprayed at a 90 deg angle alternately with the raster passes on the remainder of the crown. When the gun was positioned for the 90 deg deposition, the piston was rotated at 30 rpm in the fixture, while during the raster passes, the 15 deg incremental rotation previously described was used. Figure 62 depicts the contour of the uncoated and coated piston after the second successful attempt. As can be seen, the coating is relatively uniform and of acceptable thickness.

The fire deck was sprayed in essentially the same manner as the piston, using an incremental angular rotation after each raster pass sequence. Figure 63 shows the as-sprayed piston and fire deck.

Table XIX lists the coating system constituent elements and their nominal thicknesses as deposited on the single-cylinder engine components.

Table XIX.
Coating system constituent thickness.

Component	SI pad-- mm (in.)	NiCrAlY bond coat-- mm (in.)	SYSZ-- mm (in.)	SYSZ/HYSZ-- mm (in.)
Fire deck	1.016 (0.040)	0.127 (0.005)	0.254 (0.010)	1.448 (0.057)
Piston	--	0.152 (0.006)	0.279 (0.011)	1.194 (0.047)
Valves				
*Center to 0.90 in. dia	--	0.127 (0.005)	0.254 (0.010)	1.143 (0.045)
Outer diameter, intake	--	0.127 (0.005)	0.254 (0.010)	0.127 (0.005)
Outer diameter, exhaust	--	0.127 (0.005)	0.254 (0.010)	0.381 (0.015)

5.3.3 Final Machining of Coated Components

The coating surfaces were machined, where necessary, with single-point carbide tooling using relatively slow speeds and feed rates and shallow depths of cut as detailed in subsection 4.2. Figure 64 shows the coated valves, fire deck, and piston, respectively, after finish-machining. Both the fire deck and piston were used in the as-sprayed condition, except for minor machining at the respective outside diameters and a light blending around the valve seats on the fire deck. The valve faces required machining to reduce the coating thickness over the valve seat region as noted previously.

5.4 ENGINE TESTING

5.4.1 Approach

Selected TBC were evaluated by engine testing in an uncooled LHR diesel engine operating environment. This evaluation followed coating design and analysis (Task I) and coating screening tests (Task II). The test engine, shown in Figure 65, is a single-cylinder research engine that had been adapted to operate without a water coolant. The reciprocating components and cylinder head are typical of a heavy-duty diesel truck engine. The bore and stroke, 130 mm and 139 mm (5.12 in. and 5.47 in.), respectively, and the operating speed range, 800 to 2100 rpm, are typical of a diesel engine in this size class. The piston, fire deck, and valves of this engine were modified to test the selected PS/HYSZ TBC.

The power level to which the single-cylinder engine was operated during testing of the coated components was 34.3 kW (46 hp), (205 kW [275 hp] equivalent in a six-cylinder engine) at 1900 rpm. This is equivalent to a loading of 1.17 MPa

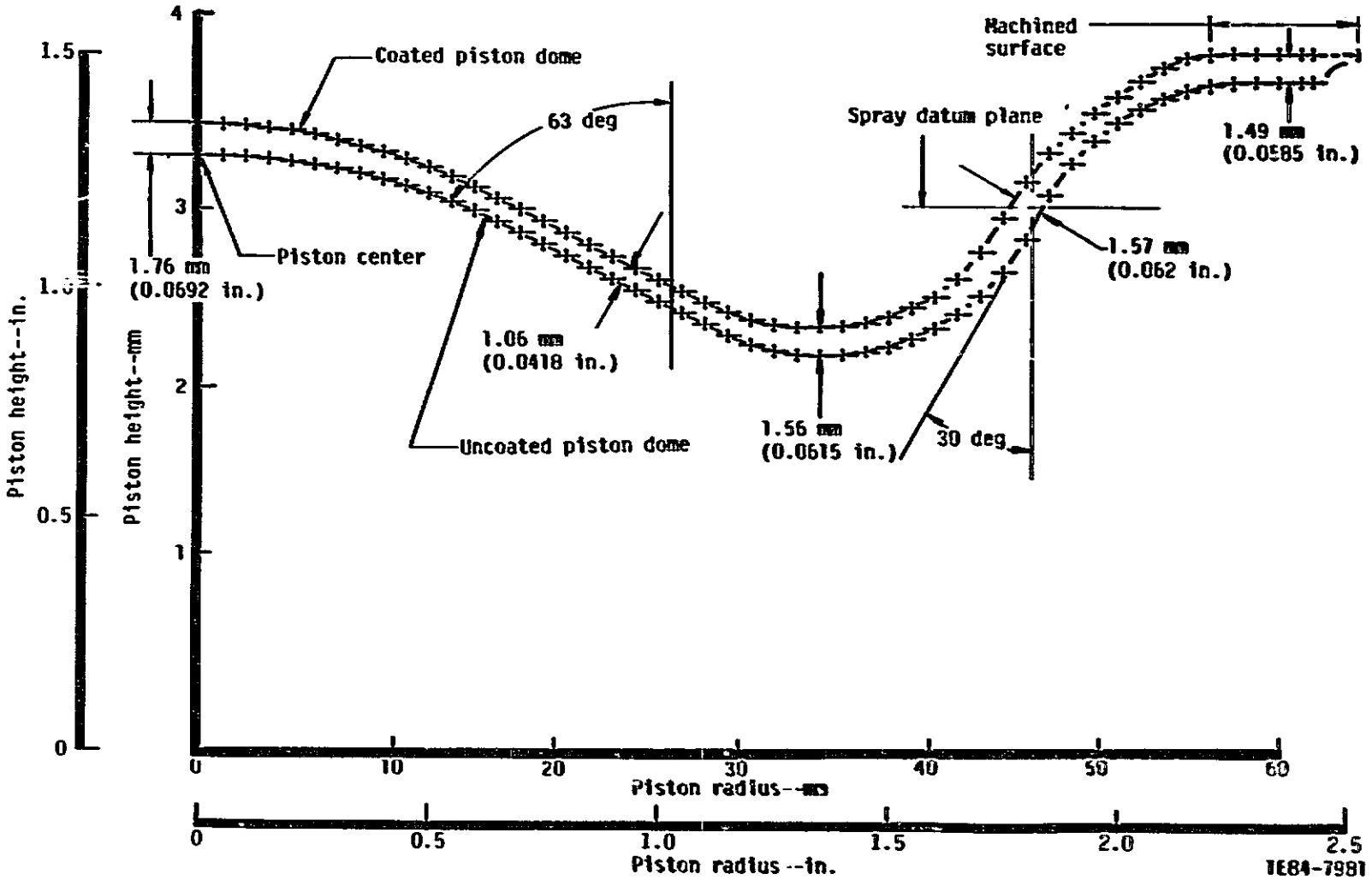

Figure 62. Uncoated/coated piston contour.

ORIGINAL PAGE IS
OF POOR QUALITY

ORIGINAL PAGE IS
OF POOR QUALITY

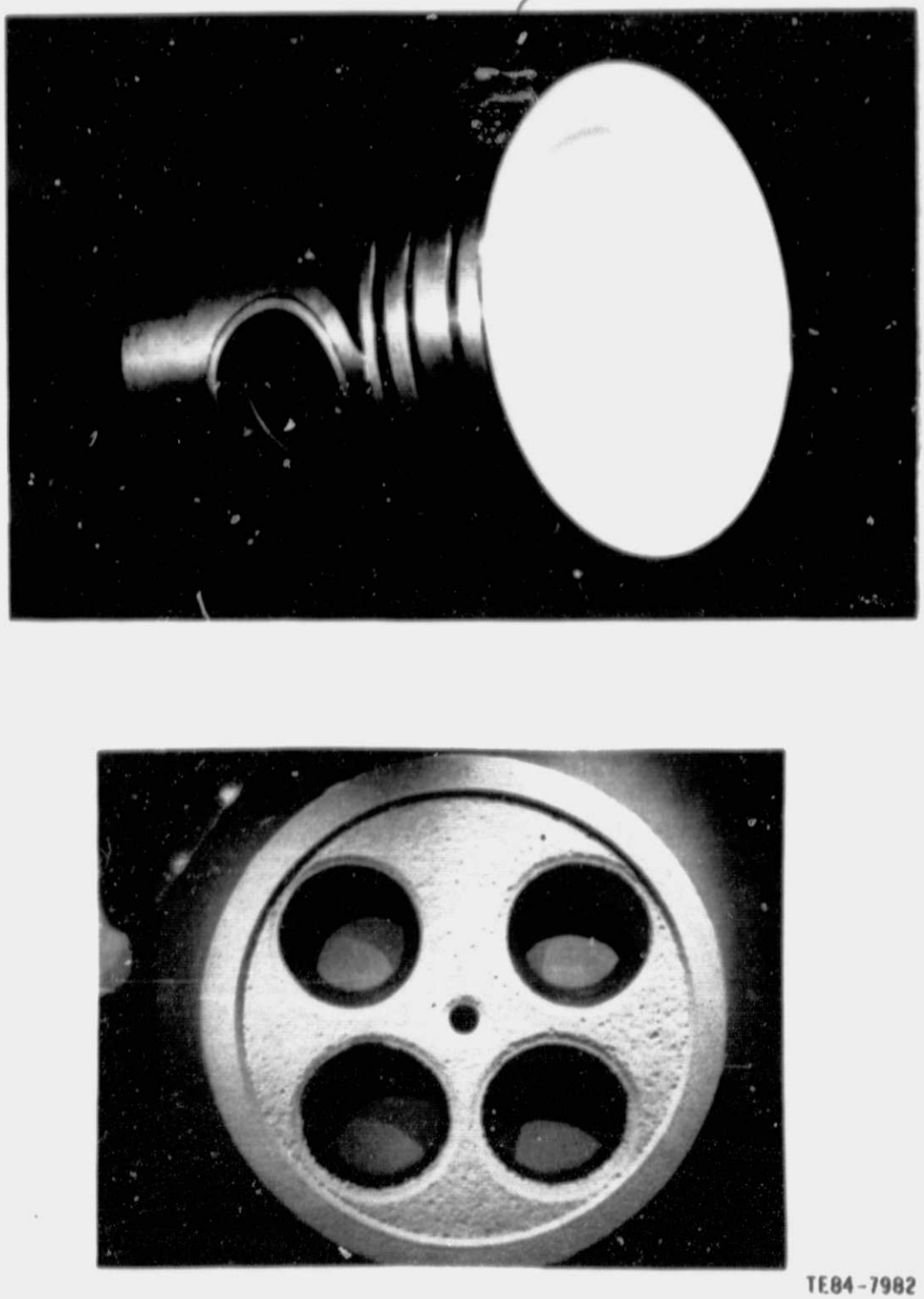

TE84-7982

Figure 63. Spray-coated piston (top) and fire deck (bottom).

ORIGINAL PAGE IS
OF POOR QUALITY

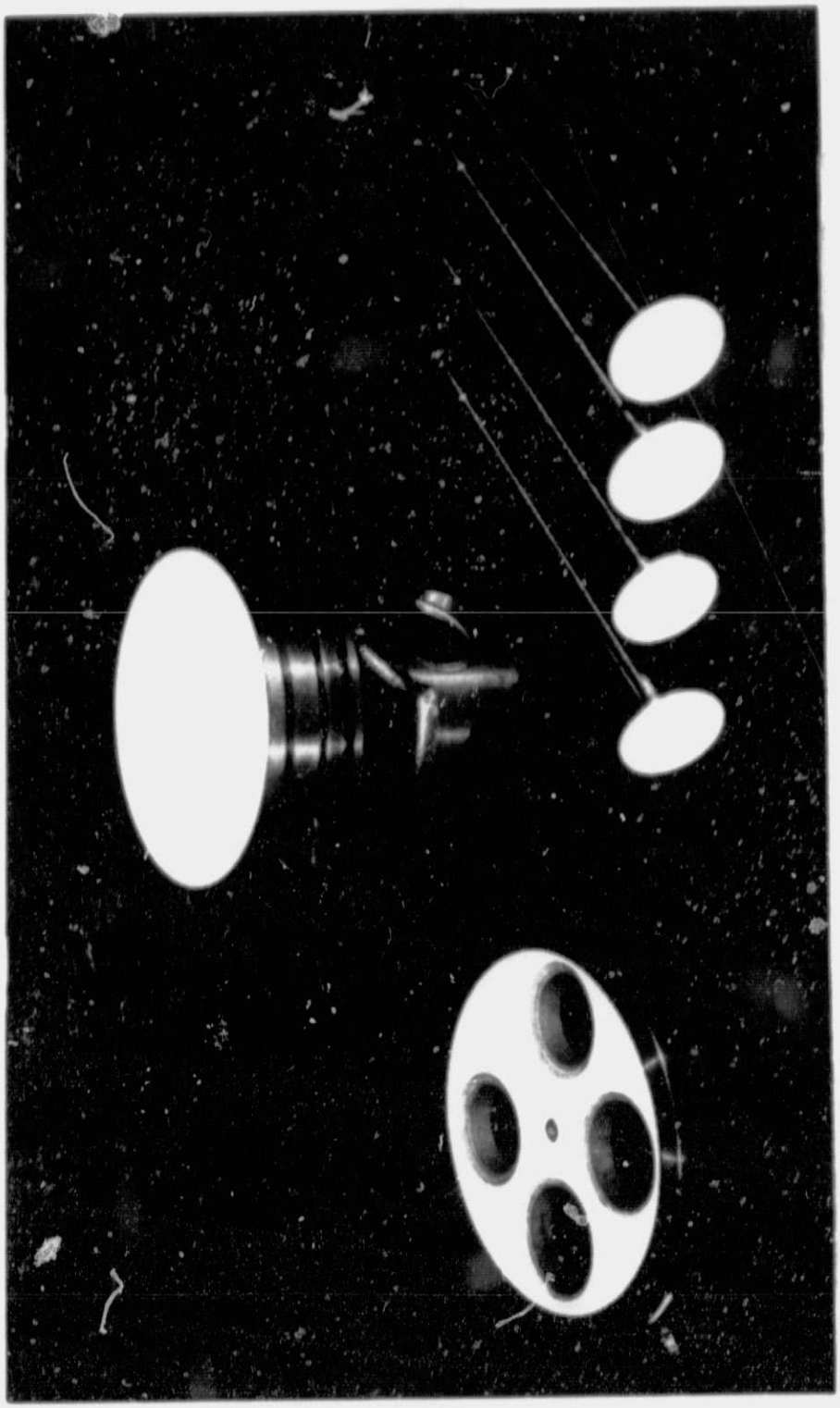

IEM-7983

Figure 64. Finish-machined coated components.

ORIGINAL PAGE IS
OF POOR QUALITY

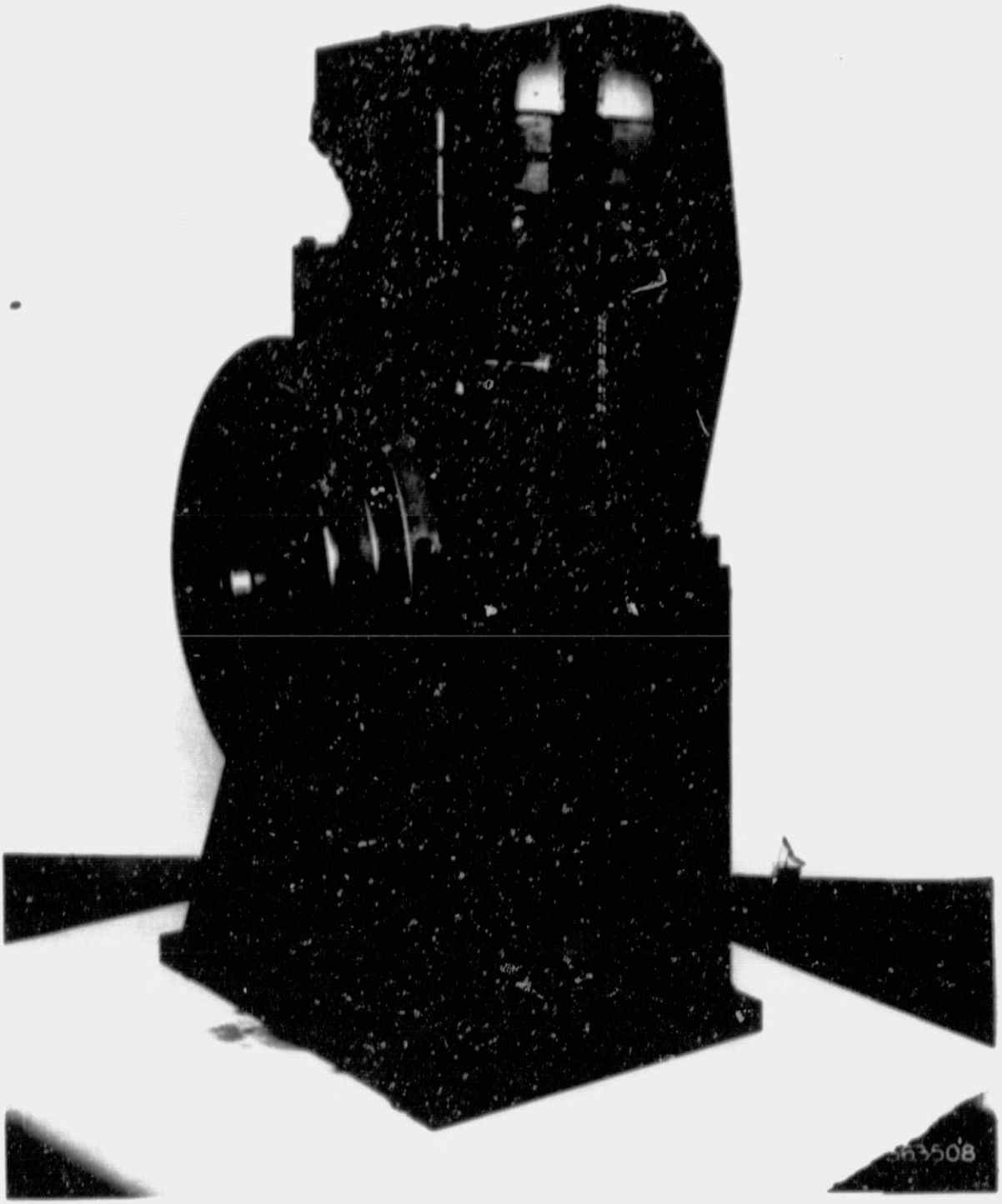

TE84-7984

Figure 65. Single-cylinder diesel test engine.

(170 lb/in.^{2}) BMEP. Table XX shows a comparison of thermal and mechanical loading of the engine test conducted in this program with the reported performance of another diesel engine using TBCs (Reference 1).

Table XX.
Comparison of engine loading.

Engine	Power--kW/cylinder (hp/cylinder)	Speed--rpm	BMEP--MPa (lb/in.^{2})	Air/fuel ratio	Average cycle gas temperature--°C (°F)
Uncooled single-cylinder LHR test engine with DEN3-326 coated components					
Power level 1	34.3 (46)	1900	1.172 (170)	26.9	850 (1563*)
Power level 2	23.1 (31)	1300	1.165 (169)	27.6	841 (1545*)
Uncooled multicylinder engine (Reference 1)					
Power level 1	28.3 (38)	2100	0.696 (101)	39.5*	714 (1317*)
Power level 2	20.1 (27)	1300	0.793 (115)	36.8*	736 (1357*)

*Estimated

The testing of the coated components was carried out in two phases. First, each component (piston, fire deck, and valves) was tested individually in the engine. These individual proof tests, 4 hr in duration, served two purposes. First, testing each component individually prevented the possible destruction of a successfull coated component in the event another coated component suffered an immediate failure. This consideration was the primary purpose of the individual tests. The second reason for testing the components individually was to assess their effect on engine performance. The engine was operated at the prescribed power rating during each proof test, thus exposing each component to the same conditions it would experience when tested in combination with the other coated components. The components were inspected and photographed at the conclusion of the 4-hr tests.

In the second phase of coating system evalution in the engine, all coated components were installed together. The engine was operated at the same conditions as in the proof tests until 10 hr of testing were completed (14 hr on each part). The cylinder head was removed to inspect and photograph the coated surfaces. The engine was reassembled and tested for an additional 10 hr under the same operating conditions, thus accumulating a total test time of 24 hr on each component. The engine was then disassembled to evaluate the condition of the coated components.

5.4.2 Engine Test Results

Engine testing of the coated piston, fire deck, and valves was conducted in the following two phases:

- o Phase I--an individual 4-hr test of each component (to prevent damage to the other coated components if an early failure occurred)
- o Phase II--20-hr test with all of the coated components installed (the head was removed at 10 hr to inspect the condition of the coated surfaces)

The engine was operated at the test conditions (power levels) shown in Table XXI during both phases of testing. The tests were conducted at each of the six test conditions for approximately 30 min, continuing to rotate through the test matrix until the planned test time was accumulated. Typically, in Phase I testing, the engine was operated through the six-point test plan once with operation at the last point, 1.17 MPa (170 lb/in.^{2}) BMEP, 1900 rpm, extended to 1 hr to complete the 4-hr proof test. In Phase II testing, the engine was operated at each test condition an average of six times.

Table XXI.
Single-cylinder LHR diesel engine test conditions.

Speed - rpm	Intake temperature - °C (°F)	Intake[1] pressure - MPa (psia)	Exhaust[1] pressure-- MPa (psia)	Torque - Nm (ft-lb)	BMEP - MPa (psi)	Power-- kW (hp)
1300	46.7 (116)	0.24 (35.0)	0.24 (35.0)	12.2 (8.97)	0.83 (120)	16.6 (22.2)
1300	46.7 (116)	0.24 (35.0)	0.24 (35.0)	146.9 (108.3)	1.00 (145)	20.0 (26.8)
1300	46.7 (116)	0.24 (35.0)	0.24 (35.0)	169.2 (124 8)	1.15 (167)	23.1 (30.9)
1900	46.7 (116)	0.24 (35.0)	0.24 (35.0)	121.5 (89.6)	0.83 (120)	24.2 (32.4)
1900	46.7 (116)	0.24 (35.0)	0.24 (35.0)	150.0 (110.6)	1.02 (148)	29.8 (40.0)
1900	46.7 (116)	0.24 (35.0)	0.24 (35.0)	172.4 (127.1)	1.17 (170)	34.3 (46.0)

[1]Intake and exhaust pressures were 0.22 MPa (32.6 psia) for Phase I testing.

In this test program the engine was operated at the specified power levels with the fuel flow adjusted accordingly. The intake and exhaust pressures (simulating turbocharger boost) and intake temperature were held constant for all six test conditions. Intake and exhaust pressures were adjusted upward 7% during Phase II testing to maintain the airflow and air/fuel ratios tested in Phase I. The decrease in airflow was the result of increased temperatures in the cylinder when all of the coated components were tested together.

The engine operated normally throughout the testing, and performance was noted as the test points were repeated. All engine testing in this program was conducted at 0.83 MPa (120 lb/in.^{2}) BMEP power levels or above.

5.4.2.1 Coating Endurance

The coated components survived the engine testing with minimum distress. The absence of scoring on the cylinder wall indicated that little, if any, coating material separated from the components and became entrapped between the piston and cylinder liner. The condition of each component is described in the following subsections.

Piston

The piston was coated with a 1.52 mm (0.060 in.) thick HYSZ coating, as shown in Figures 66 and 67. The coating was machined at the rim to achieve the proper piston-to-head clearance. Figure 68 shows the piston after completion of the Phase I (4-hr) test. A small crack developed during this test, as noted in the figure. This crack was nearly centered in one of the eight fuel injector spray plums on the exhaust side of the engine. The crack was not observed with the naked eye but was recorded in the photograph under different lighting conditions.

Figures 69 and 70 show the condition of the piston coating after 14 hr and 24 hr of testing, respectively. The crack noted after 4 hr of testing did not noticeably enlarge in size and, further, no other cracks or spalling of coating appeared. Mud flat cracking observed in the thermal shock test samples was not observed in the piston coating surface. Also, no noticeable surface erosion was detected.

Fire Deck

The fire deck TBC system consisted of a 1.52 mm (0.060 in.) HYSZ coating applied over a 1.02 mm (0.040 in.) thick SI pad, as shown in Figure 66. The pad, brazed to the Waspaloy fire deck, was cut back around the valve seats and center hole so that the ceramic coating covered the edges of the pad at those locations, thereby preventing pad infiltration with combustion products. Figure 71 shows the coated fire deck prior to testing. Note the pockmarked, as-sprayed flat surface of the fire deck. This surface texture is typical of coatings applied to an SI pad. The initial layers of coating fill the porous outer layer of the pad, and this surface characteristic is carried forward as additional coating is applied.

Figure 72 shows the coated fire deck after the initial 4-hr test. Combustion soot was wiped from the surface by hand, accenting the pockmarked surface observed before testing. Some spalling of the coating is shown at the o.d. of the coated surface. The spalling occurred at the thin region between the exhaust valve openings on the rim of the fire deck. This region is outside the bore of the cylinder, and marks on the coating suggest interference existed between the coating and the top surface of the cylinder liner. This interference may have contributed to the spalling of the coating in this region. No other cracks or spalling were observed in the coating surface after 4 hr of testing. Figure 73 is included to show another view of the fire deck with the coated valves installed after 4 hr of testing. The view in Figure 73 is more comparable to photographs taken later in the testing sequence.

Figure 74 shows the fire deck and valves after 14 hr of testing was completed. A small crack in the coating existed between the exhaust valves near the location of the maximum calculated surface temperature. Minor additional spalling

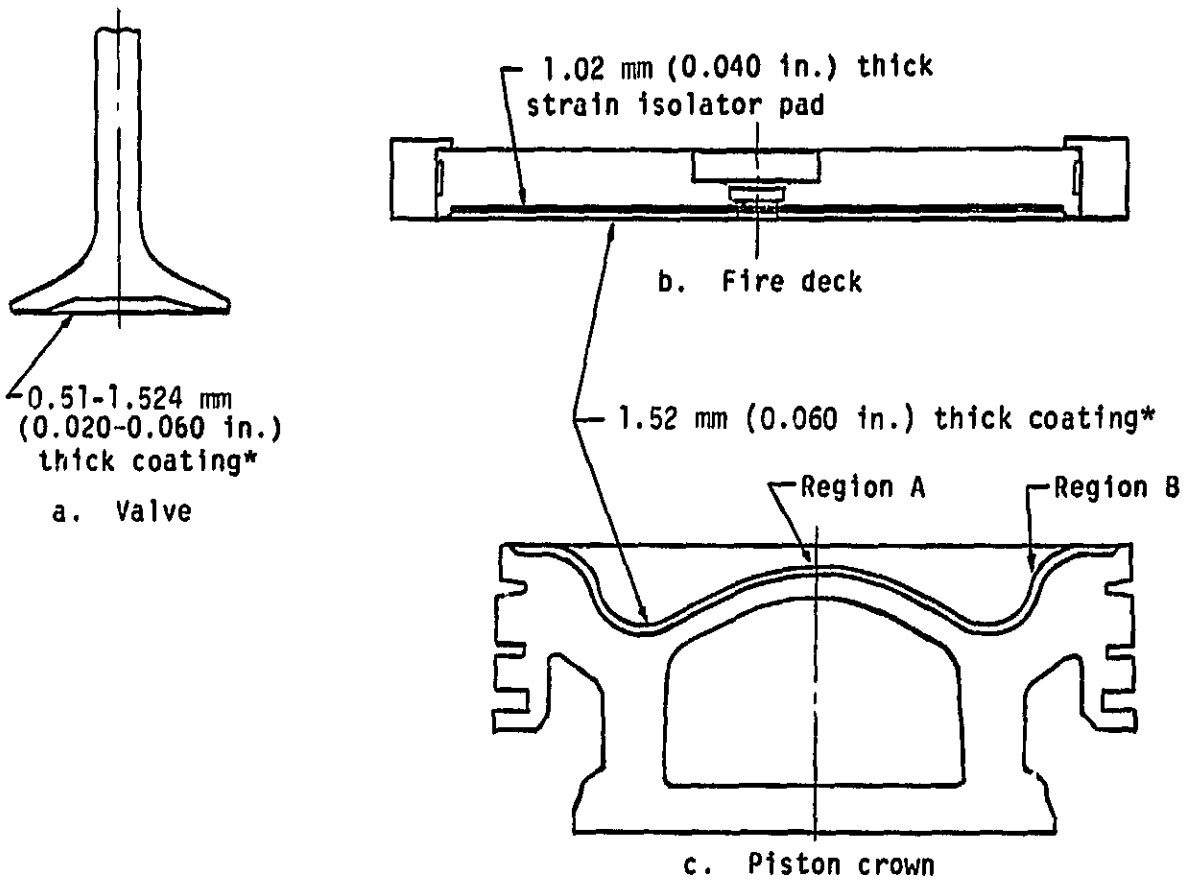

*Allison plasma sprayed hollow particle yttria stabilized zirconia thermal barrier coating

TE84-7985

Figure 66. Cross sections of coated engine components.

ORIGINAL PAGE IS
OF POOR QUALITY

TE84-7986

Figure 67. A piston with a thermal barrier coating before testing.

ORIGINAL PAGE
OF POOR QUALITY

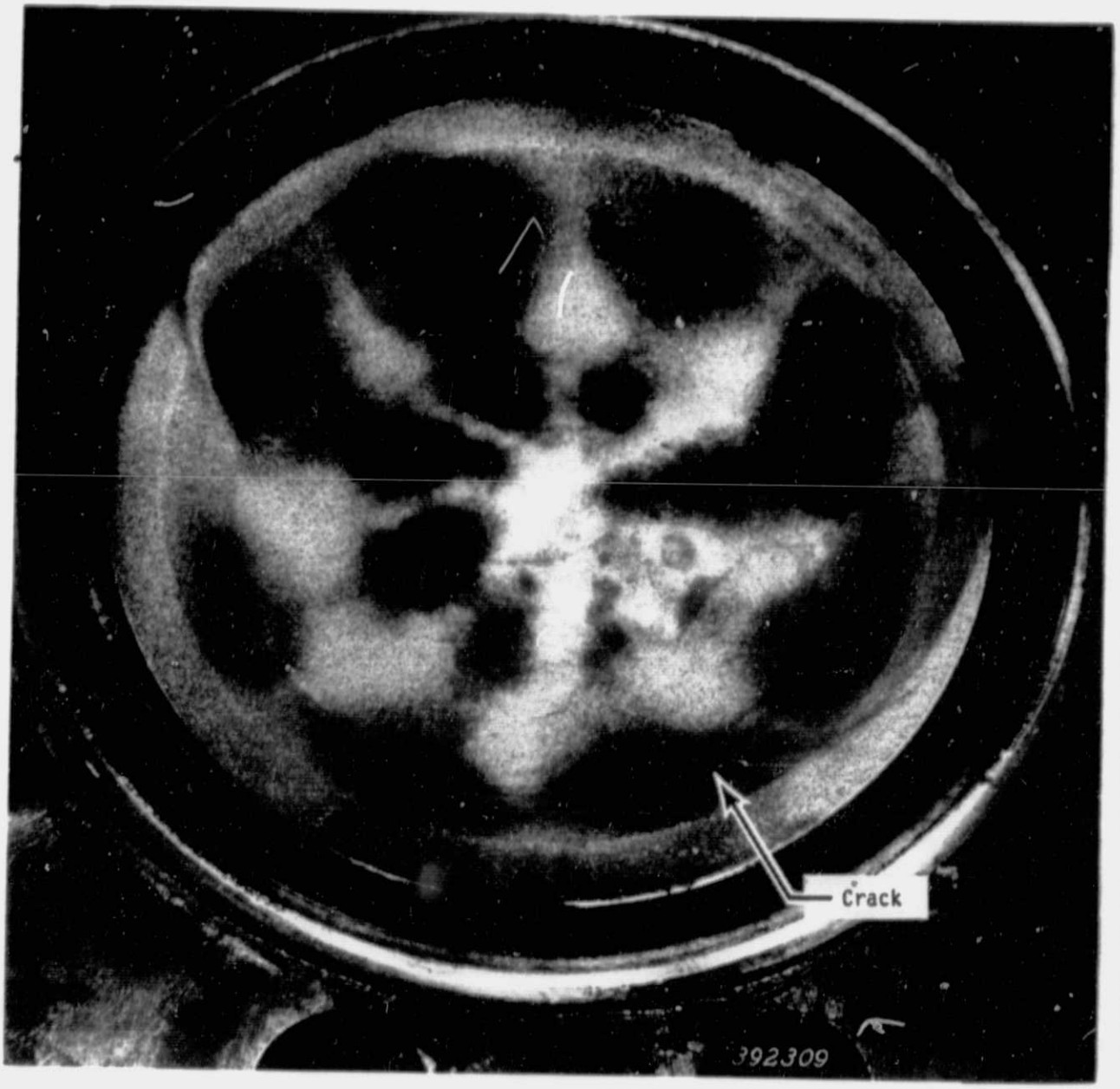

TE84-7987

Figure 68. A coated piston after 4 hr of testing.

ORIGINAL PAGE IS
OF POOR QUALITY

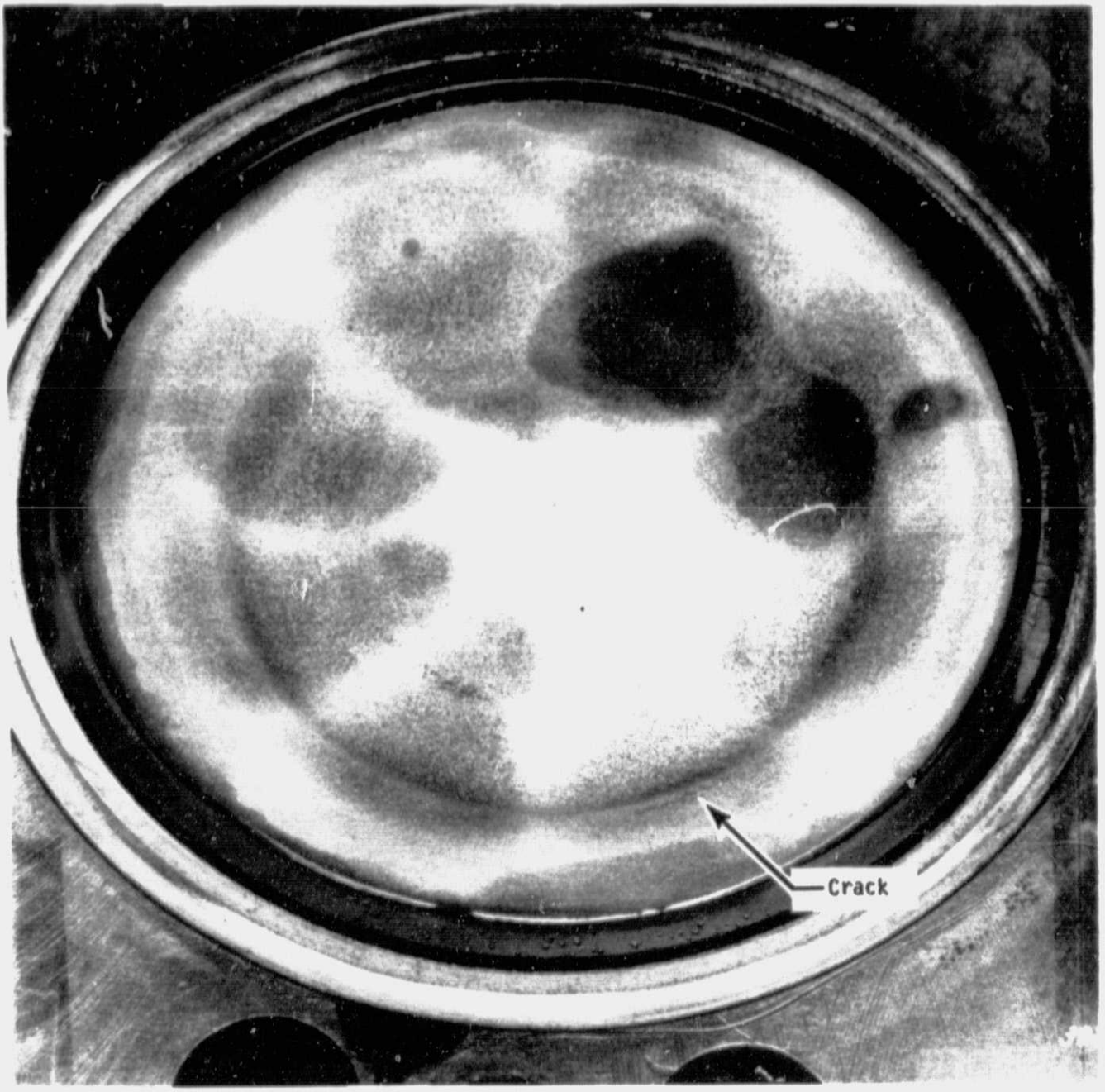

Figure 69. A coated piston after 14 hr of testing. TE84-7988

OF POOR QUALITY

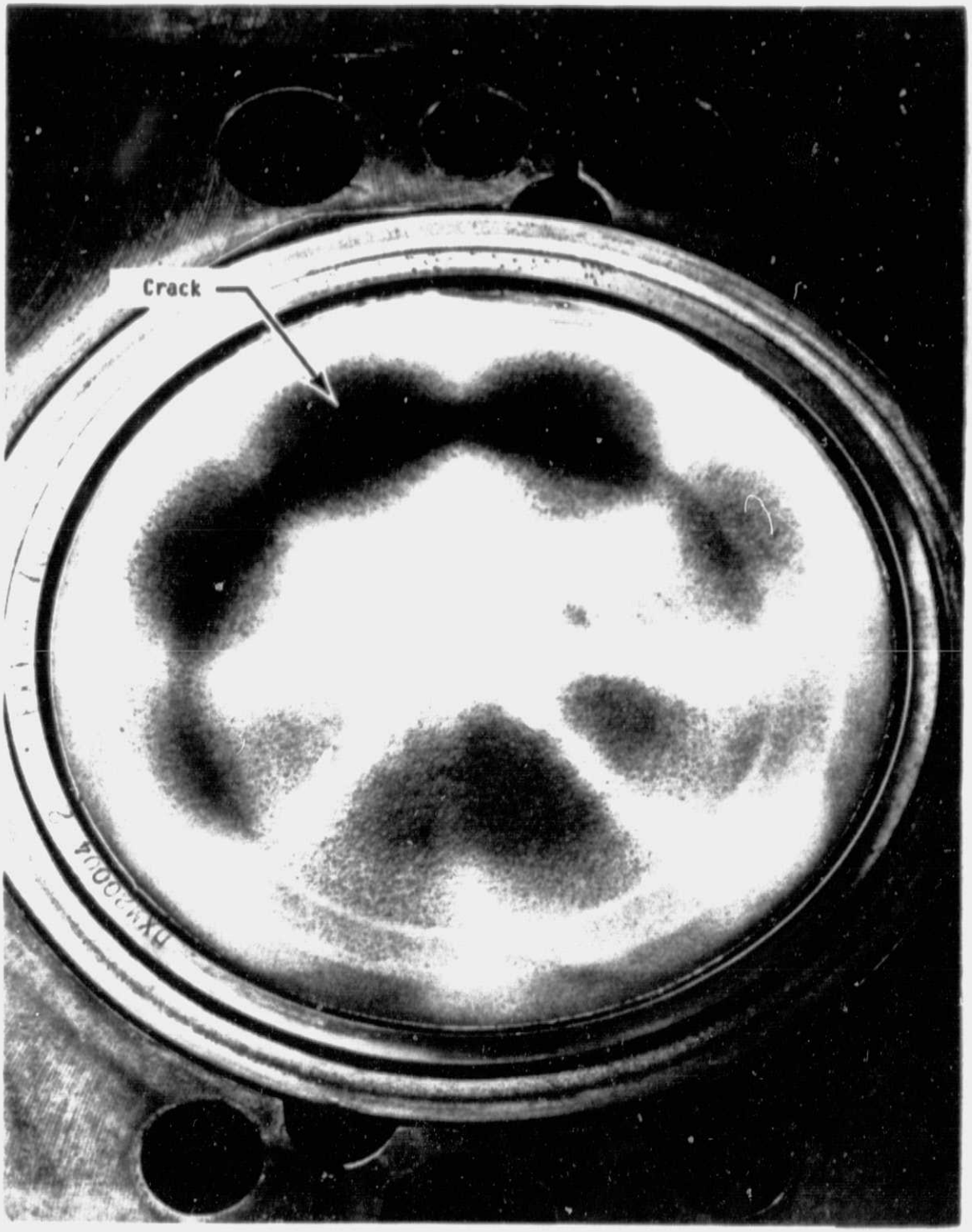

TE84-7989

Figure 70. A coated piston after 24 hr of testing.

ORIGINAL
OF POOR

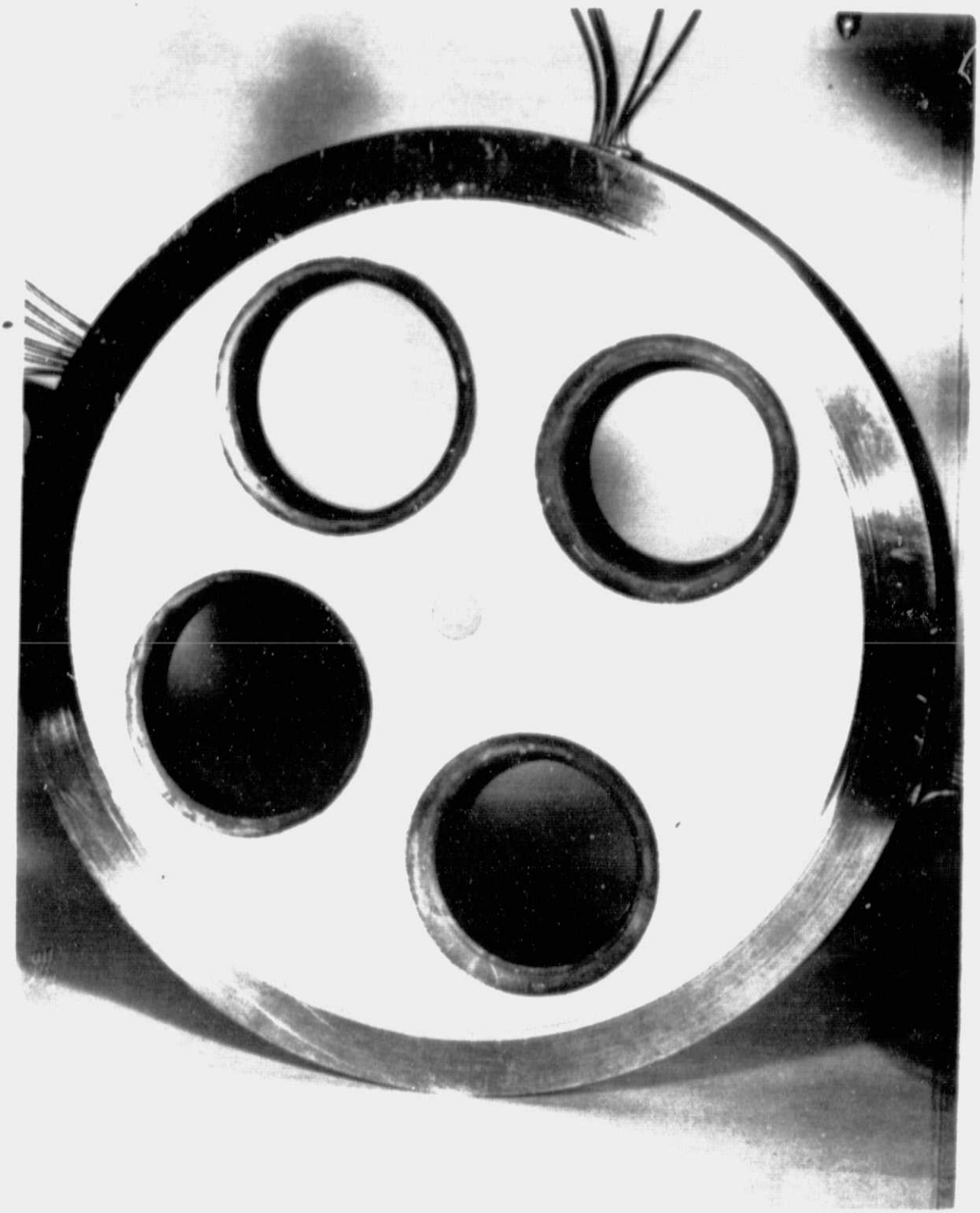

TE84-7990

Figure 71. A fire deck with a thermal barrier coating before testing.

ORIGINAL PAGE IS
OF POOR QUALITY

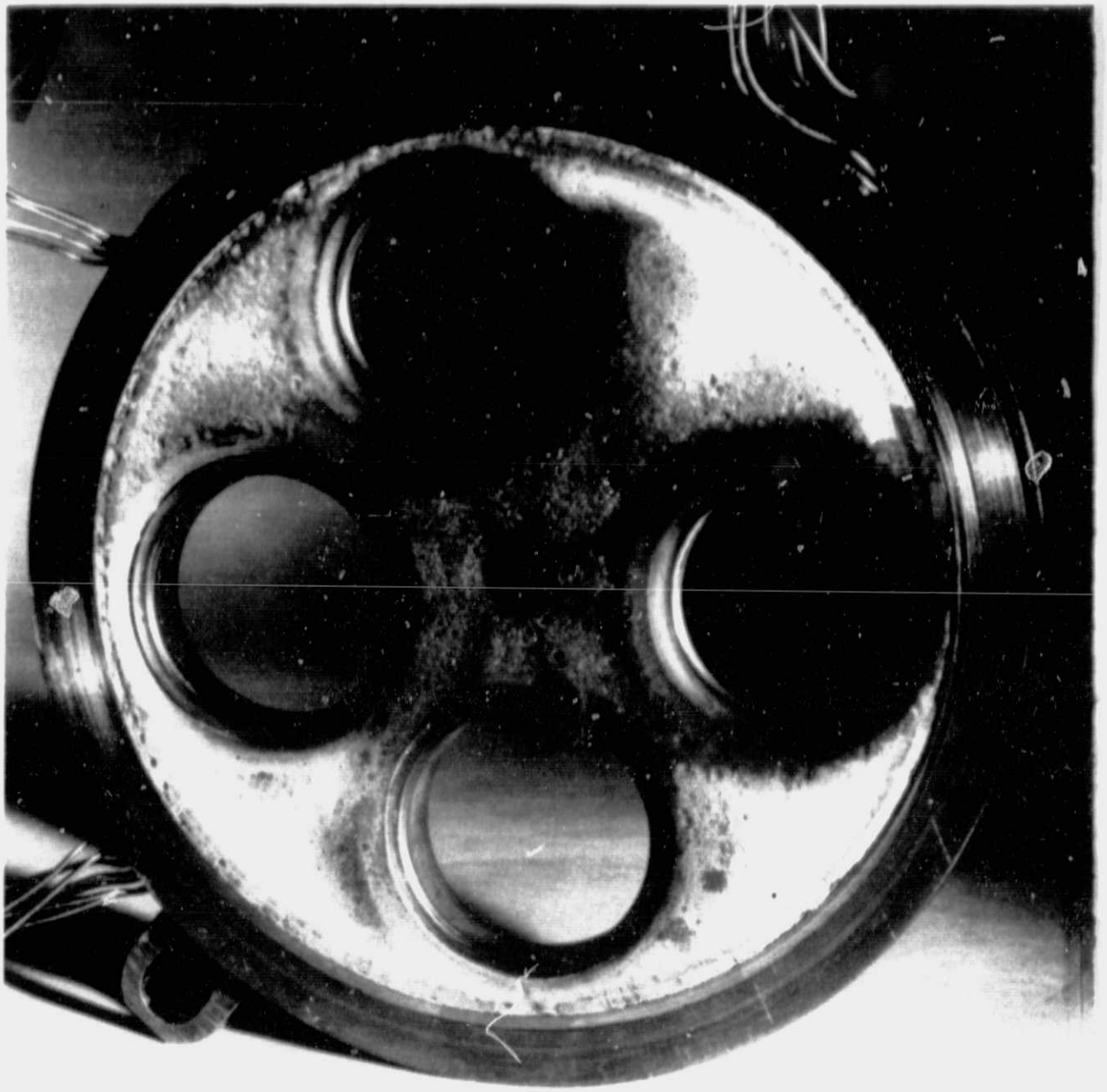

Figure 72. A coated fire deck after 4 hr of testing. TE84-7991

ORIGINAL PAGE IS
OF POOR QUALITY

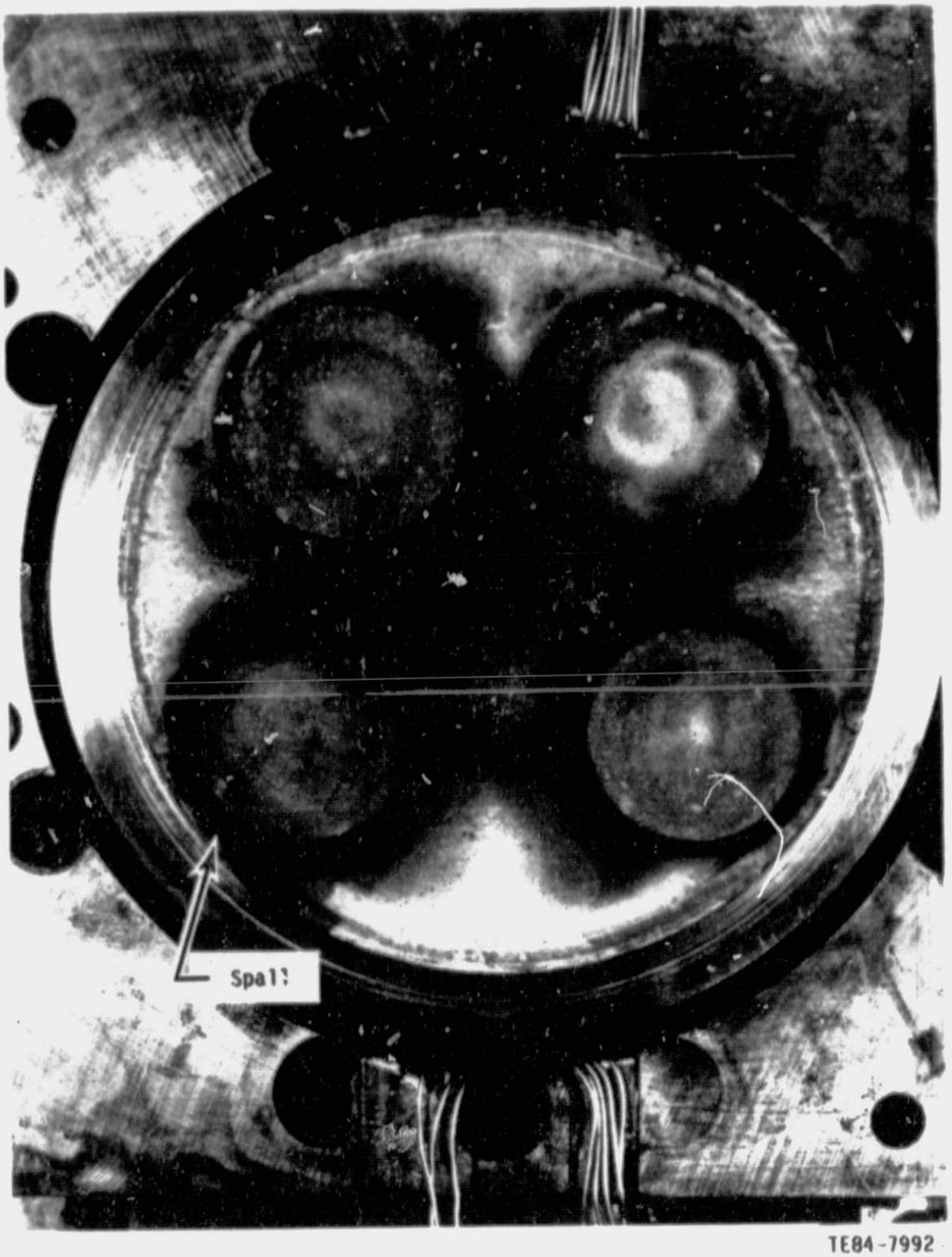

Figure 73. A coated fire deck and coated valves after 4 hr of testing.

ORIGINAL PAGE IS
OF POOR QUALITY

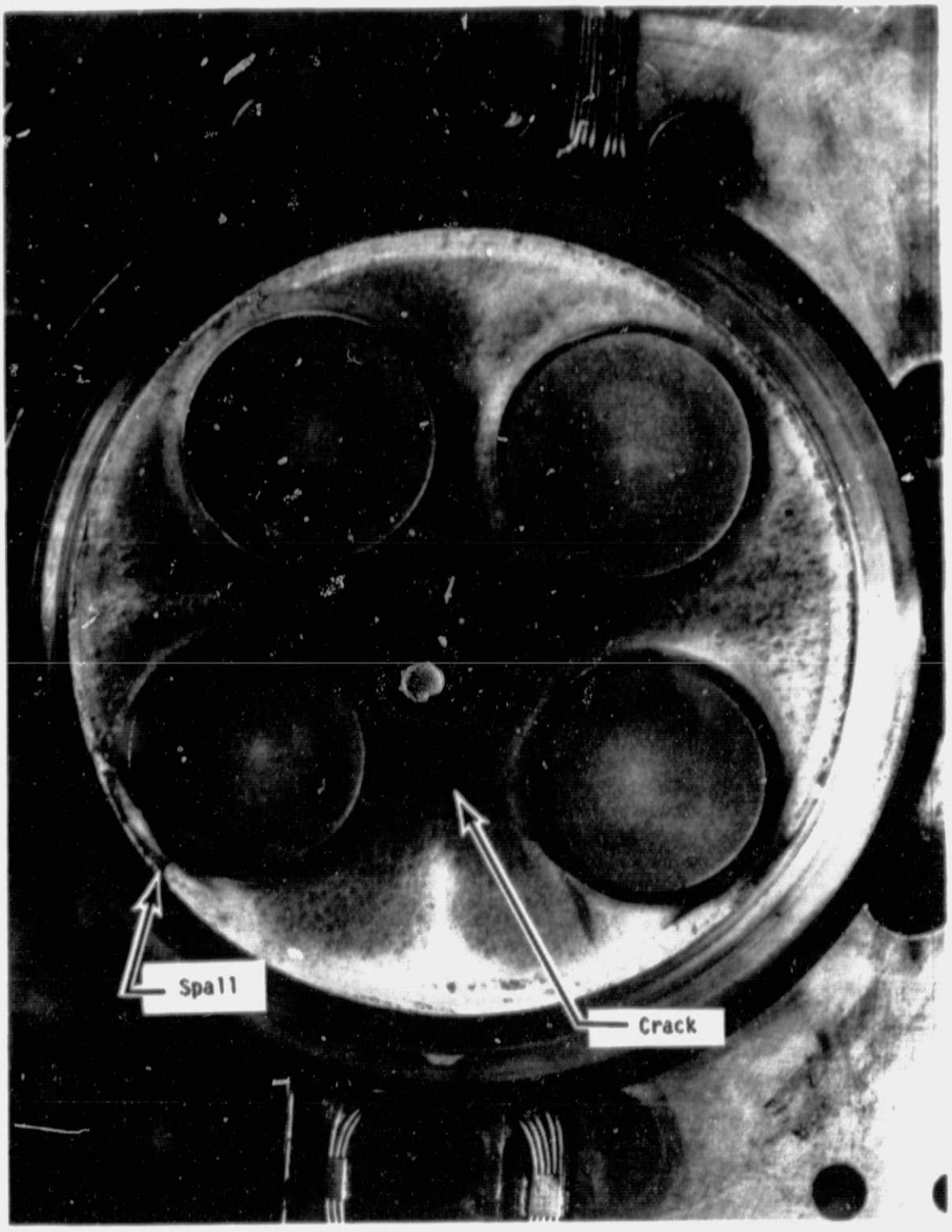

TE84-7993

Figure 74. A coated fire deck and coated valves after 14 hr of testing.

of the coating over the cylinder liner is indicated. No other spalling of the coating had occurred, and mud flat cracking was not observed.

Figures 75 and 76 show the condition of the coated fire deck and valves after completing the 24-hr test. The crack noted after 14 hr of testing had increased in length and showed indications of defining an oval-shaped spall about 7.6 mm by 15.2 mm (0.3 in. by 0.60 in.). The depth of the crack was not determined nor was it possible to estimate if the spall was about to separate from the fire deck surface. No other large cracks or mud flat cracking were observed in the fire deck surface, and no erosion damage was observed.

Valves

The intake and exhaust valves were coated with a 1.52 mm (0.060 in.) thick coating that tapered to 0.51 mm (0.020 in.) thick at the o.d. of the intake valves and to 0.76 mm (0.030 in.) thick on the exhaust valves, as shown in Figure 66.

Figure 77 shows the coated valves before testing. The coating was fully machined to retain the original valve dimensional configuration. This configuration was necessary to ensure that valve-to-piston interference did not occur during engine operation.

The condition of the valves after testing is shown in Figure 78 (after the 4-hr test), Figure 74 (after 14 hr of testing), and Figures 75 and 79 (after 24 hr of testing). The condition of the coating on all four valves was excellent after the 24-hr test. No erosion, edge cracking, or mud flat cracking was observed on any valve.

Summary of Condition of Coated Engine Components

The following statements summarize the condition of the coated components after engine testing:

- The coatings on all components were free of visual erosion damage.
- The coatings on all components were free of mud flat cracking like that observed in the static thermal shock tests.
- The coating on the piston showed no signs of spalling. One small crack developed during the initial test but did not enlarge during subsequent testing.
- There was indication of one small area of impending spalling on the combustion surface of the fire deck, but it did not separate during testing. This area represents about 1.3% of the coated surface of the fire deck. Spalling did occur at the o.d. of the fire deck but may have been induced by unintended contact with the top of the cylinder liner.
- The coating on all valves was free of any distress after testing.
- The coated insulating rings used in this test program performed as intended without suffering any spalls.

The coatings on the tested components were not exposed to destructive inspection techniques.

ORIGINAL PAGE
OF POOR QUALITY

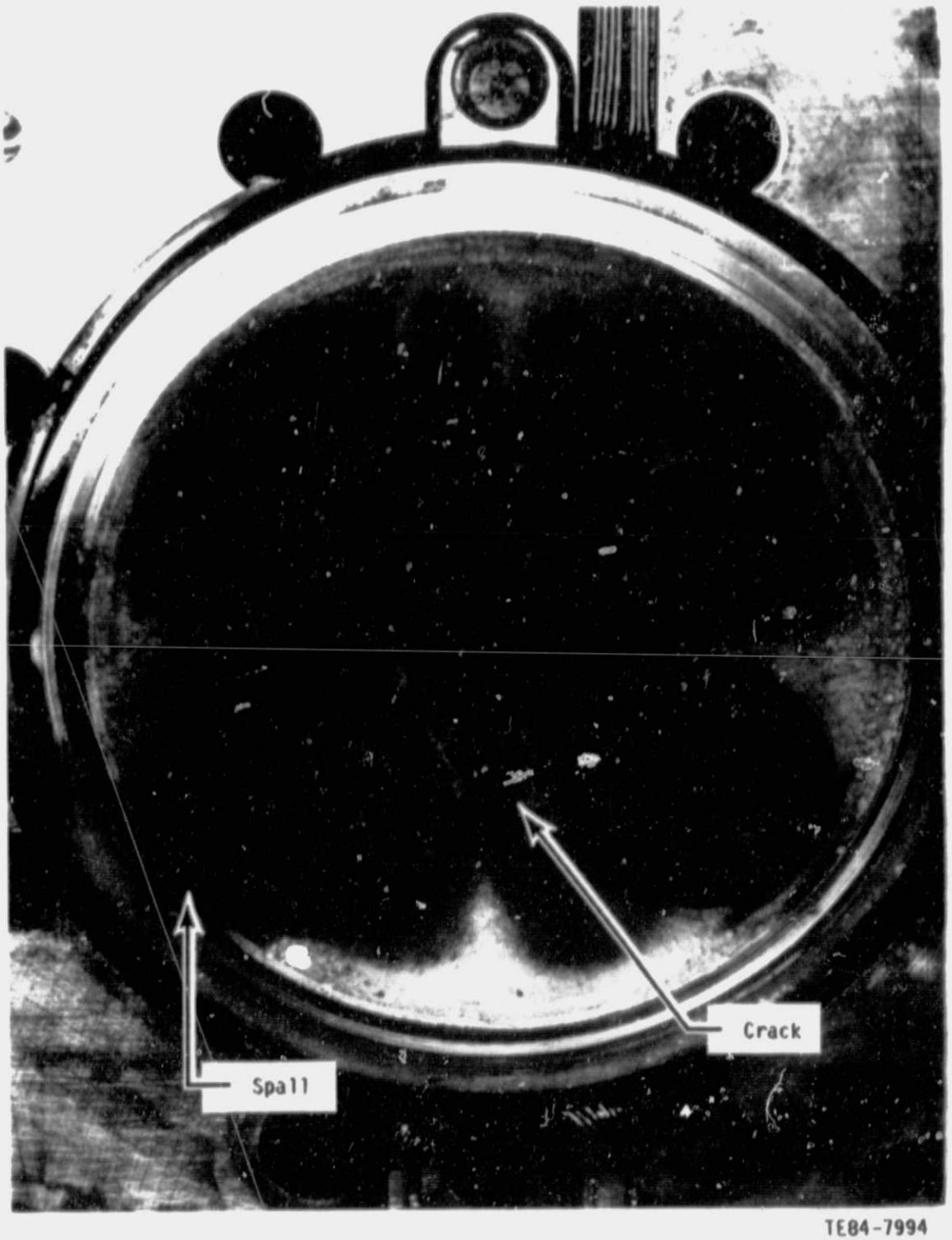

TE84-7994

Figure 75. A coated fire deck and coated valves after 24 hr of testing.

ORIGINAL PAGE IS
OF POOR QUALITY

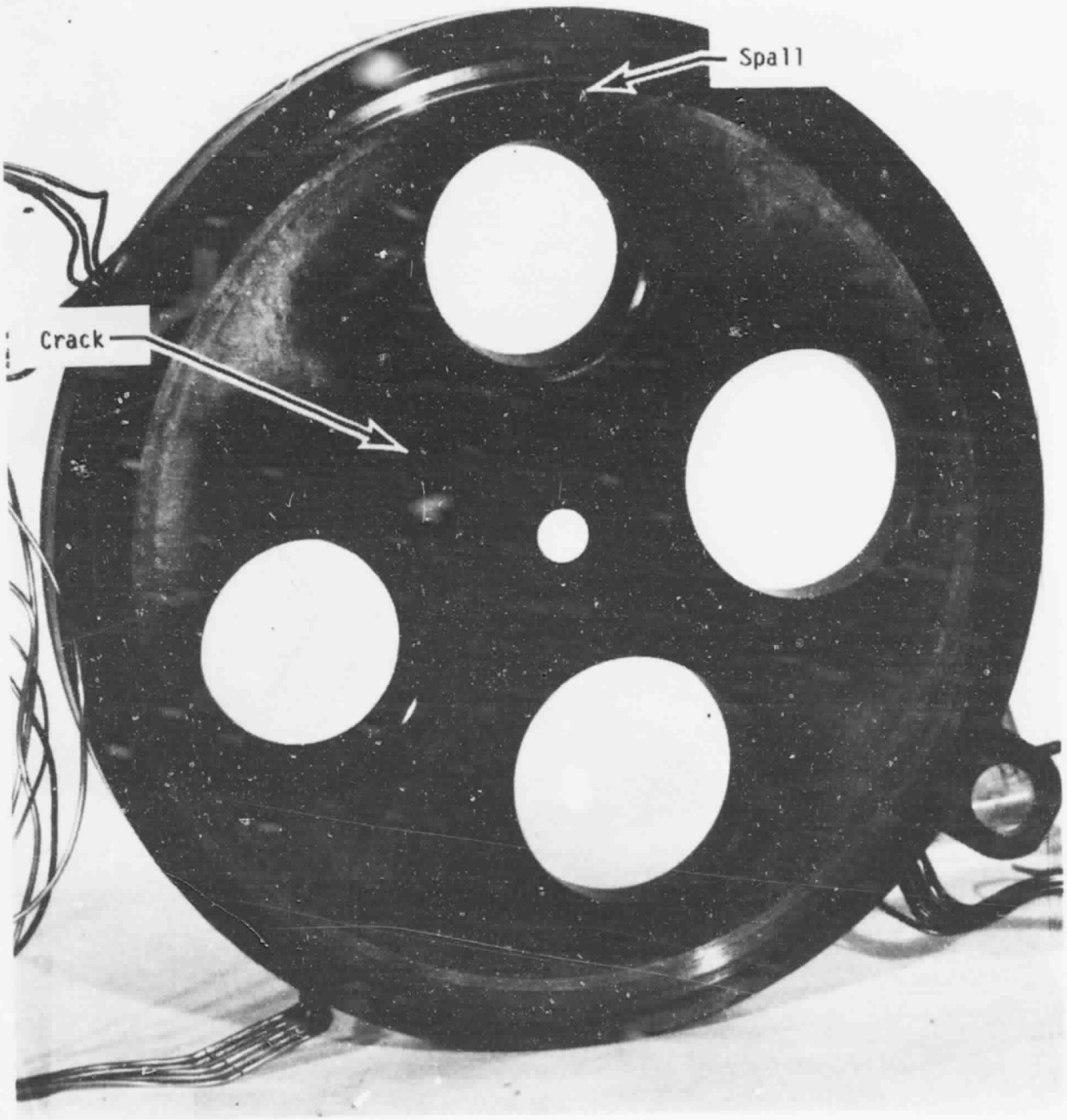

TE84-7995

Figure 76. A coated fire deck after 24 hr of testing.

ORIGINAL PAGE IS
OF POOR QUALITY

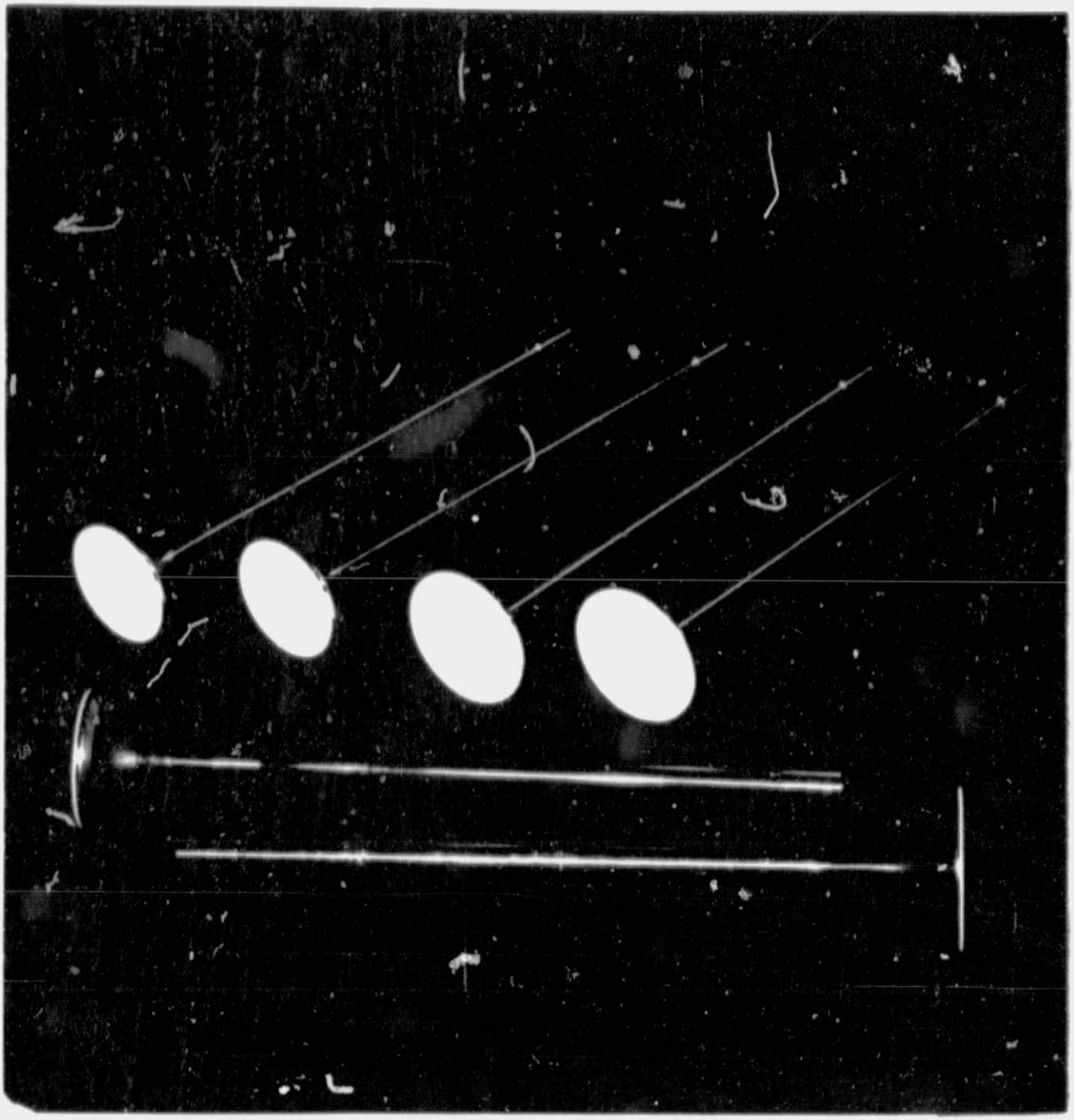

TE84-7996

Figure 77. Valves with thermal barrier coatings before testing.

ORIGINAL PAGE IS
OF POOR QUALITY

Figure 78. Coated valves after 4 hr of testing.

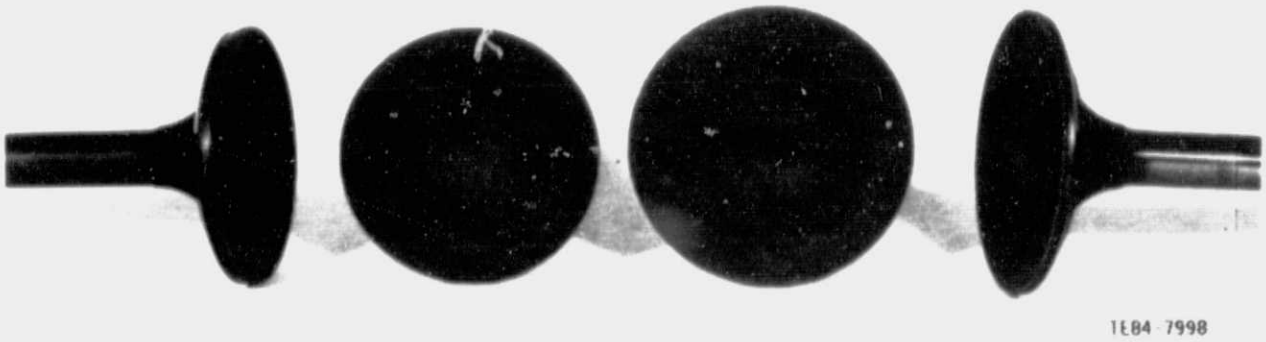

Figure 79. Coated valves after 24 hr of testing.

5.4.2.2 Comparison of Engine Performance and Fire Deck Metal Temperature with Coated and Uncoated Components

Engine operating parameters--speed, torque, airflow, fuel flow, and exhaust temperature--and specific engine component temperatures were recorded during engine testing. These data allowed comparison of engine performance and exhaust gas and temperatures of the fire deck metal for the coated and uncoated engine configurations.

Exhaust Gas Temperature

Increased exhaust gas temperature was the major observed change in engine operating parameters with the installation of the coated components. Figure 80 shows the exhaust gas temperatures with all of the coated components installed and with all of the uncoated components installed versus air/fuel ratio at 1900 rpm. The exhaust gas temperature increased 30°C (54°F) at 26.9 air/fuel ratio with the coated components installed. The difference was about 28°C (50°F) at reduced power levels. Increased exhaust gas temperature was also observed at reduced engine speed. Figure 81 shows that at 1300 rpm, the exhaust gas temperature of the coated engine configuration was about 30°C (54°F) greater than for the uncoated engine configuration throughout the power ranges tested.

Metal Operating Temperature of the Fire Deck

Reduced metal operating temperatures of the fire deck were also observed with the application of the TBC system. The comparison of fire deck temperatures was made on a different basis than that for the exhaust temperature. The comparison of the metal temperatures of the coated and uncoated fire deck was based on data collected with the engine configured as follows:

- o case I--uncoated fire deck, uncoated valves, coated piston
- o case II--coated fire deck, coated valves, coated piston

This comparison demonstrated the effect of applying the TBC to the complete cylinder head surface while eliminating the additional effect that changing piston configuration would have on in-cylinder gas conditions (temperatures).

The coated and uncoated fire decks used in the tests were instrumented with thermocouples (20 on the coated fire deck and 16 on the uncoated fire deck). This instrumentation allowed determination of the reduction in the metal temperature of the fire deck as a result of applying the TBC system. Figure 82 shows the thermocouple installation on the reverse side of the coated fire deck. The uncoated fire deck was instrumented in a similar manner.

The measured temperature profile along the symmetrical fire deck centerline for the coated and uncoated fire decks are shown in Figure 83 for engine operation at 1900 rpm, 26.9 air/fuel ratio, and 1.17 MPa (170 lb/in.^{2}) BMEP. The reduction in the metal temperature of the coated fire deck varied from 42°C (75°F) between the exhaust valves to 71°C (160°F) between the intake valves. The metal temperature at the o.d. of the fire deck assembly changed only slightly with the addition of the TBC. Figure 83 shows a considerable temperature gradient existing in the fire deck from the exhaust side to the intake side. The fire deck is heated by exhaust gas flowing through the exhaust port passages and cooled by the intake charge flowing through the intake port passages. The reduction in metal temperatures on the exhaust side is diminished

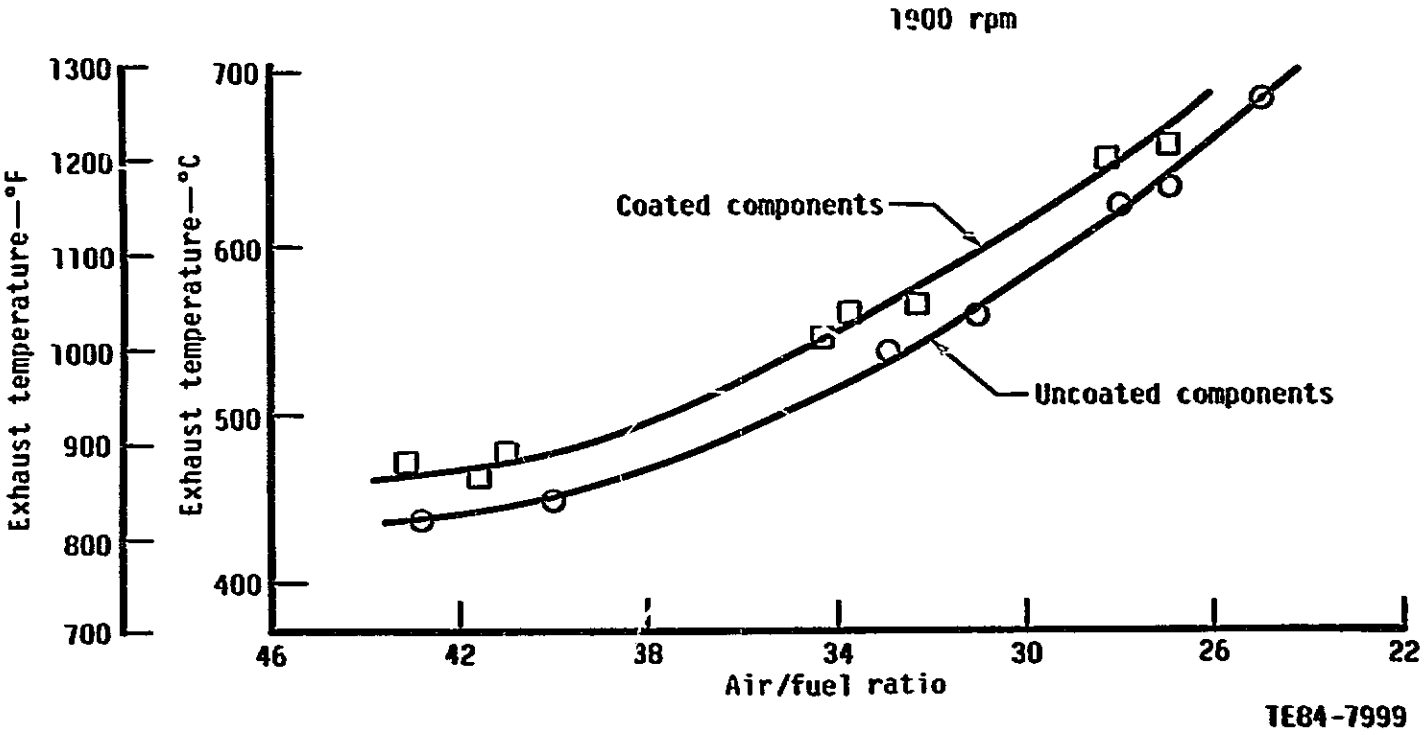

Figure 80. Exhaust gas temperature versus air/fuel ratio at 1900 rpm.

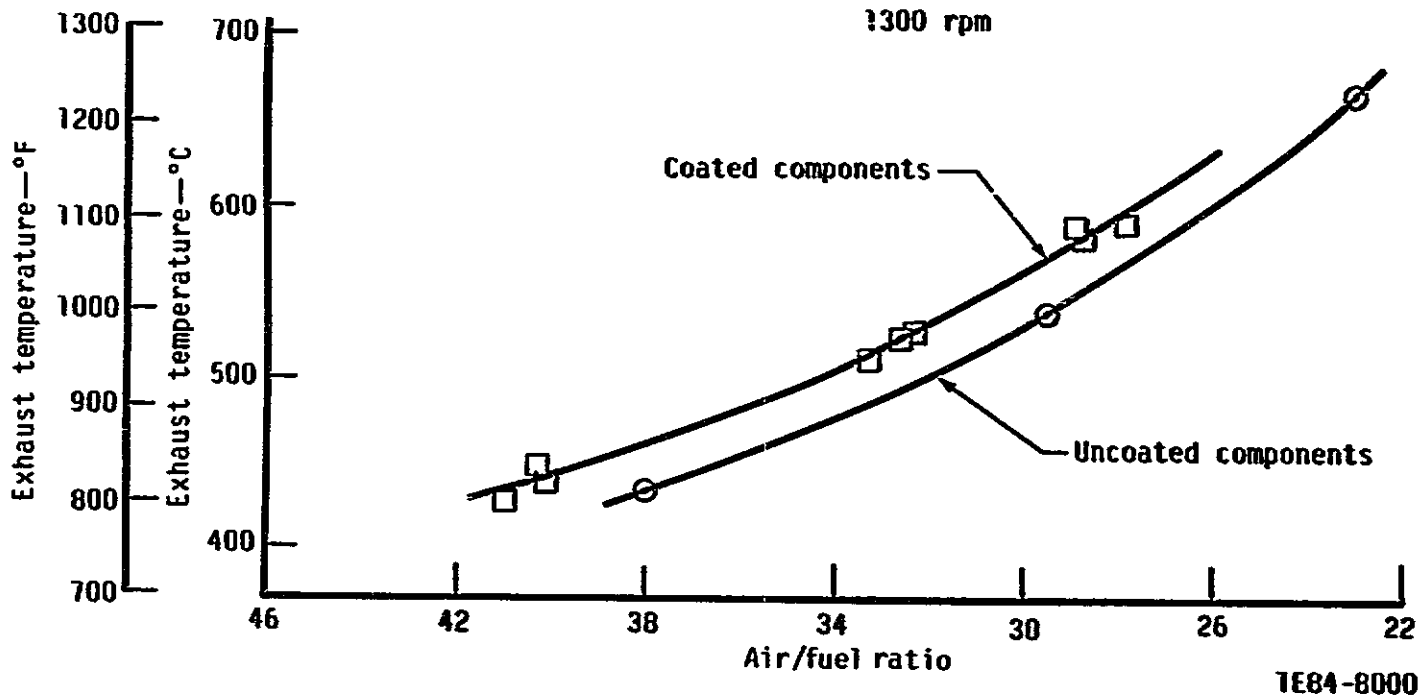

Figure 81. Exhaust gas temperature versus air/fuel ratio at 1300 rpm.

ORIGINAL PAGE IS
OF POOR QUALITY

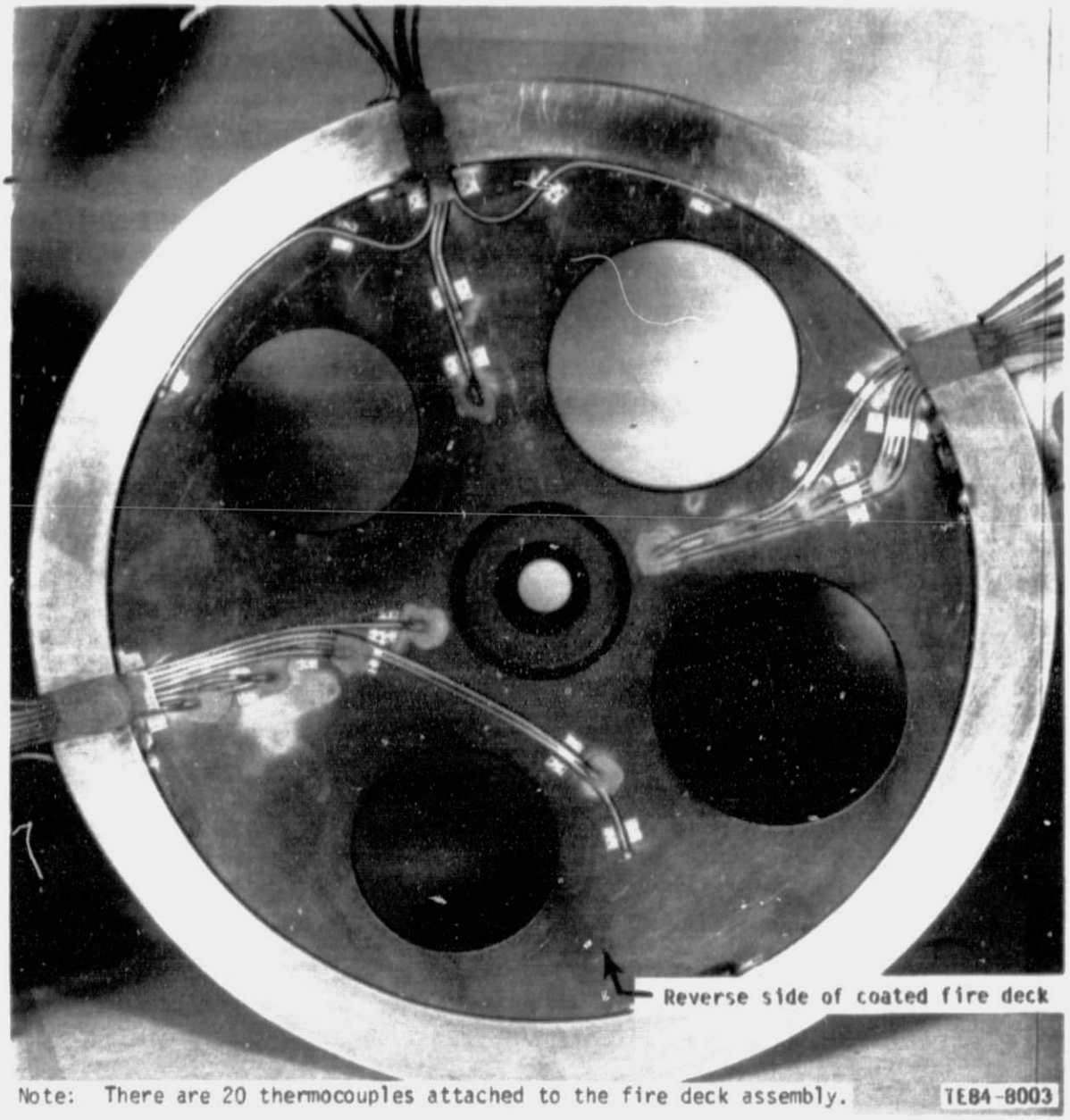

Figure 82. Thermocouple instrumentation on a coated fire deck.

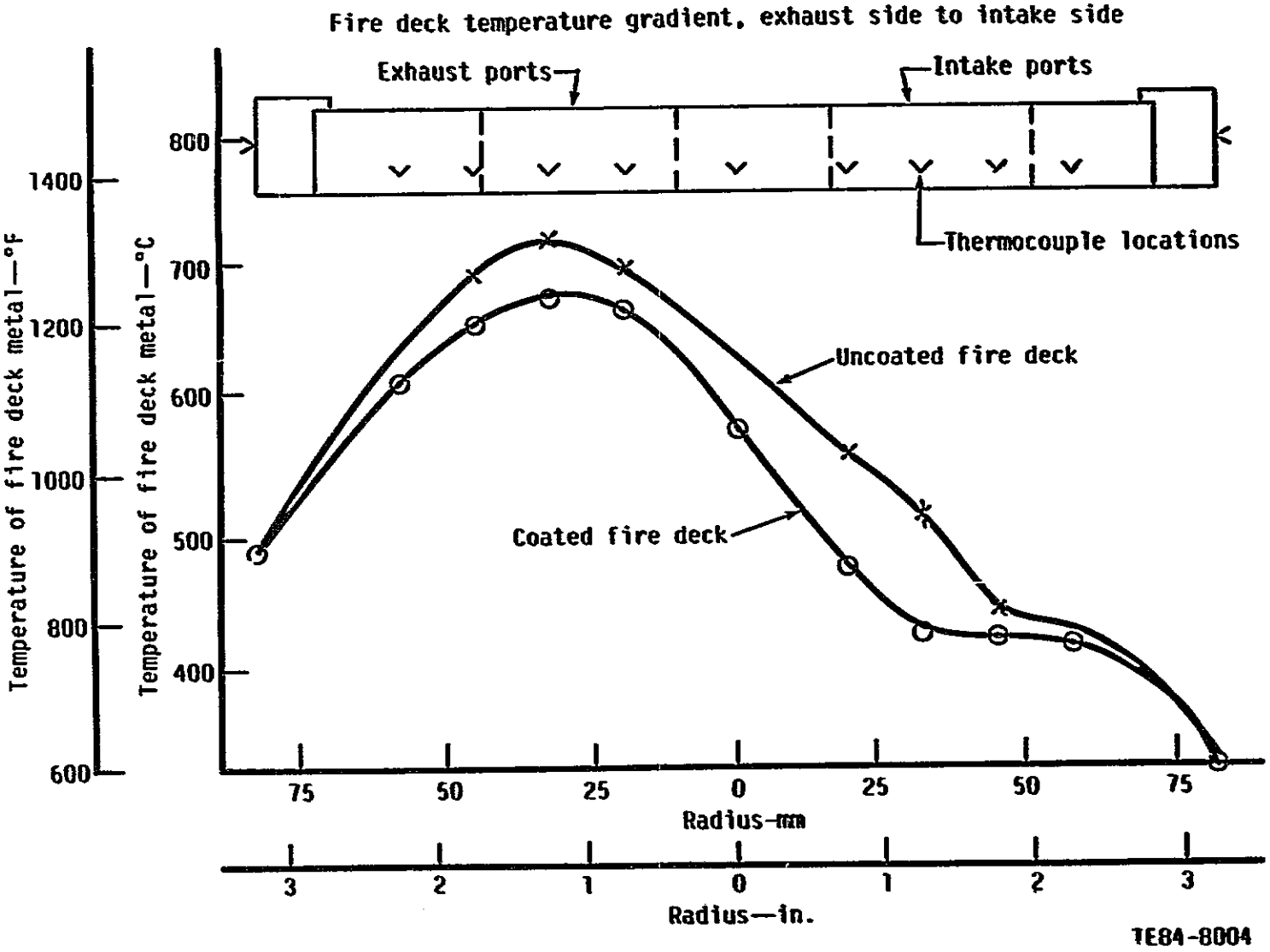

Figure 83. Metal temperatures of the fire deck along symmetrical centerline.

because the exhaust gas passing through the exhaust passages of the coated fire deck was 28°C (50°F) hotter than that passing through the uncoated fire deck. Thermal barrier treatment of the fire deck port passages was not included in the scope of this program but gains could be made in retaining heat in the working gas by treating this portion of the fire deck also.

Reduction in the metal temperatures of the fire deck at two locations in the fire deck as a function of air/fuel ratio is shown in Figure 84 for engine operation at 1900 rpm. A significant portion of the reduction in the metal temperatures of the fire deck is maintained as engine power is reduced.

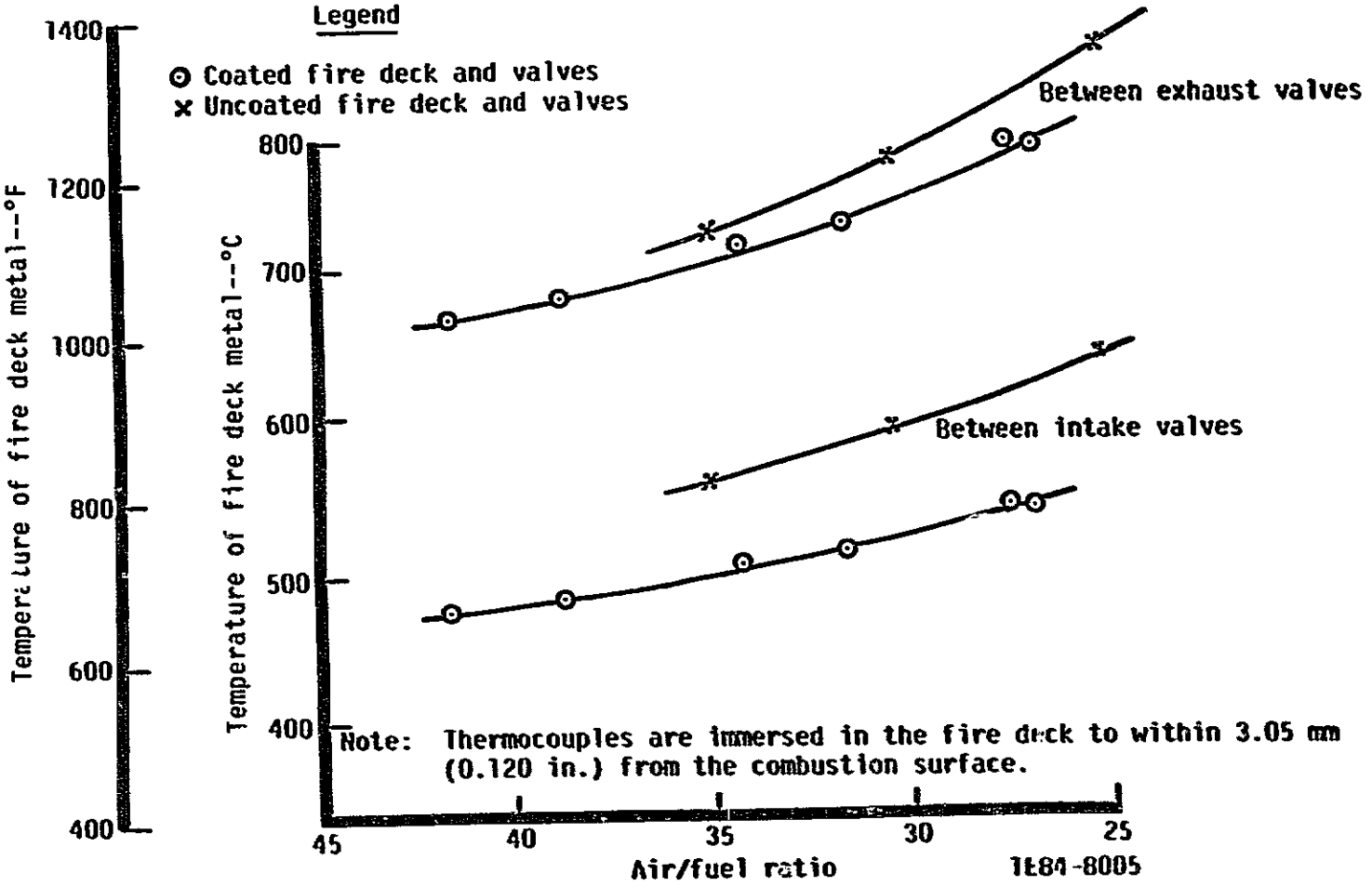

Figure 84. Reduction in metal temperatures of the fire deck versus air/fuel ratio.

VI. CONCLUSIONS AND RECOMMENDATIONS

6.1 DESCRIPTION OF INVESTIGATION

This program was undertaken to systematically develop an enhanced capability TBC for diesel engine components. First, static screening tests were conducted to evaluate the thermal conductivity, erosion resistance, corrosion/oxidation resistance, and thermal shock resistance of seven increased thickness developmental TBC systems. Three of the coating systems incorporated a strain isolator (SI) pad. Systematic development of the PS parameters of an advanced coating system based on an HYSZ powder was also undertaken. A PS/HYSZ coating developed by Allison was judged superior in the static screening tests and, thus, applied to the modified piston, fire deck, and valves of an uncooled single-cylinder LHR diesel engine. These components were engine tested for a planned total of 24 hr at power levels from 0.83 MPa to 1.17 MPa (120 lb/in.^{2} to 170 lb/in.^{2}) BMEP.

6.2 PROGRAM GOALS

The following three primary objectives were goals in this program effort:

- to demonstrate an enhanced capability coating system with increased thickness (greater than state-of-the-art 0.76 mm (0.030 in.) coating thickness) in an LHR diesel engine environment
- to evaluate in a diesel engine environment an SI concept that relieves shear strain at the coating/metal substrate interface
- to increase the exhaust gas heat energy by reducing heat loss through walls in the cylinder to the engine structure and other cooling media. This reduction would increase energy available to exhaust heat recovery devices, which, in turn, would improve the overall efficiency of the engine system.

6.3 RESULTS AND CONCLUSIONS

1. An advanced capability thermal barrier was demonstrated successfully in a diesel engine environment. The PS/HYSZ coating with a thickness of 1.52 mm (0.060 in.) was engine-tested for 24 hr with little visible indication of coating distress.

2. The thickness of the PS/HYSZ coating was defined by constraints encountered in modifying components of the test engine to accept the TBCs. Therefore, the maximum thickness capability of the PS/HYSZ coating was not determined in this program.

3. The feasibility of using a metallic SI between a ceramic coating and the base metal substrate was also demonstrated with 24 hr of testing. The tested fire deck coating system incorporated a 1.02 mm (0.040 in.) thick 50% dense SI designed for the diesel engine application.

4. The presence of the TBCs in the cylinder increased the exhaust gas temperature about 30°C (54°F) over a broad range of test conditions. This magnitude of increase was not calculated in the heat transfer analysis of the coated components. This increase suggests that the radiation heat transfer characteristics of the coatings may differ from those for uncoated components. A reduction in metal temperature of 42°C to 86°C

(75°F to 155°F) at specific locations in the coated fire deck also demonstrated the thermal effectiveness of the coating.

5. The morphology of the PS/HYSZ coating was not fully optimized during this program. It did, however, demonstrate a 10% reduction in thermal conductivity when compared to SYSZ coatings.

6.4 RECOMMENDATIONS

1. The PS/HYSZ coating should undergo additional engine durability testing to accumulate at least 100 hr of test time. The testing should include transient as well as steady-state engine operations. Engine loading should be increased if the coatings continue to perform satisfactorily at power levels tested in this program.

2. Engine components should be designed to allow testing of PS/HYSZ coating thicknesses up to 2.54 mm (0.100 in.). A 2.54 mm (0.100 in.) thick coating would achieve a thermal effectiveness equal to a monolithic zirconia component approximately 7.62 mm (0.300 in.) thick.

3. The radiation heat transfer characteristics of the zirconia-based coatings should be evaluated to determine the full capability of the coatings to reduce heat loss form the engine cylinder.

4. The necessity of the SI pad in the overall coating system was not determined in this program. Evaluation of the SI should be continued to determine its suitability to be included as a necessary component in a viable TBC system.

5. The development of the PS/HYSZ coating should be continued. Further reduction in thermal conductivity and improvement in durability may be achieved through improved PS techniques that enhance the retention of the hollow particle morphology.

APPENDIX A

LIST OF TERMS, ABBREVIATIONS, AND SYMBOLS

The following list defines terms, abbreviations and symbols used throughout this report. In most instances, these terms are used in place of their length equivalents.

abs	absolute
BMEP	break mean effective pressure (a measure of engine output)
BSFC	brake specific fuel consumption
coating	implies a plasma-sprayed coating
EJ	exajoules (joules x 10^{18})
FEM	finite element model or method
fire deck	lower portion of cylinder head exposed to the combustion gases (the valves seat on the fire deck)
HYSZ	hollow particle yttria-stabilized zirconia material powder
LHR	low heat rejection design or treatment
NiCrAlY bond coat	nickel, chromium, aluminum, yttria bond coat material used in Allison-applied coatings
o.d.	outer diameter
piston crown	the top portion of the piston assembly, the top surface of which is exposed to the combustion gases
PS	plasma-sprayed
PS/HYSZ coating	an Allison-applied plasma-sprayed coating incorporating solid and hollow particle yttria-stabilized zirconia material powders
psia	$lb/in.^2$ absolute
psig	$lb/in.^2$ gage
PSZ	plasma-sprayed zirconia
SEM	scanning electron microscope
SI	a sintered metallic strain isolator pad
SYSZ	solid particle yttria-stabilized zirconia material powder
TBC	thermal barrier coating
vendor coating A	a vendor-applied coating identified as coating A
vendor coating B	a vendor-applied coating identified as coating B
XEDA	X-ray energy dispersion analysis
YSZ	8% yttria-stabilized zirconia
1-D	one-dimensional
2-D	two-dimensional
3-D	three-dimensional
80/20 SYSZ/ Eccosphere coating	an Allison-applied plasma-sprayed coating system incorporating solid particle yttria-stabilized zirconia and Eccosphere material powder
ΔT	temperature drop

REFERENCES

1. R. Kamo and W. Bryzik, "Cummins/TACOM Advanced Adiabatic Engine," SAE Paper 840428, February 1984.

2. F. E. Ames, "A Study of the Thermal Conductance of Thermal Barrier Coating Systems," Allison Report EDR 11889, September 1984.

3. Curt H. Liebert, "Emittance and Absorptance of NASA Ceramic Thermal Barrier System," NASA Technical Paper 1190, June 1978.

4. Insulated Oil-Cooled Piston Assembly, U.S. Patent No. 4,270,494 dated 2 June 1981, assigned to General Motors Corporation.

5. Insulated Oil-Cooled Piston Assembly, U.S. Patent No. 4,253,430 dated 3 March 1981, assigned to General Motors Corporation.